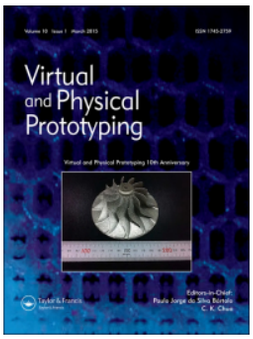

Taylor & Francis
Taylor & Francis Group

Virtual and Physical Prototyping

ISSN: 1745-2759 (Print) 1745-2767 (Online) Journal homepage: www.tandfonline.com/journals/nvpp20

A critical review on additive manufacturing of refractory alloys from a data analytics perspective- beyond nickel-based superalloys

Duck Bong Kim , Mahdi Sadeqi Bajestani , Md Abdul Karim , Saiful Islam , Oleg N. Senkov , Peter K. Liaw , Hojun Lim , Paul Witherell , Yousub Lee , Peeyush Nandwana , Xuesong Fan , Wonjong Jeong , Jiwon Mun , Yongho Jeon & Ho Jin Ryu

To cite this article: Duck Bong Kim , Mahdi Sadeqi Bajestani , Md Abdul Karim , Saiful Islam , Oleg N. Senkov , Peter K. Liaw , Hojun Lim , Paul Witherell , Yousub Lee , Peeyush Nandwana , Xuesong Fan , Wonjong Jeong , Jiwon Mun , Yongho Jeon & Ho Jin Ryu (16 Jan 2026): A critical review on additive manufacturing of refractory alloys from a data analytics perspective- beyond nickel-based superalloys, Virtual and Physical Prototyping, DOI: 10.1080/17452759.2025.2604453

To link to this article: https://doi.org/10.1080/17452759.2025.2604453

Published online: 16 Jan 2026.

VIRTUAL AND PHYSICAL PROTOTYPING
https://doi.org/10.1080/17452759.2025.2604453

Taylor & Francis
Taylor & Francis Group

REVIEW ARTICLE

OPEN ACCESS Check for updates

A critical review on additive manufacturing of refractory alloys from a data analytics perspective- beyond nickel-based superalloys*

Duck Bong Kim[a], Mahdi Sadeqi Bajestani[b], Md Abdul Karim[c], Saiful Islam[a], Oleg N. Senkov[d], Peter K. Liaw[e], Hojun Lim[f], Paul Witherell[g], Yousub Lee[h], Peeyush Nandwana[i], Xuesong Fan[j], Wonjong Jeong[k], Jiwon Mun[k], Yongho Jeon[l] and Ho Jin Ryu[k]

[a]School of Environmental, Civil, Agricultural and Mechanical Engineering, University of Georgia, Athens, GA, USA; [b]Transportation Research Institute (IMOB), Hasselt, Belgium; [c]Department of Computer Science, Engineering, and Mathematics, University of South Carolina Aiken, Aiken, SC, USA; [d]Air Force Research Laboratory, Wright-Patterson AFB, Dayton, OH, USA; [e]Department of Materials Science and Engineering, University of Tennessee, Knoxville, TN, USA; [f]Department of Computational Materials, Sandia National Laboratories, Albuquerque, NM, USA; [g]Systems Integration Division, National Institute of Standards and Technology (NIST), Gaithersburg, MD, USA; [h]Computational Sciences and Engineering Division, Oak Ridge National Laboratory, Oak Ridge, TN, USA; [i]Materials Science and Technology Division, Oak Ridge National Laboratory, Oak Ridge, TN, USA; [j]Materials Joining Group, Oak Ridge National Laboratory, Oak Ridge, TN, USA; [k]Department of Material Science and Engineering, Korea Advanced Institute of Science and Technology, Daejeon, South Korea; [l]Department of Mechanical Engineering, Ajou University, Gyeonggi-do, South Korea

ABSTRACT

Refractory alloys (RAs) are promising materials due to their exceptional physicochemical properties, but most research remains at the laboratory scale. For broader adoption, advancements in manufacturing are essential. Because their high stability makes conventional methods like machining and casting difficult, additive manufacturing (AM) is emerging as an effective approach for fabricating refractory alloy components. However, AM's repeated non-equilibrium thermal cycles introduce undesired features (e.g. defects, anisotropic microstructures, and residual stresses), which are magnified due to RAs' unique properties. This paper comprehensively reviews the state-of-the-art methods of AM for refractory alloys. It explores data analytics techniques to establish design rules based on multi-fidelity experimental and computational methods. Furthermore, it investigates integrated, collaborative efforts to harmonise standalone databases, information, knowledge, and predictive models at multi-physics, multi-stage, and multi-scale. Unlike the existing literature that focuses primarily on material systems or process fundamentals, this work provides an integrated perspective on AM of refractory alloys from a data analytics standpoint, highlighting the roles of integrated computational materials engineering (ICME), verification, validation, and uncertainty quantification (VV&UQ), and digital twin-driven qualification in overcoming data scarcity and accelerating rapid qualification.

ARTICLE HISTORY
Received 2 September 2025
Accepted 10 December 2025

KEYWORDS
Additive manufacturing; refractory alloys; data analytics; thermo-physicochemical properties; high-temperature applications

1. Introduction

Refractory metals, such as tungsten (W), molybdenum (Mo), niobium (Nb), tantalum (Ta), and rhenium (Re), have significant potential for engineering applications in extremely harsh environments due to their exceptional physicochemical properties, microstructural stability, and outstanding mechanical properties at elevated temperatures [1,2]. For example, pure W features intrinsic properties such as a high melting point (3420°C), great hardness, large thermal conductivity (175 W/m.°C), excellent strength at room and elevated temperatures, and radiation-shielding capability. Therefore, W-based alloys have been widely used in electronics, medical, and nuclear applications [3]. Similarly, each refractory metal exhibits distinct attractive properties, and alloys based on these metals are used

CONTACT Duck Bong Kim DBKim@uga.edu School of Environmental, Civil, Agricultural and Mechanical Engineering, University of Georgia, Athens, GA 30602, USA; Yongho Jeon princaps@ajou.ac.kr School of Environmental, Civil, Agricultural and Mechanical Engineering, University of Georgia, Athens, GA 30602, USA; Ho Jin Ryu hojinryu@kaist.ac.kr Department of Material Science and Engineering, Korea Advanced Institute of Science and Technology, 291, Daehak-ro, Yuseong-gu, Daejeon 34141, South Korea

in various industries [4]. Despite their advantageous properties, manufacturing refractory metals is inherently complex and requires specialised techniques due to poor machinability, intrinsic brittleness, and oxidation issues. If these limitations could be adequately addressed, refractory metals and alloys would have a significant impact on advanced technological applications, particularly in aerospace and nuclear applications [5,6].

The broad adoption of refractory alloys (RAs) for practical industrial applications is mainly hindered by a lack of knowledge about their manufacturability [7,8]. First, the sizes and geometrical complexity of refractory RAs fabricated by conventional manufacturing processes (e.g. powder metallurgy, casting, and machining) are limited. Second, the cost of RAs is significantly higher than that of most conventional alloys due to the inclusion of expensive elements and the associated cost of processing them [9]. Third, the design rules among process-structure–property-performance (PSPP) relationships of RAs have not been thoroughly investigated, due to the lack of cost-efficient, integrated experimental and computational modelling methods. Due to these limitations, it is challenging to fabricate RAs using conventional methods, especially for large-sized structures with complex shapes [10]. To address these issues, manufacturing engineers and material scientists are increasingly exploring the additive manufacturing (AM) processes to utilise the promising features of refractory metals for structural and functional parts [11].

AM provides several attractive advantages, e.g. complexity-free fabrication, suitable solutions for one-off or small batches of production parts, sustainable manufacturing due to low material waste, and reduction of lead times [12]. Moreover, AM can support the production of intricate parts with excellent mechanical properties, essential for applications in high-temperature environments, such as turbine components in aerospace. Therefore, metal AM processes potentially offer the best solution to fabricate functional and structural components from RAs. To address the first limitation mentioned in the previous paragraph, AM supports complex part fabrication and scalable manufacturing capabilities by utilising layer-by-layer stacking mechanisms. To overcome the second limitation, AM offers near-net shape fabrication, which is suitable for manufacturing structures (e.g. for aerospace applications) with a high buy-to-fly ratio (BTF), resulting in reduced material waste and overall cost. To manage the third limitation, AM can leverage advanced sensors and utilise cost-efficient high-throughput experimental methods (HTEM) to characterise the relationships among process, structure, property, and performance (PSPP) for 'alloy-on-demand' fabrication [13,14].

The layer-by-layer deposition in the AM process creates many of its own challenges, such as the non-equilibrium, repeated thermal cycles, which induce solidification-remelting-recrystallization in the previously deposited layers [15]. Consequently, this process generates several unwanted features, e.g. (1) heterogeneous microstructures and defects [16] and (2) the residual stress developed due to extreme thermal gradients [17]. In the case of additively manufactured refractory alloys (AM-RAs), these unwanted features are magnified due to the exceptional physicochemical properties of refractory elements [18]. Accordingly, current AM-RAs often have deteriorated mechanical and chemical properties due to a lack of fundamental knowledge of AM-RAs. Understanding non-equilibrium thermodynamics, the enormous compositional space, and the unusual kinetic properties in RAs is necessary to establish a control framework that mitigates these unwanted features. In this regard, data analytics (DA), which is defined as 'a process of examining data to extract and create valuable information for decision-making', can be considered one of the possible solutions to address the issues and challenges in AM-RAs [19].

The DA techniques have been widely used in AM for high-performance alloys (e.g. Inconel 625 and Ti-6Al-4V) for better process understanding and improvement of mechanical properties [20]. The goals of DA for AM are to establish methods and design rules for near-optimal process planning, real-time process control, part qualification, and performance assurance [21]. Physics-informed, data-driven modelling approaches with uncertainty consideration are an effective tool for investigating and establishing those attributes [22,23]. Nevertheless, in addition to the complexity arising from the multi-physics and multi-scale aspects of AM, there are several critical issues in AM-RAs, such as the lack of databases on physicochemical properties in RAs and the extensive resource requirements for conducting experiments [24]. Such a database should initially include thermophysical parameters (e.g. thermal conductivity, heat capacity, diffusion coefficients), mechanical properties under service-relevant conditions (e.g. fatigue, creep, corrosion), and microstructural descriptors linked to process parameters (e.g. grain morphology, defect density, texture). Equally important is the adoption of standardised data formats and open-access platforms to facilitate integration with machine learning (ML) frameworks. Developing such a resource would directly support the reduction of uncertainty and enable more reliable, data-driven, and physics-informed modelling for AM-RAs.

The objectives of this paper are to (1) review the state-of-the-art in AM-RAs, (2) identify current technical

limitations and critical research challenges from a DA perspective, and (3) outline future research and development directions. RAs and AM classifications will be presented in Section 2. The metal AM-RAs will be reviewed in Section 3. The DA techniques for AM-RAs will be investigated from a microscopic perspective in Section 4, while Section 5 introduces an integrated framework from a macroscopic perspective. Section 6 will summarise the findings and discuss future directions in research and development to accelerate the development of AM-RAs.

2. Background

2.1. Classification of refractory metals and alloys

Refractory metals are a group of metallic elements highly resistant to heat and wear. These metals (e.g. W, Mo, Nb, Ta, and Re) have melting points above 2400°C and high creep resistance. A wider definition, which is used by the materials science community, identifies refractory metals as those having melting points above 1800°C and thus includes nine additional elements, such as zirconium (Zr), hafnium (Hf), vanadium (V), chromium (Cr), technetium (Tc), ruthenium (Ru), osmium (Os), rhodium (Rh), and iridium (Ir). The physical properties of these metals are summarised in Table 1. Their density ranges from 6.11 (V) to 22.59 g/cm^3 (Os), specific heat from 0.13 (W, Os, and Ir) to 0.49 (V) J/g.°C, thermal conductivity from 22.7 (Zr) to 174.0 (W) W/m.°C and heat of fusion from 135.8 (Ir) to 422.0 (V) J/g. Interestingly, all refractory metals have a low coefficient of thermal expansion, in the range from 4.5×10^{-6}/°C (W) to 9.6×10^{-6}/°C (Ru). V, Nb, Ta, Cr, Mo, and W have a body-centred cubic (BCC) crystal structure. Tc, Re, Ru, and Os have a hexagonal-close-packed (HCP) crystal structure, whereas Rh and Ir have face-centred cubic (FCC) crystal structures. Zr and Hf have an HCP crystal structure at room temperature and transform to a BCC structure at higher temperatures.

Refractory metals can be alloyed with other refractory or non-refractory metals to improve mechanical properties through different strengthening mechanisms, such as solid-solution and precipitation strengthening [25]. These alloys are referred to as refractory-metal-based alloys or simply refractory alloys. Conventional refractory alloys are based on a single refractory metal and contain other alloying elements with total concentrations generally not exceeding 30 at. %. They encompass thirteen different groups (among the fourteen elements, Tc is radioactive and cannot be used as a base element), as shown in Table 1, and each group is named after the base element, e.g. Nb alloys, Mo alloys, W alloys, etc.

In 2010–2011, a new approach involving refractory high-entropy alloys (RHEAs) was introduced, driven by the goal of exploring the vast and complex composition space [26,27] and developing a new generation of high-temperature materials capable of functioning under temperatures and loading conditions beyond those of Ni-based superalloys [28,29]. Since their introduction, RHEAs have gained considerable attention for their ability to maintain strength at temperatures of at least 1600°C and their distinctive thermo-physicochemical properties [30–34]. RHEAs are defined as alloys composed of four or more refractory elements (referred to as principal elements), with each element having a concentration between 5 and 35 atomic percent. Additionally, RHEAs can include non-principal elements, which are not necessarily refractory metals and have concentrations below 5 at. % [31]. Figure 1 shows the year-wise number of publications for different refractory metals fabricated by AM processes. Research activity on AM of refractory alloys has shown a steady increase over the past decade, with tungsten being the earliest

Table 1. Common physical properties of refractory elements.

Category	Metal	A (g/mol)	ρ (g/cm^3)	T_m (°C)	T_b (°C)	C_p (J/g.°C)	λ (W/m.°C)	α (×10^{-6} /°C)	ΔH_f (J/g)	r (×10^{-12} m)	Crystal Structure
Refractory metals	Ta	180.95	16.65	3017	5458	0.14	57.5	6.5	199.0	146	BCC
	W	183.84	19.25	3422	5555	0.13	174.0	4.5	192.5	139	BCC
	Nb	92.91	8.57	2477	4744	0.27	53.7	7.31	328.3	146	BCC
	Mo	95.94	10.22	2623	4639	0.25	138.5	5.1	390.7	139	BCC
Wider definition	Cr	52.00	7.14	1857	2672	0.45	93.7	6.6	325.0	128	BCC
	Hf	178.49	13.31	2233	4603	0.14	23.0	6.6	142.9	159	HCP/BCC
	Zr	91.22	6.51	1857	4409	0.27	22.7	5.8	219.0	160	HCP/BCC
	V	50.94	6.11	1902	3409	0.49	30.7	8.3	422.0	134	BCC
	Tc	98.91	11.50	2157	4877	0.25	50.6	7.1	240.7	136	HCP
	Re	186.21	21.02	3186	5596	0.14	48.0	6.6	177.2	137	HCP
	Ru	101.07	12.37	2334	4150	0.24	117.0	9.63	237.5	134	HCP
	Os	190.23	22.59	3050	5020	0.13	88.0	6.58	167.2	135	HCP
	Rh	102.91	12.45	1964	3695	0.24	87.2	8.5	208.9	134	FCC
	Ir	192.22	22.56	2466	4428	0.13	147.0	6.5	135.8	136	FCC

Atomic mass (A), density (ρ), melting point (T_m), boiling point (T_b), specific heat (Cp), thermal conductivity (λ), coefficient of thermal expansion (α), heat of fusion (ΔH_f), and atomic radius (r).

system reported in 2009 and rhenium introduced in 2016. This upward trend reflects growing recognition of the potential of refractory alloys for high-temperature and extreme-environment applications. The bibliometric analysis underscores both the timeliness of this review and the urgent need to consolidate fragmented knowledge across different alloy systems into a systematic framework.

Although RHEAs occupy a wider composition space than conventional refractory alloys, their definition is compositionally limited and excludes a large amount of refractory multi-principal element alloys (RMPEAs) with the number of principal elements less than five and/or a concentration of an alloying element more than 35 at.%. To address these restrictions, a new class of refractory alloys, referred to interchangeably as refractory complex concentrated alloys (RCCAs) or RMPEAs, has recently been introduced and is being investigated extensively [34]. These alloys are based on two or more principal refractory elements, and they also may contain other non-principal alloying elements (refractory or non-refractory). Non-refractory elements, such as Al, Ti, and Si, are often added to RCCAs to reduce density, control the microstructure and phase composition, and improve properties. By definition, RCCAs occupy much larger composition space than RHEAs. In fact, RHEAs can be considered as a special subclass of RCCAs with high configurational entropy. Depending on their composition, RCCAs have a wide range of properties, and their melting temperature (Tm) can reach up to 3500°C. Moreover, these alloys display a linear correlation between their densities and melting temperature [35], indicating that the high-temperature strength and specific strength of these alloys tend to increase with higher T_m [36]. Refractory superalloys (RSAs) are a special group of RCCAs with unique microstructure and mechanical properties [37]. These alloys contain two nanometer-sized coherent phases, disordered BCC (A2) and ordered B2, or γ′, and mimic the microstructures of Ni-based superalloys. This two-phase microstructure has high thermal stability in some RSAs and provides superior strength retention at temperatures up to 1200°C. Another group of materials is high-entropy superalloys (HESA), which can exhibit superior creep resistance and yield strength. For instance, Li et al. [38] designed Ni-5.82Fe-15.34Co-2.53Al-2.99Ti-2.90Nb-15.97Cr-2.50Mo (wt.%) HESA with a yield strength of 1346 MPa at room temperature and 1061 MPa at 750°C and a density of 7.98 g/cm^3.

2.2. AM processes for refractory alloys

Compared to conventional manufacturing processes, it has been shown that AM processes encompass significant benefits during the fabrication of customised, highly complex, and one-off parts [3]. AM is considered a sustainable manufacturing process and has advantages in depositing high BTF ratio structures, HTEM capability [39], and fabrication of functionally graded materials (FGMs) and multi-materials [40]. Consequently, AM can serve as an optimal solution to facilitate the paradigm shift from 'apply the alloy you have' to 'engineer the alloy you need.' In addition, it has a significant

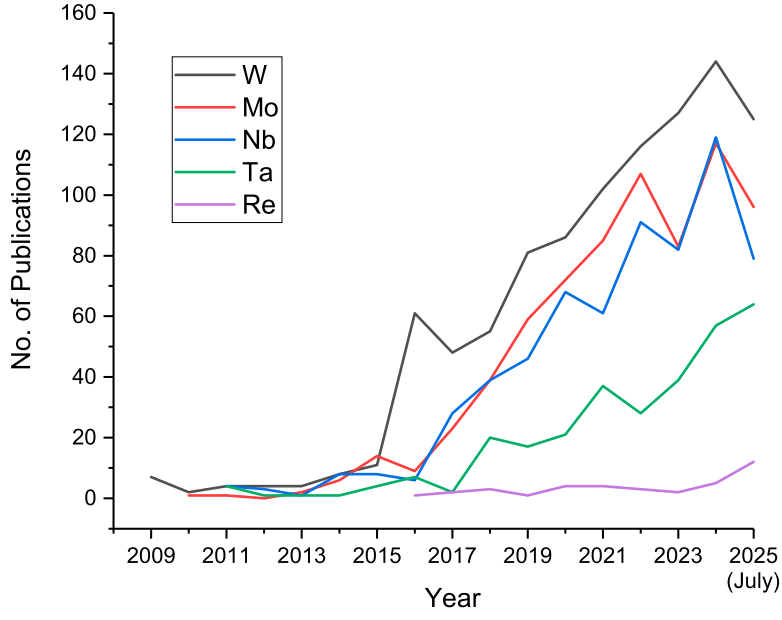

Figure 1. Year-wise number of publications in Scopus and Google Scholar databases for different refractory alloys fabricated by additive manufacturing processes [31].

potential to open a material and manufacturing renaissance era via additive manufacturing of RA and RHEA [41].

According to the American Society for Testing and Materials (ASTM) F42 Committee [42], AM processes can be classified into seven groups: powder bed fusion (PBF), directed energy deposition (DED), material extrusion, vat photo-polymerization, binder jetting, material jetting, and sheet lamination (SL). Among these, PBF and DED processes are considered the most suitable processes for the fabrication of refractory alloys due to the requirement for higher energy to melt these materials. These processes can be further classified according to the types of energy sources utilised (e.g. laser, electron beam, and arc) and feedstocks used (e.g. powder or wire), as illustrated in Figure 2. A detailed discussion of the AM processes employed to fabricate RAs will be provided in Section 3.

2.3. Data analytics

The design space (i.e. window map) of AM-RAs is vast and complex since it requires investigation of numerous process parameters (e.g. power, moving speed, layer thickness, interpass temperature, and feeding rate). Along with the increase in parameters, the required number of experiments for process optimisation grows exponentially, a phenomenon known as the 'curse of dimensionality.' Furthermore, any change in a process parameter can lead to significant variations in the corresponding microstructures, properties, and performance characteristics. Accordingly, establishing PSPP linkage can be very complicated due to the curse of dimensionality [44] in AM-RAs, as discussed in Section 1. In this context, it is hypothesised that the DA and its techniques can be the potential solution to tackle this challenge. DA can be categorised into four areas: (1) physics-based analysis, (2) data-driven analysis, (3) physics-informed data-driven analysis, and (4) its engagements with uncertainty analysis. In this paper, we categorised them into (1) Microscopic DA: predictive model and computational approach for understanding the underlying physics from the low-level perspective, and (2) Macroscopic DA: qualification and decision-support with uncertainty consideration from the high-level integrative perspective.

From the low-level perspective (unit mathematical model), the mathematical formulations and simulation encompass data-driven, physics-based, surrogate, and physics-informed data-driven models [45,46].

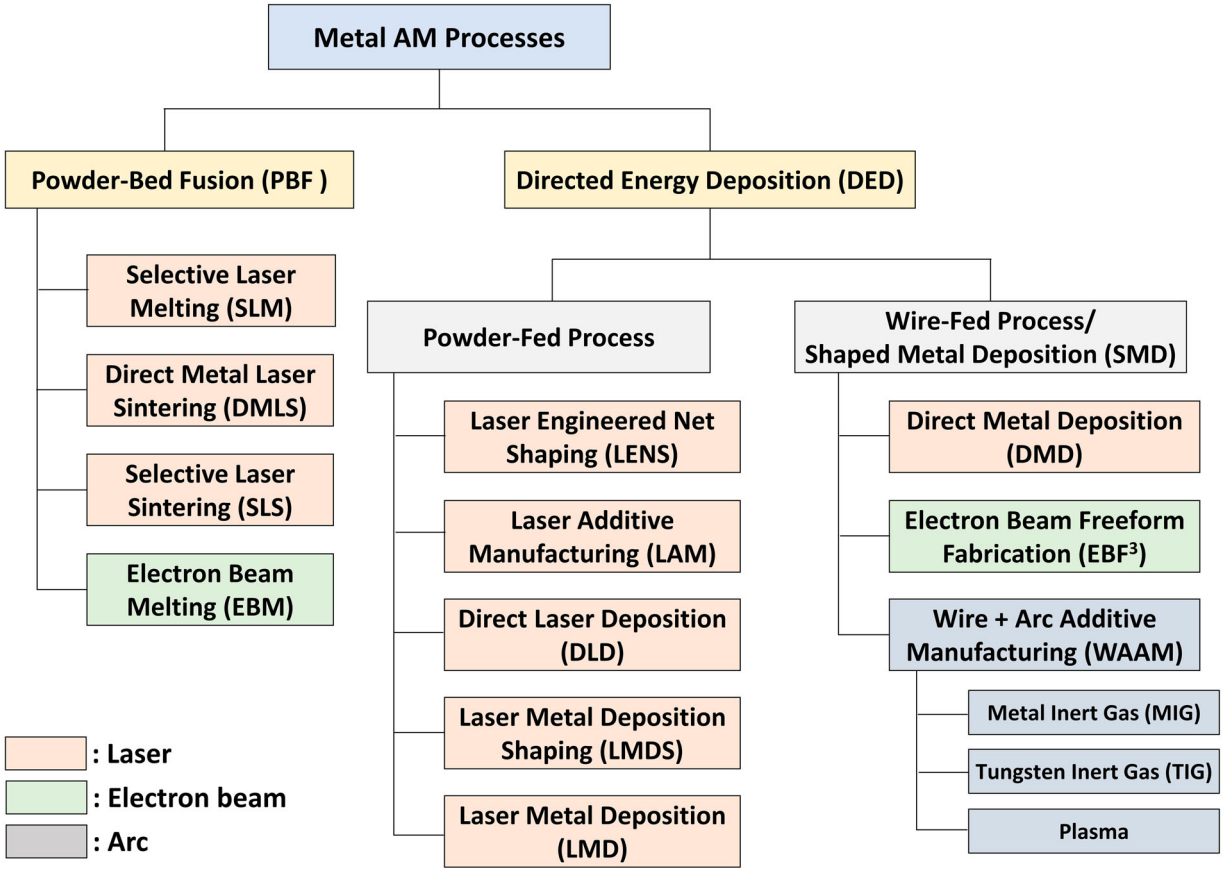

Figure 2. Classification of metal AM processes [43].

Nevertheless, the curse of dimensionality of AM [47] and an enormous compositional design space in RCCAs [48] limit the effectiveness of the design rule establishment through a data-driven approach (e.g. design of experiments (DoE) and ML). To overcome this issue, HTEM, one of the low-fidelity experimental methods for screening new alloys [49], can be cost-effectively utilised to establish the design rule [50]. In this regard, high-fidelity physics-based models such as computational fluid dynamics (CFD) can be implemented to study and understand the underlying physical phenomena during the fabrication process at different length scales. To overcome the high computational costs [51], surrogate models (e.g. response surface, artificial neural network, and kriging models) can be developed by reducing high-order models into low-order approximations [48]. Moreover, artificial intelligence (AI)/ML can be integrated with experimental results utilising big data analytics techniques [52]. In addition, dimension reduction schemes (e.g. principal component analysis (PCA)) can also be used to reduce dimensions in high-dimensional microstructures/properties [53]. However, implementing big data analytics of AM-RAs is challenging due to the requirement for expensive experiments. Perhaps the most appealing approach to utilise big data analytics in AM is a physics-informed data-driven approach [45].

Given the complexity of the processes, AM lends itself nicely to physics-based guidance. The accuracy and reliability of the physics-informed data-driven approach can be enhanced by integrating uncertainty quantification analysis [54]. A DA framework is necessary to provide (1) the unit mathematical model for the PSPP design establishment with uncertainty management and (2) the means to understand the mechanisms at the microscopic level. However, the foundational knowledge and investigation efforts are significantly lacking in this regard. For AM-RA, decisions are still made based on experience since neither the capabilities nor the resources are available to manage the conflicting and complicated problems. The details will be discussed in Section 4.

From a high-level perspective (top-down or systems engineering), DA can be viewed as performance assurance (PA), which includes quality assurance (QA), and encompasses approaches such as integrated computational materials engineering (ICME) [55]. The objective of ICME is to (1) select materials to satisfy requirements or develop new alloys, (2) determine and optimise manufacturing process conditions, and (3) fabricate the new alloy structures. The ultimate goal of PA is to satisfy conflicting requirements, e.g. the customer's requirements, the manufacturer's profit, and government regulations (e.g. air pollution), which are related to multi-criteria decision-making (MCDM) techniques. The QA enables us to ensure the predefined part properties before, during, and after the AM process while managing the process repeatability and product reproducibility [56]. These high-level DA approaches have several critical hurdles: (1) the high uncertainty and complexity, and (2) the inability to deal with multiple conflicting objectives. In short, decision-making is a complex problem due to the multiple conflicting objectives of stakeholders, making it considerably challenging to determine a near-optimal solution that satisfies all requirements and constraints. However, DA's foundational knowledge and integration efforts for AM-RAs' fabrications are significantly lacking. To accomplish these, a generalised framework will be required for managing heterogeneous, multiple conflicting objectives, uncertainty, and uncertainty propagation. The details will be discussed in Section 5.

2.4. Scope and contributions

Several review papers on additive manufacturing and/or refractory alloys and/or data analytics have recently been published. This paper aims to distinguish itself by providing a comprehensive, well-balanced, and concise review in terms of AM-RAs from the DA perspective. The current study distinguishes itself from the other reviews outlined in Table 2 by presenting a critical analysis of AM for RAs from a data analytics perspective, aiming to accelerate the development of materials beyond Nickel-based superalloys. While other reviews primarily focus on material systems [2,3,57–59] or general applications of ML in AM [60,61], the present study integrates the AM process within a comprehensive digital thread. Its innovative approach is rooted in addressing the fundamental complexity and data scarcity inherent to AM-RAs through advanced computational and analytic frameworks. The paper outlines future research directions centred on adopting physics-informed machine learning (PIML) and transfer learning (TL) to address the limitations of experimental data. Crucially, this paper stands out by investigating the integration of advanced concepts like Integrated Computational Materials Engineering (ICME), verification, validation, and uncertainty quantification (VV&UQ), and digital twin-driven rapid qualification for AM-RAs, providing a five-stage macroscopic view (design, process planning, fabrication, post-processing, and test/qualification) to achieve quality assurance.

There are several critical research questions (RQs) to utilise the benefits of the AM-RAs.

Table 2. Comparison of existing review papers and the present study.

Year, Ref.	Primary focus/Materials	Contribution/ Novelty	Role of data-driven approaches and ML
2025, [2]	RHEAs, RHE-Cs*, RHE-Ce*	Detailed coverage of synthesis methods and mechanical, corrosion, and radiation properties of RHE materials. Classifies the use of RHEA in composite materials (as matrix or reinforcement)	Secondary. Focuses primarily on materials science and experimental results
2022, [3]	AM of refractory metal W and W alloys	Technical analysis of crack suppression strategies: remelting, scanning strategies, substrate heating & effects of alloying elements	Minimal. Focuses on experimental optimisation of processing parameter windows
2022 [57]	AM of W, W-based alloys & composites	AM fundamentals as applied to W, including equations for dynamic viscosity, temperature profiles/cooling rates, and quantitative descriptions of scanning parameters	Identified as future opportunity. Suggests deep learning/ML could guide LPBF processes and clarify complex molten pool fluid dynamics
2022, [60]	ML, BDA*, and DfAM* for aerospace	ML/BDA/IoT and DfAM specifically in AM for the aerospace sector	Central for design, optimisation, monitoring, quality control, and improving the product lifecycle
2022 [61]	Application of ML for AM	Systematic review, including keyword co-occurrence and clustering analysis, to map research hotspots. Provides statistical insights into ML research in AM	Central. Reviews and classifies ML technologies across core AM domains, focusing on defect detection, monitoring, and process modelling
2022, [59]	AM of W and W-based alloys (e.g. W-Ta, W-Ni-Fe)	Summaries in tabular format of the wide range of experimental processing parameters used in literature and their empirical consequences on W printability	Implicit/Traditional Modelling. Focus is on synthesising existing experimental data to define usable process windows (printability maps)
2025, [58]	Mo-Re alloys, focusing on strengthening mechanisms, multi-scale simulations	Highlighting the 'rhenium effect' and discussing key research gaps (e.g. micro-mechanisms underlying peak ductility and hot-zone embrittlement in welding)	Secondary. Discussed within the framework of multi-scale computations, mentioning machine-learning potentials
This study	AM of RAs from a data analytics perspective	Integrated framework using ICME, VV&UQ, Predictive Analytics, and digital twin-driven rapid qualification methods. Also addresses advanced techniques like TL and PIML to overcome limited experimental data	Central. DA, ICME, PIML, TL, multi-fidelity modelling, and Verification, Validation, and Uncertainty Quantification (VV&UQ) are core themes

RHE-Cs: Refractory High-Entropy Composites, RHE-Ce: Refractory High-Entropy Ceramics, * BDA: Big Data Analytics, DfAM: Design for Manufacturing.

RQ1: What are the limitations, critical research issues, and technical challenges for AM-RAs?

RQ2: What are the DA techniques used to investigate multi-physics and multi-scale phenomena, as well as the defect formation? And what are the limitations of the existing DA techniques?

RQ3: What are the verification/validation and uncertainty quantification (VV&UQ) and performance assurance (PA) criteria in AM-RA?

RQ4: What are the design rule establishment approaches in AM-RA?

RQ5: What are the digital twin-driven qualification methods?

RQ6: What are the future research and development tasks for the AM-RAs?

We structured our review paper based on responses to these questions, as indicated in Figure 3. In Section 3, we review the current state-of-the-art in terms of AM-RAs, and in Section 4, we identify the current limitations and their critical research issues in design, process planning, fabrication, post-processing, and test/qualification from the microscopic DA perspective. Section 5 discusses VV&UQ, design rule establishment, ICME, PA, and digital twin-based qualification from the macroscopic DA perspective. We summarise the lessons learned from this review and identify future research directions in Section 6.

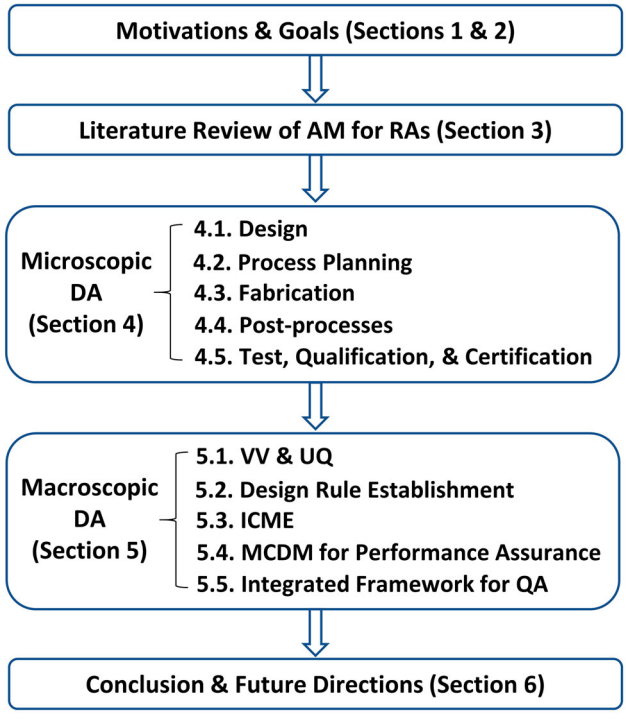

Figure 3. Structure and overview of this review and outlook of AM-RAs.

3. Literature review of AM for RAs

In this Section, the literature related to AM-RA of W, Mo, Nb, Re, and Ta will be discussed, and their microstructural

Table 3. Properties of AM Refractory metals and alloys.

		Process	Structure		Property/Performance		
	Material	Type	Phases	Grain size (μm)	Hardness (HV)	Tensile (T) Compressive (C) (MPa)	Reference
W-based	Pure W	EBM	–	66–100	–	120-282(T, 800 °C)	[68]
		LPBF	BCC	11.3-224.7	300–467	933–1036 (T)	[63,65,66,90–103]
		LDED	BCC	–	710	–	[104,105]
		EBM	–	224–427	366–380	–	[106]
		WAAM	–	–	–	–	[107]
	W-Ta	LPBF	BCC	5.18-6.43	454.28	1393 (C)	[108–113]
	W-Fe	LMD	BCC + Intermetallics	–	400–750	3200 (C)	[114]
	W-Mo	LPBF	BCC + W_2C/Mo_2C	–	–	–	[115]
	W-Nb	LPBF	–	–	11.7	–	[75]
		EBM	–	∼30	418–696	1892 (C)	[116]
	W-Ni	LPBF	–	–	300–355	–	[117]
		LMD	–	–	–	420–580 (T)	[118]
	W-Ni-Fe	LPBF	BCC + FCC	–	555 MPa	839–1198 (T)	[71,119–121]
		LDED	BCC + FCC	23.8-25.5	5.7-6.0 GPa	872–1037 (T)	[72,119,122]
	W-Ni-Cu	LPBF	BCC + FCC	–	330–410	–	[123]
	W-Oxides (Y_2O_3)	LPBF	–	–	462.5	–	[67,124]
	W-Carbides (TaC, TiC, ZrC)	LPBF	W + W_2C	2.5-15	670–810	–	[73,125,126]
Mo Based	Pure Mo	LPBF	–	–	–	350 (C)	[76]
		LPBF	–	–	∼212	∼340 (T)	[77]
		PBS	–	–	–	400 (C)	[127]
		LBPF	–	–	–	∼1000 (C)	[79]
		EBPBF	BCC	–	–	–	[80]
		LPFS	–	–	340	–	[44]
	Mo + C	LPBF	α Mo + HCP Mo_2C	10∼20	350	–	[128,129]
		LPBF	α Mo + HCP Mo_2C	13.4	–	–	[130]
	Mo + TiC	EPBS	α Mo + FCC (Ti)C + HCPMo_2C	–	–	–	[79]
	TZM	LPBF	–	–	–	–	[131]
		LPBF	–	–	–	–	[81]
		WAAM	–	–	188∼194	192 (T)	[7,82]
		LPBF	BCC + FCC	1.5-4.8	–	–	[132]
		LPFS	–	–	–	–	[74,133,134]
	Mo-8.5Si-5.6B	LPBF	α Mo + Mo_5SiB_2 + Mo_5Si_3	–	815	–	[135]
	Mo-16.5Si-7.5B	LPBF	α Mo + Mo_3Si + Mo_5SiB_2	–	–	–	[83,84,136]
	Mo-6.7Si-13.3B-5Ti-5C	EBM	α Mo + Mo_5SiB_2 + TiC	–	1000∼1638	-	[137]
	Mo-5Si-10B-10Ti-10C	LPBF	α Mo + Mo_5SiB_2 + TiC	–	1100∼1300	-	[138]
		LPBF	–	–	–	180 (C)	[139]
	Mo – 47.5Re	PBS	–	–	–	1000 (C)	[78]
	W-2.5Ta, W-7.5Ta, W-15Ta	LPBF	BCC	–	420–470	1200–1500 (C)	[140]
Nb Based	Pure Nb	EPBF	BCC	∼250	-	135–141 (T)	[86]
		LPBF	–	70	230–370	639 (T)	[85]
	Nb-W-Mo-Zr	EBM	BCC + Nb_2C, (Nb,Zr)C	–	–	–	[141]
		LPBF	BCC + ZrO_2+ Nb_2C + (Nb,Zr)C	–	–	679 (T)	[87]
	Nb-10Hf-1Ti	LPBF	-	28	–	595–674 (T) 627–674 (C)	[88]
Ta Based	Pure Ta	EBM	BCC	–	–	–	[142]
		LPBF	–	69–138	205–445	570–650 (T)	[89,143–150]
		LPFS	–	–	–	–	[151,152]
		LWPS	–	–	99–114	218–261 (T)	[153]
	Ta-Ti	LPBF	BCC + HCP	–	–	235–320 (T)	[154]

features (e.g. grain size, morphology, and phase), observed defects (e.g. cracks and porosity), and mechanical properties (e.g. hardness, tension, and compressive strength) will also be thoroughly reviewed. The corresponding information is summarised in Table 3.

3.1. Pure W and W-alloys

Various researchers have investigated AM for pure W since it is typically used in nuclear fusion reactors as a plasma-facing material. It requires better thermo-physico-chemical properties, including high melting points and great thermal conductivity [62]. However, AM for W is challenging, and researchers have reported porosity, cracks, oxidation, and heterogeneous microstructures in the deposited structures [3]. This may contribute to the high ductile-to-brittle transition temperature (DBTT) (∼200-400°C) and high residual stresses, leading to crack formation and propagation [63,64]. Cracks primarily nucleate at the tungsten oxides formed during the solidification process [65–67] and propagate along the high-angle grain boundaries [63,64].

To overcome cracking, Ledford et al. [68] preheated the powder up to about 1800°C before deposition and

successfully fabricated crack-free W components utilising electron beam melting (EBM). These samples showed mechanical strengths (282 MPa at 800°C) intermediate between those of cast and wrought materials. Ren et al. [69] were able to produce crack-free W samples using different scanning velocities to control the thermal gradient, thereby reducing residual stress formation. The substrate was preheated to temperatures of 1150 and 1500°C during the process. Moreover, Ren et al. [69] and Guo et al. [66] recently achieved the highest compressive strength of 1760 and 902 MPa for the pure W. To mitigate porosity, as studied by Dorow-Gerspach et al. [70] the substrate was preheated to 1000°C and high densification (relative density >99%) was achieved using a laser power of 170 W. The high preheat temperature presents a challenge because W has a very low recrystallization temperature.

To further improve printability and enhance properties, the impact of different alloying elements and secondary-phase particle combinations has been studied. The alloying elements, including Cu, Fe, Mo, Ni, Ta, and their combination, have relatively low melting points compared to W. Hence, they melt first and act as binders to connect the W powders. Chen et al. [71] and Wang et al. [72] prepared crack-free samples by applying W-7Ni-3Fe material using selective laser melting (SLM) and laser melting deposition (LMD), and the prepared samples showed mechanical properties of 1198 and 1037 MPa in tensile tests, respectively. In addition, it was reported that the addition of secondary-phase particles, especially ZrC [73] and Y_2O_3 [67], was shown to refine grain size and help inhibit cracking behaviour. Crack-free tungsten alloys, such as W-Cu [74], and W-Nb [75], were successfully deposited using the carefully selected process parameters (e.g. a scanning speed of 360 mm/s and volumetric energy density of 476 J/mm^3).

3.2. Pure Mo and Mo-alloys

The AM processing of pure Mo and Mo-based alloys has mainly focused on the fabrication of pure Mo, TZM (Mo-0.48Ti-0.09Zr-0.02C), and Mo-Si-B series alloys. In the case of pure Mo, most investigations have focused on the PBF, and the effect of high DBTT (~100°C) on crack generation was identified as a common challenge [76–78]. Furthermore, the manufacturing of pure Mo by wire-based EBM and arc melting was also studied. In the case of wire + arc additive manufacturing (WAAM), defects, including cracks and pores, were found and quantitatively and statistically analyzed through 3D computed tomography (CT) [79,80]. Various researchers have tried to mitigate these issues by minimising the thermal gradient through process optimisation, adding alloying elements, and carbide/oxide additives. Rock et al. [79] reported the fabrication of crack-free and dense pure Mo by electron beam PBF by raising the preheat temperature of the build plate to 1000~1200°C. In addition, using the PBF process, crack-free Mo-TiC MMCs were also fabricated from Mo + TiC powder, which was prepared via the mechanical alloying (MA) process. No cracks were formed during the AM processing of a TZM alloy by PBS, but the density was found to be relatively low (maximum 80%) [81].

When using WAAM to process TZM, micro-cracks were formed, and large grain sizes (compared to laser powder bed fusion (LPBF)) were found [7,82]. Oxide particles were dispersed in the inter-dendritic phase regions, resulting in grain refinement and fracture toughness enhancements. The Mo-Re series alloys have also been investigated as space propulsion materials for ultra-high temperature applications. The addition of 47.5 wt.% Re to Mo was shown to decrease the DBTT by about 250°C and significantly increase the mechanical strength [83,84]. The ultimate compressive strength was measured to be around 400 MPa in unalloyed Mo, while for Mo-47.5 Re, it was up to 1000 MPa, which the authors attributed to the solid solution strengthening effect.

3.3. Pure Nb and Nb-alloys

Nb alloys are mainly used in aviation components with a high BTF ratio, and research on alloys in practical use is being actively conducted to reduce component manufacturing costs. Using AM for pure Nb has led to crack-free deposited structures, a success which can be attributed to the intrinsic ductility characteristic of Nb at room temperature [85,86]. Liu et al. [85] deposited pure Nb with LPBF and investigated the effect of oxygen content on the mechanical properties. The results indicated that although a high oxygen content reduced the tensile elongation by about 90%, the ultimate tensile strength (UTS) (639 MPa) considerably improved when compared to previous studies. Chen et al. [87] prepared Nb521 (Nb–5W–2Mo–1Zr) parts using LPBF and found that the microstructure was composed of a Nb matrix containing fine, ~100 nm in size, Nb_2C, (Nb, Zr) C, and ZrO_2 precipitates. Due to the formation of nano-sized ZrO_2, the sample had a UTS of 679 MPa, indicating a higher strength than other AM-processed Nb. In addition, Awasthi et al. [88] prepared C103 (Nb-Hf-Ti) samples using LPBF and measured the oxygen

concentration. The results showed that the oxygen content (455 ppm) exceeded the ASTM B654/B654 M threshold by 255 ppm, which was attributed to the oxygen content (444 ppm) of the powder used.

3.4. Pure Re and Ta and their alloys

Since pure Ta has excellent corrosion resistance and biocompatibility, it is commonly used in medical implants. Research on porous structures with low elastic moduli and large surface areas has been actively conducted using powder-bed processes. In the study of Lian et al. [89], the mechanical properties of pure Ta manufactured by LPBF were assessed as a function of volumetric energy density (157-342 J/mm^3) and revealed that process conditions with lower volumetric energy densities resulted in an increase in mechanical properties due to the rise in grain boundary density.

3.5. Refractory medium/high entropy and RCCAs

Refractory alloys can be categorised into four broad classes based on their formation entropy and the number of individual alloying elements, namely refractory low, medium, and high entropy alloys, and refractory complex concentrated alloys. Among them, RHEAs achieve better stability due to their high entropy and absence of brittle intermetallic phases. As a result, they exhibit exceptional thermo-physicochemical properties that have attracted the AM community's attention. Compared to traditional methods (e.g. casting, powder metallurgy, and vacuum arc melting) for fabricating these alloys, AM has demonstrated superiority due to its advantages of higher precision, greater efficiency, and better accommodation for complex-shaped parts. Different AM processes have been employed to fabricate RHEA. Dobbelstein et al. [155,156] successfully prepared RHEAs TiZrNbHfTa and TiZrNbTa using a laser metal deposition (LMD) method. In other studies, using EBM, Zadorozhnyy et al. [157] and Katz-Demyanetz et al. [158] fabricated BCC-structured TiVZrNbTa and $Al_{0.5}CrMoNbTa_{0.5}$, respectively.

Studies have been conducted to control the concentration of Nb in the basic composition of $TiZrHfNb_x$ to significantly improve ductility by suppressing the 'ω' phase formation and subsequent embrittlement [159]. The RHEA WMoTaNb has been fabricated utilising different AM techniques such as DED, SLM, and selective

Table 4. Refractory medium and high entropy alloys, structures, and properties.

		Process	Structure				Property/ Performance		
Entropy	Material	Type	Phases	Grain size (μm)	Porosity	Crack	Hardness (HV)	Tensile (T) Compressive (C) (MPa)	References
RMEA	NbMoTa	LPBF	-	25	–	o	–	–	[162]
	NbMoTi	LPBF	FCC + BCC	41	×	×	445.84	–	[163]
	Nb-40Ti-20Ta	LPBF	BCC	12	o	o	217–337	1000 (C)	[164]
RHEA	WNiFeCo	LPBF	BCC + intermetallic	–	–	×	–	–	[71]
	WMoTaNb	LPFS	BCC	0–10	×	×	493	–	[39,165]
		LPBF	BCC	13.4	-	-	826	–	[161]
	WMoTaNbC	EBM	BCC	12.3	×	×	720	1200 (C)	[160]
	WMoTaNbV	LPBF	BCC	16.3	-	o	-	–	[166]
	W_XNbMoTa	LPFS	BCC	20	×	-	459.2-497.6	–	[167]
	WMoTaTi	LPBF	BCC + HCP	10	×	×		–	[168]
	WMoTaNbVFeCoCrNi	EBM	BCC + FCC + Laves	–	o	o	819–853	915 (C, 1200°C)	[169]
	NbMoTaTiNi	LPFS	BCC+γ	0.8-2.1	×	×	1000	–	[170]
	$NbMoTaTi_{0.5}Ni_{0.5}$	LPBF	-	10	×	×	-	2297 (C, 25°C) 651 (C, 1000°C)	[162]
	NbMoTaTi	LPBF	-	22	o	o	–	–	[162]
	NbMoTaNi	LPBF	-	8	o	o	–	–	[162]
	$Ni_5Cr_4WFe_9Ti$	LPBF	FCC	2	–	–	–	650–1000 (T)	[171]
		LPBF	FCC	0.3-1	×	×	-	960 (T)	[172]
	CoCrNbNiW	LPFS	BCC + FCC	75	–	–	515.4	–	[173]
	Co-26Cr-5Mo-5W	LPBF	FCC + HCP	–	×	×	-	–	[174]
	AlCoFeNiSmTiVZr	LPBF	FCC + IM	40–50	×	-	258~1080	–	[175]
	TiZrNbHfTa	LPFS	BCC	–	×	-	509	–	[155]
	TiZrHfNbx	LPFS	BCC, BCC+ω	162- 219.5	o	o	1000	–	[159]
	TiZrNbTa	LPFS	BCC	–	–	–	220~440	–	[156]
	TiNbCrVNiAl	LPFS	bcc+σ+Ti2Ni	1–35	–	–	400~1000	–	[176]
	TiVZrNbTa	EBM	BCC	1–3	–	–	–	–	[157]
	$Fe_{49}Cr_{18}Mo_7B_{16}C_4Nb_6$	WAAM	α-Fe matrix + particles	–	–	–	680~1000	–	[177]
	$AlMo_{0.5}NbTa_{0.5}TiZr$	LPFS	BCC + interdendritic HCP	–	–	–	–	–	[178]
	$Al_{0.5}CrMoNbTa_{0.5}$	EBM	BCC	–	–	–	–	–	[158]
	$CoCrMoNbTi_{0.4}$ + CNT	LPFS	BCC + HCP + TIC	–	–	-	1000	2000 (C)	[179]
RCCA	NbTaTiZr	LPFS	-	–	–	o	–	–	[180]
	MoNbTaVTiCu	LAM	BCC	–	o	×	–	–	[181]
	Nb–40Ti–20Ta	LPBF	BCC	11.14-12.04	o	×	217–227	2026 (C)	[164]

EBM [155,160,161]. In the study of Melia et al. [39], both WMoTaNb RHEAs and RCCAs were investigated by combining microscopy and high-throughput mechanical testing to vary the W, Ta, Nb, and Mo content, respectively. Since WMoTaNb RHEA prepared by SEBM exhibited severe cracking behaviour, Xiao et al. [160] investigated the WMoTaNbC RHEA, which contains 0.5 wt.% of graphite to suppress cracks. The effect of adding Ti, Ni, and $Ti_{0.5}Ni_{0.5}$ to the NbMoTa refractory medium entropy alloy (RMEA) was analyzed by Zhang et al. [162].

In NbMoTa, NbMoTaTi, and NbMoTaNi, both micro–macro cracks were formed, but in the case of the $NbMoTaTi_{0.5}Ni_{0.5}$ sample with both Ti and Ni added, formability was significantly improved by forming Ni_3Ta (Ti, Nb, Mo) with low stacking fault energy (SFE). According to the existing literature, most RHEA systems currently studied and developed are single-phase BCC solid-solution structures. A few alloys have two or more phase structures, as listed in Table 4. Three markers of '–', '×', and 'o' are used in the table, which indicate 'the study has not investigated', 'has not observed', and 'has observed' the corresponding characteristic, respectively.

3.6. Smart or functional materials

3.6.1. Shape memory alloys

Shape memory alloys (SMAs) have been used in a wide spectrum of applications (e.g. biomedical) due to their ability to recover large inelastic strains. Several groups of alloys exhibit shape memory behaviour, including copper-based alloys (e.g. Cu-Zn and Cu-Al), iron-based alloys (e.g. Fe-Mn-Si and Fe-Ni-C), and Ni-Ti systems (nitinol) [182]. RAs have extraordinary thermo-physicochemical properties, and combining them with elements that exhibit shape memory features can lead to numerous potential applications. Yi et al. [183] fabricated Ti-Nb SMA utilising vacuum arc melting and observed that mechanical properties improved as the Co content increased from 0.5 to 3.0 at.%.

Although AM is a promising approach to fabricating SMAs, limited investigations have been conducted in this regard [184]. Khimich et al. [185] fabricated porous and dense samples of low-modulus Ti-Nb alloy using laser AM. They observed uniaxial grains with identical microstructure features and phase compositions in both cases. The use of AM with shape memory alloys has been comprehensively reviewed in the study of Mehrpouya et al. [186]. HTEM can be a viable solution for developing and synthesising new SMAs based on refractory alloys since it can produce bulk structures of chosen compositions. This feature will be discussed in detail in Section 4.

3.6.2. Multi-materials

A key characteristic of Directed Energy Deposition (DED) is the capability to produce functionally graded materials (FGMs) and multi-material components by incorporating multiple feeding systems. When selectively depositing different materials within a single part, DED can enhance the part's functionality, reduce the number of required components, and simplify the assembly process [187]. Other metal AM processes, such as LPBF, have also been used to fabricate multi-materials. Functionally graded materials can enhance mechanical properties as well as the chemical resistance of a final part, thereby strengthening the part performance, as discussed in [188,189]. For example, bimetallic structures (BSs) have been employed in aerospace applications, and NASA reported using Inconel/GRCop84 BS in heat exchangers and channel-cooled nozzles [190].

For refractory alloys, the above issues are significantly amplified due to their exceptional thermo-physicochemical characteristics. For example, with the melting temperature of a refractory metal such as W ($T_m = 3422°C$) exceeding the vaporisation temperature of iron ($T_v = 2862°C$), traditional welding of steel to tungsten is infeasible. Table 5 shows the refractory alloy-based BS, which indicates several studies have been conducted. For instance, in the case of Cu-W bimetallic structure, Wei et al. [191] and Tan et al. [192] employed LPBF. The former used a stainless-steel (SS) interlayer, which causes good bonding due to the solid-state and grain boundary diffusion. In another study [193], bimetallic structures of Inconel 625 and W7Ni3Fe were manufactured using DED-based AM, as shown in Figure 4(a). Jadhav et al. [194] manufactured a defect-free BS of Ti6Al4V-NbZr1 by WAAM, as shown in Figure 4(b). They achieved a maximum UTS of 567 MPa, which is comparable to that of conventionally and additively manufactured NbZr1. In addition, an integral structure of a W-Cu composite and NbZr1 alloy was successfully fabricated in the study of Karim et al. [195] as shown in Figure 4(c).

As noted by Reichardt et al [196], fabricating FGMs and bimetallic additively-manufactured structures (BAMSs) has numerous challenges: (1) alloy compatibility and obtaining good metallurgical bonding between dissimilar alloys, (2) intermetallic formation and solubility limitations, (3) thermal property mismatch (e.g. different coefficients of thermal expansion (CTE)), and (4) difficulty in the measurement of residual stress/

Table 5. Refractory alloy-based BS.

AM process	Combination		Comments	Ref.
	Base	Alloying		
WAAM	W7Ni3Fe	Inconel 625	Defect-free BS of W7Ni3Fe-Inconel 625 by WAAM	[193]
	NbZr1	Ti6Al4V	Achieved the maximum ultimate tensile strength of 567 MPa	[194]
	NbZr1	W-Cu	An integral structure of W-Cu composite and NbZr1	[195]
	Ta	Mo-W	– A dense network of cracks at the interface of Ta-Mo – A sharp change in the microstructural evolution at the W-Mo interface	[40]
LPBF	W	CuA	Good bonding (solid-state, grain boundary diffusion) with SS interlayer	[191]
	W	Cu	Porosities and cracks at the interface	[192]
LMD	W7Ni3Fe	Inconel 718	– 100% improvement in thermal diffusivity and yield strength – 50% reduction in modulus of elasticity	[11]
	TA15	Ti2AlNb	Tensile strength of 909.27 MPa and elongation of 6.73%.	[197]
	TA15	Ti2AlNb	Tensile strength of 1025 MPa and elongation of 7.3%	[198]
	Ti2AlNb	γTiAl	From substrate, elastic modulus gradually increases from 105 to164 GPa	[199]
	Ti	Mo	From substrate yield (681–579), ultimate tensile (791–686 MPa) and elongation (10–25%).	[200]
	TiZrNbTa[a]		Increasing the Zr to Nb results in finer and harder multiphase microstructures.	[156]

[a]Compositionally graded.

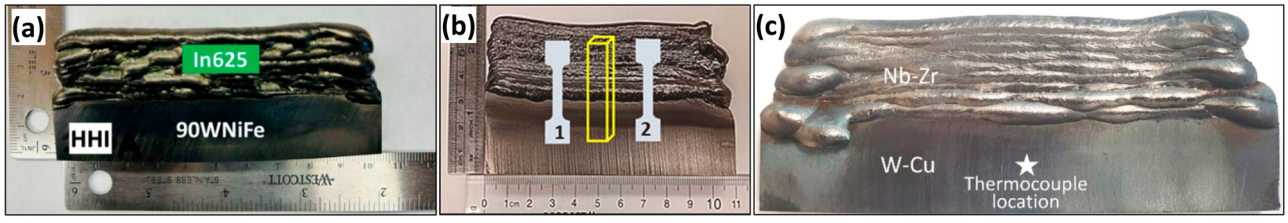

Figure 4. Bimetallic structures (a) Inconel 625-90WNiFe [193], (b) Ti6Al4V-NbZr1 [194], and (c) W-Cu-NbZr1 by WAAM [195].

strain at the interface due to limited gauge volume (which is approximately 1 mm while the intermetallic interface is in scale of hundred micrometers). Additionally, a lack of knowledge about weld-pool dynamics, intermetallic formation, and residual stress significantly complicates the process.

3.6.3. High-throughput experimental methods (HTEM)

Refractory alloys and RHEAs/RCCAs encompass vast compositional regions in which novel materials with interesting structural and functional properties may be discovered. However, this potential is accompanied by the challenge of effectively producing and screening these alloys. Conventional approaches based on casting, simulation, and experimental characterisation are too time-consuming to cover such a large compositional space. Thus, high-throughput synthesis offers a reduced-complexity solution for investigating a broad range of compositions in the material and analytics space. For instance, Dobbelstein et al. [201] performed a high-throughput synthesis of the Ti-Zr-Nb-Hf-Ta system using DED. They analyzed the compositionally graded variants of the RHEA and characterised the mechanical and microstructural properties. Moorehead et al. [202] combined high-throughput materials synthesis with characterisation and modelling techniques to fabricate arrays of high-entropy alloys in the Mo-Nb-Ta-W system utilising powder DED, as exhibited in Figure 5. Other researchers have also studied this approach for different alloy compositions, for example, CoCrFeMnNi and CoCrFeNiTi high-entropy alloys [203,204] and MoNbTaW and WMoVTaNbAl refractory high entropy alloys [39,205]. However, HTEM still requires a great number of experiments, which are time-consuming and cost-intensive. Moreover, in the case of the AM-RA, microstructural defects and poor mechanical properties (as detailed in Section 4.2) complicate their fabrication. To address these issues, the integration of high-throughput methods with ML [206,207] and CALculation of PHAse Diagrams (CALPHAD) [208] has been investigated.

3.7. Summary of the current state-of-the-art in AM of RAs

RAs inherently have several manufacturing issues, such as (1) rapid oxidation, (2) brittleness at room

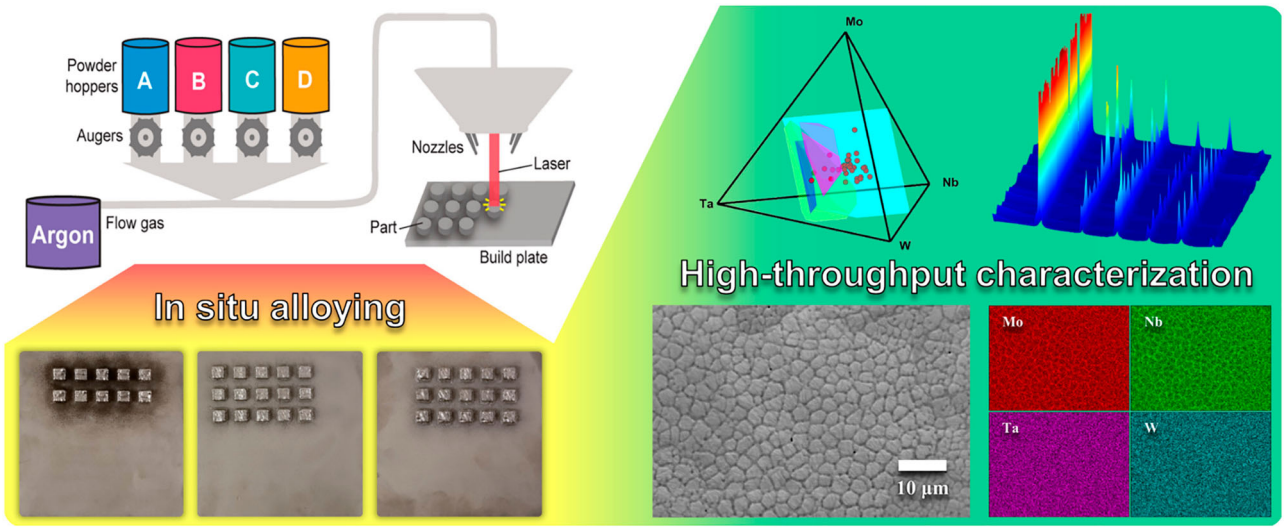

Figure 5. High-throughput synthesis of Mo-Nb-Ta-W high-entropy alloys via additive manufacturing [202].

temperature, and in some cases (3) phase instability [34,209]. AM components experience non-equilibrium thermal cycles and are characterised by inherent uncertainty and complexity. This section summarises the state-of-the-art studies on AM-RAs, and the following themes emerge:

- Many RAs are susceptible to rapid oxidation at elevated temperatures, which has hindered their broader application. To address this, various effective strategies have been developed to protect refractory alloys in high-temperature environments. The application of protective coatings and the incorporation of elements that favour the formation of protective oxide layers (e.g. Al, Cr, Ti, or Si) have been shown to be possible solutions.
- RAs typically have a BCC crystal structure, and their stress–strain behaviour strongly depends on temperature. In addition, since they have higher DBTT, mostly above room temperature, they exhibit brittleness at room temperature, and AM intensifies this behaviour.
- AM induces unwanted defects (e.g. pores, cracks, and micro-segregations) and microstructural heterogeneities, which makes the AM-RA processing challenging. Post-processing is required to remove these defects and improve mechanical properties, which will be discussed in Section 4.4.
- Residual stresses are developed in AM structures due to the thermal gradients caused by rapid cooling and heating and repeated phase transformations. In AM-RAs, residual stresses are a critical issue due to the significant difference between melting and preheat temperatures. Also, residual stresses are reported to affect the DBTT, a critical phenomenon of BCC materials.
- Refractory alloys have a stochastic nature, and this is intensified by the inherent complexities and uncertainties in AM, highlighting that process repeatability and part reproducibility can be a concern in AM-RAs. For example, fatigue and creep performance of AM-RA structures is highly dependent on the manufacturing parameters, refractory alloy elements, and process-induced defects. This trend magnifies the importance of VV&UQ for quality assurance.

The AM-RAs show great potential for high-temperature applications. The next section will discuss this topic from a data analytics perspective. Many research groups have investigated the manufacturability of RAs to determine near-optimal parameters for fabricating crack-free parts with high relative density and improved mechanical properties. In general, high residual stresses and DBTT have been shown to induce crack formation in AM-processed pure refractory metals, decreasing their mechanical properties and thermal conductivity. To address this issue, and advance manufacturability, recent studies focus on optimising AM process parameters and incorporating alloying elements to influence residual stresses and solidification behaviour.

4. Technical challenges and research opportunities from the data analytics perspective

The AM research for refractory alloy structures is still in its early stages, and advancements continue to face several challenges, as discussed in Section 3. First,

refractory alloys are considered rare and expensive materials. Thus, it is difficult for research groups with limited resources to engage in this area of research (e.g. AM systems and materials). Second, due to the unique thermo-physicochemical properties, RAs introduce significant complexity and uncertainty into their AM processing. For instance, due to the high melting point and thermal conductivity of W, it is challenging to deposit multi-layer components without defects. Third, the PSPP relationship has not yet been comprehensively investigated, and fundamental processing knowledge is significantly lacking. Currently, most AM processes for RAs depend on empirical knowledge and experience to determine the process parameters, often through Edison or DoE methods. Trial-and-error methods often fail to understand the AM processes for RAs comprehensively. Therefore, to ensure the required quality and performance of deposited RA structure, the relationships among PSPP should be characterised through mechanisms such as design rules [210]. DA techniques, such as modelling, simulation, and optimisation have been recognised as the key enablers for design rule establishment [211]. By integrating experimental and computational methods, meaningful data and predictive models can be developed, enabling an integrated framework to support better decision-making, which will be discussed in Section 5.

This section will discuss technical challenges and research opportunities in AM of RA structures from the DA perspective. Considering unique features (e.g. excessive residual stresses due to the high thermal gradient, complexity in compositional refractory elements, and a wide range of physiochemical properties in refractory elements), innovative and transformative approaches are required for the design and manufacturing of refractory alloys. Based on the AM digital thread concept [212], the subsections are organised into five stages: design, process planning, fabrication, post-processing, test, qualification, and certification.

4.1. Design

AM technologies provide significant design flexibility to fabricate complex components, customise products, minimise material waste, and develop customised products. The following sections will discuss two aspects of design in the AM processes: geometric design, which includes topology optimisation (TO) and generative design (GD), and alloy design. In addition, the applications of DA and ML in enhancing the design process will also be reviewed.

4.1.1. Geometric design

Geometric design, specifically Design for Additive Manufacturing (DfAM), is a practice aimed at encouraging designers to explore and create innovative design concepts optimised for additive manufacturing. Leveraging the unique capabilities of AM, its goals often include improving performance through unique design decisions or lowering the BTF, reducing structural weight without sacrificing performance, and minimising environmental impact [213–215]. These objectives are essential for refractory alloys that contain heavy elements (e.g. W, Ta, and Mo), resulting in high densities (e.g. 12.36 and 9.94 g/cm^3 for WNbMoTaV and TiZrHfNbTa, respectively). In addition, RAs are expensive and difficult to machine, which further complicates their fabrication. Therefore, DfAM methods (i.e. TO and GD) are required to address these challenges.

TO is an iterative approach implemented to optimise part design while preserving performance requirements and constraints [216]. The growing emphasis on sustainable mobility and higher energy efficiency has encouraged research into lightweight and ready-to-assemble parts by utilising the freeform fabrication capability in AM [217,218]. Research in employing TO for refractory alloys is relatively immature. Kumaran et al. [219] proposed TO for AM of (SS316L and AlSi10Mg) piston. They fabricated the sandwich structure by involving two different AM techniques: the PBF process (lower AlSi10Mg portion) and the DED process (an upper AlSi10Mg portion). Introducing extra AM-related constraints, such as support structures/overhangs, minimum printable features, anisotropic material properties, and thermal strain/stress into TO results in more complex boundary conditions. Consequently, TO methods face additional challenges in identifying the optimal solution using an efficient and fast-converging simulation process [220,221]. In addition, TO requires iterative simulations, creating challenges when adopting current thermo-mechanical simulations to perform multiple iterations for TO. The more commonly used inherent strain-based approach has limitations in accounting for dynamically changing strains caused by phase transformations, geometry-heat source interactions, and complex geometries. Consequently, such approaches rely on qualitative optimisation rather than quantitative optimisation due to a lack of accuracy in predicting distortion and residual stress. An example of related research conducted by Mishra et al. [222] emphasises using TO for controlling a heat history during the deposition process to obtain desired mechanical properties, as shown in Figure 6.

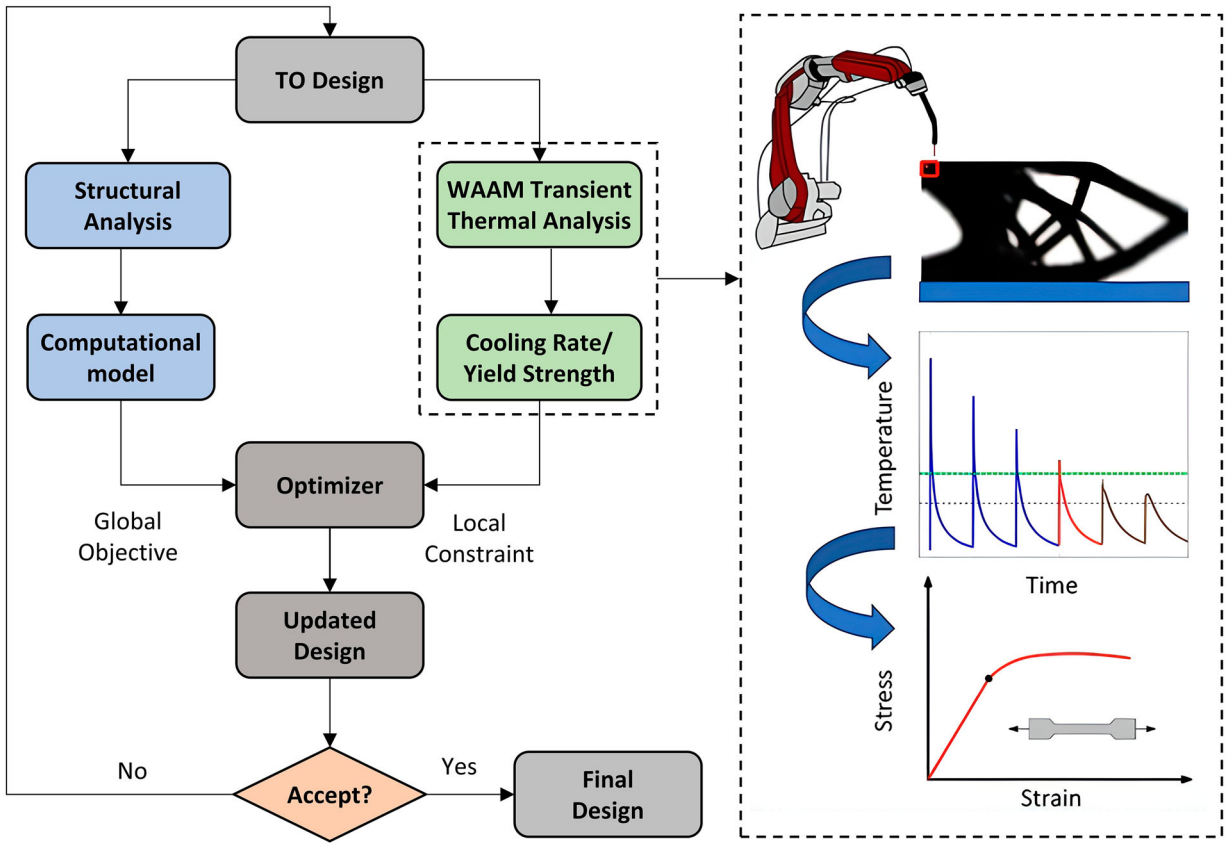

Figure 6. Design for material properties of additively manufactured metals using topology optimisation [222].

GD is an increasingly popular approach that can create potential solutions for designers by exploring the design space using rule-based or algorithm-based systems. Although TO be a common practice in industry, the advent of GD may allow for further critical refinement of parts while maintaining the required functionality. In addition, the advantages of GD are enhanced when combined with AM, which allows for material savings and improves part performance [223].

Researchers have recently integrated TO with GD approaches, such as generative adversarial networks (GANs), and proposed a new concept, deep generative design, which derives the learning capability from the iteration process and existing design datasets [224]. Li et al. [225] proposed generative adversarial network-based topology optimisation for the design of 2D microstructures with extreme material properties. In addition, Venugopal et al. [226] investigated structural and thermal generative design using a reinforcement learning-based search strategy for AM. They proposed computationally efficient methods for exploring generative designs of structurally and thermally loaded parts with improved functional performance and additive manufacturability. These concepts strive to more effectively incorporate existing AM knowledge – such as design constraints, design rules, and manufacturability – into the GD process, enabling the exploration of more suitable AM design solutions. In the context of GD for AM-RAs, further research is needed to integrate AM-specific constraints and develop efficient decision-making tools that assist designers in defining optimisation criteria and categorising potential solutions.

Generative AI is increasingly recognised for its ability to produce a wide range of design alternatives, making it an important tool in the design field and reshaping traditional methodologies. This technology acts as a collaborator in the design process by generating novel and diverse design forms. Through ML and pattern recognition, generative AI analyzes large datasets of designs, which enables it to produce innovative solutions [227,228]. In addition, the human-in-the-loop concept has also been at the center of attention in different stages of the manufacturing processes, for a collaborative decision support [229,230]. In addition, Data-driven design frameworks are emerging, but are limited by the scarcity of high-quality, labelled datasets and the difficulty of capturing the interplay between geometry, process parameters, and final properties [231]. Digital metallurgy and tessellated design frameworks, supported by ML, are enabling the creation of functionally graded and compositionally complex geometries, but require further development in integrating

real-time feedback and multi-material compatibility [232,233].

4.1.2. Alloy design

The possible combinations of refractory alloys are almost infinite, and it is impossible to investigate all possible combinations with the limitations of resources. It is significantly challenging to deposit, test, and characterise the compositions and properties [234]. The vast compositional space of refractory alloys makes traditional trial-and-error alloy design inefficient. ML and high-throughput computational methods are now used to predict phase stability, mechanical properties, and corrosion resistance, enabling rapid screening and optimisation [235,236]. In addition, explainable ML models and multi-objective optimisation frameworks have successfully identified new high-performance alloys, but challenges remain in model interpretability, transferability to new alloy systems, and the integration of domain knowledge [237,238].

To characterise the PSPP, an efficient method for establishing new design rules is necessary. The motivation for innovating new alloys is based on the hypothesis of exceeding the performance limitations of pure metals or currently available alloys in engineering applications. The new alloys may be designed via efficient experimental methods (e.g. HTEM), as discussed in Section 3.6.3. However, HTEM still requires time-consuming and cost-intensive experiments. Moreover, microstructural defects and poor mechanical properties in AM-RA (for more details, see Section 4.2) complicate their fabrication. To address these issues, Liu et al. [239] performed a comparative study of predicting high entropy alloy phase fractions with traditional ML and deep neural networks using CALPHAD, as shown in Figure 7(a).

The CALPHAD-based software packages (e.g. Thermo-Calc [240]) have been developed to generate thermodynamic databases, solve for general phase equilibria, composition-dependent material properties, and generate phase diagrams [241]. Numerous research studies have been conducted using CALPHAD for alloy design. For instance, in a recent study, Singh et al. [242] validated thermal conductivity predictions on elemental solids, binary and ternary alloys, and RHEAs by comparing experimental results with thermodynamic simulations (e.g. CALPHAD). Additionally, the Thermo-Calc modules enable material-to-material calculations, allowing for the easy variation of the weight percent of specific materials within a system. For example, Ta, as an elemental addition, can act as an alloying or binding species to Re and W, forming metal carbides and metal oxides. To illustrate these phases, the stable fundamental phases in a W-Re-Ta-C system are shown schematically in Figure 7(b) [243]. HTEM and CALPHAD, as well as their integration with other computational or ML approaches, have been shown to be efficient methods for characterising the PSPP relationship in AM-RA. Although the combination of HTEM and numerical simulations has not yet been widely applied to AM of refractory alloys, recent work [244] demonstrates how combinatorial synthesis, high-throughput characterisation, and computational modelling can be integrated to accelerate the discovery of new materials. Similar approaches could serve as a blueprint for future AM-RA studies, where systematic data generation and simulation feedback loops may overcome the challenges of data scarcity.

4.2. Process planning

AM process parameters significantly impact the generated microstructures, as well as the corresponding mechanical properties and part performance [245]. The

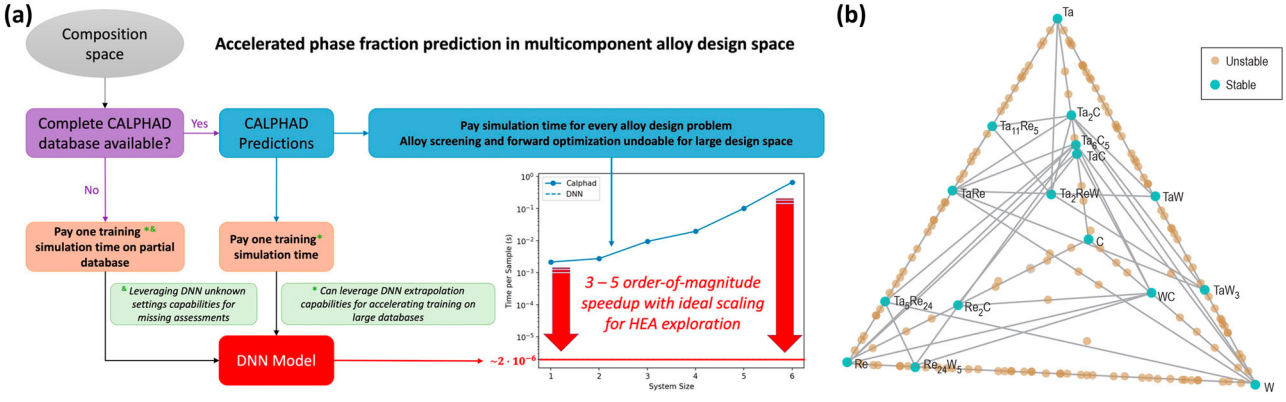

Figure 7. (a) Overview of the proposed CALPHAD surrogate pipeline [239], (b) the W-Re-Ta-C 4-species 'pyramid' of stable and unstable interactions using Thermo-Calc [243].

PSPP linkage, which may be considered design rules, must be established for the process planning. This process can be achieved through trial-and-error and DoE approaches, which are time-consuming and cost-intensive due to the curse of dimensionality and vast design space. To address these challenges, DA techniques must be employed to minimise the number of experiments and increase accuracy. Data analytics and ML are increasingly used for process parameter optimisation, melt pool modelling, and real-time process control [246–248]. In this section, we divided the process planning for PSPPs into four subsections: DA for process, structure, property, and performance. Each subsection explains the state-of-the-art research, identifies knowledge gaps, and addresses research issues, primarily from the DA perspective.

4.2.1. Process

In AM-RA, window maps can be generated to help identify optimal parameters that lead to required part quality (e.g. defect-free structures) [59]. For instance, in AM-RA, Ren et al. [103] investigated the impact of varying laser power and scanning speed on the surface morphology of W single tracks, as illustrated in Figure 8(a). Process parameters, such as interpass temperature, scanning paths, powder type, and layer thickness, are considered, adding dimensional complexity. In another study, Dong et al. [249] studied the hot deformation behaviour and processing maps of an equiatomic MoNbHfZrTi RHEA, as presented in Figure 8(b). In addition, Figure 8(c) shows the hot-processing map, where the contour indicates the power-dissipation factor, and the shaded portion represents the instability zone. Ivekovic et al. [102] further introduced the boundaries for three regions in the W–7Ni–3Fe alloy, highlighting the complexity of PSPP characterisation in refractory materials.

These window map studies, founded on data-driven/ experiment-based approaches, are costly to implement. Many researchers are instead focusing on employing computational approaches [250], including process modelling and simulation [251]. For instance, Doan [252] employed molecular dynamics (MD) simulations to investigate the mechanical behaviour and microstructure development of TaTiZrV RHEA during nanoindentation. The study indicated that the [111]-oriented substrate exhibits the highest average hardness due to the presence of a complex dislocation network. In a recent survey, Islam et al. [211] investigated an integrated experimental and computational methodology that can predict the mechanical properties of wire-arc DED refractory NbZr1 alloy. They performed a crystal plasticity (CP) simulation on the RVE of NbZr1, predicted the deformation behaviour and stress–strain curve, and explored the process-structure–property (PSP) relationship, as shown in Figure 9(a). Additionally, Vanani et al. [253] conducted an MD simulation to examine the microstructure and mechanical behaviour of Ti6Al4 V/NbZr1 bimetallic additively manufactured structures. In addition, Sharma et al. [254] developed a finite element (FE) based thermo-kinetic and thermo-mechanical computational model to simulate the process spanning from the melt pool scale to the component level for laser-based AM of pure W. Refractory high-entropy alloys are particularly difficult to process by AM processes due to their sensitivity to cracking and defects (e.g. unmelted powders and keyholes) as shown in Figure 9(b). Mooraj et al. [255] generated a normalised model-based processing diagram to identify the process window map. They achieved a nearly defect-free TiZrNbTa alloy via in-situ alloying of elemental powders during L-PBF.

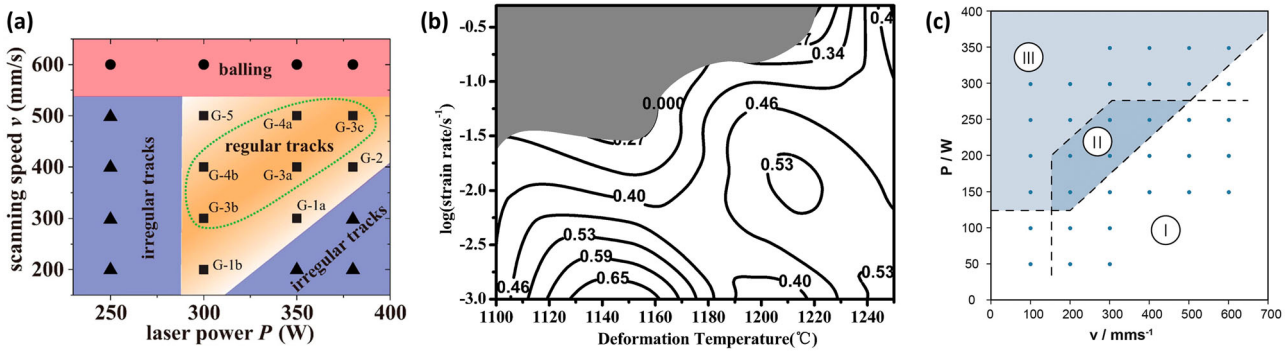

Figure 8. Processing map for (a) pure W manufactured by L-PBF [103], (b) MoNbHfZrTi RHEA (the grey part is the instability zone) [249], (c) and the boundaries for the different regions of W–7Ni–3Fe (I) low Ni content with cracks and warping, (II) Optimum region, and (III) lack of fusion with defects and a low density [102].

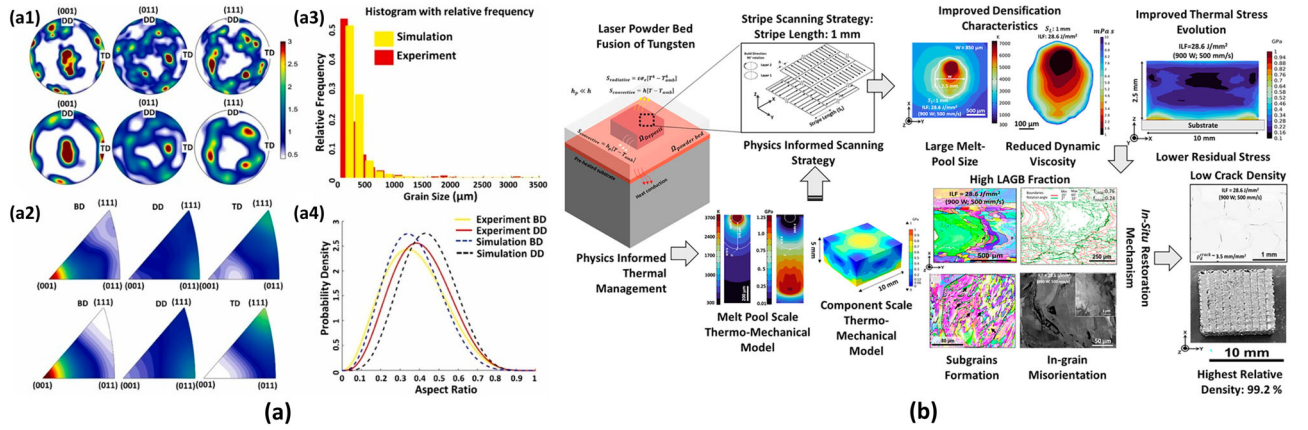

Figure 9. (a) Comparison of the grain morphology and texture between the experimental EBSD data and simulated RVE: (a1) pole figure, (a2) inverse pole figure, (a3) grain size distribution, and (a4) aspect ratio in WAAM NbZr1 [2]. (b) Laser-based additive manufacturing of tungsten: Multi-scale thermo-kinetic and thermo-mechanical computational model and experiments [28].

4.2.2. Structure

To gain a comprehensive understanding of the generated microstructure, DA approaches, particularly physics-based computational modelling methods, are perhaps the most insightful. Microstructure modelling approaches aim to link processing conditions with the resulting microscopic features of a material, including grain size, shape, and crystallographic texture. Various numerical methods, including Phase Field (PF), Cellular Automata (CA), and Potts Kinetic Monte Carlo (KMC), can be used to simulate processes such as solidification, solid-state phase transformations, recrystallization, and grain growth. These models differ in their resolution (micro – or mesoscale), computational expense, and the manner in which they incorporate fundamental physical principles. For example, PF models require careful calibration of material and model parameters, often relying on thermodynamic databases (like CALPHAD) and atomistic simulations [52].

On the other hand, the CA method uses a finite set of discrete spatial and temporal units or cells. Unlike PF and CA models that are based on fundamental physical mechanisms, the KMC method models grain evolution using a probabilistic approach. In this regard, DREAM.3D [211] and Neper [256] are commonly used software that utilise experimental information to generate 3D virtual microstructures. Figure 10 shows one example of the microstructure of the deformed additively manufactured TiZrHfNb RHEA along the horizontal direction [159].

4.2.3. Property

To perform computational modelling, temperature-dependent thermo-physicochemical properties, such as thermal conductivity, melting point, and density, among others, are necessary. However, acquiring the required properties for AM-RAs can be challenging, especially due to the lack of a universal database. A significant research opportunity exists regarding the prediction of microstructures in AM-RA components and their correlation with process variables, such as scan speed, input energy, cooling rate, and melt pool geometry. These links must be leveraged to control unwanted features such as heterogeneous microstructure, anisotropic mechanical properties, misorientations of grain boundaries, and other microstructural defects [257].

Several studies have been conducted to predict and measure the properties of additively manufactured refractory alloys. To better understand AM-RA properties relative to other processes, Mooraj et al. [255] investigated the additive manufacturing of defect-free TiZrNbTa refractory high-entropy alloy with enhanced elastic isotropy via in-situ alloying of elemental powders. Compared to its as-cast counterpart, the as-printed TiZrNbTa exhibits comparable mechanical properties with enhanced elastic isotropy. The result of this study is shown in Figure 11(a). In addition, Li et al. [235] recently manufactured and characterised novel Mo-NbW ternary alloys, using experimental observations to validate predictions from ML and CALPHAD. Their six as-cast alloys exhibit a single-phase BCC solid solution in agreement with CALPHAD studies. The predictions of hardness, based on the ULtrahigh TEmperature Refractory Alloys (ULTERA) database, were conducted by integrating the measured hardness results into the training dataset for the iteration of the surrogate model. The employed framework is shown in Figure 11(b). Although computational tools such as CALPHAD and ML provide powerful capabilities for exploring vast alloy design spaces, a clear gap persists between prediction and

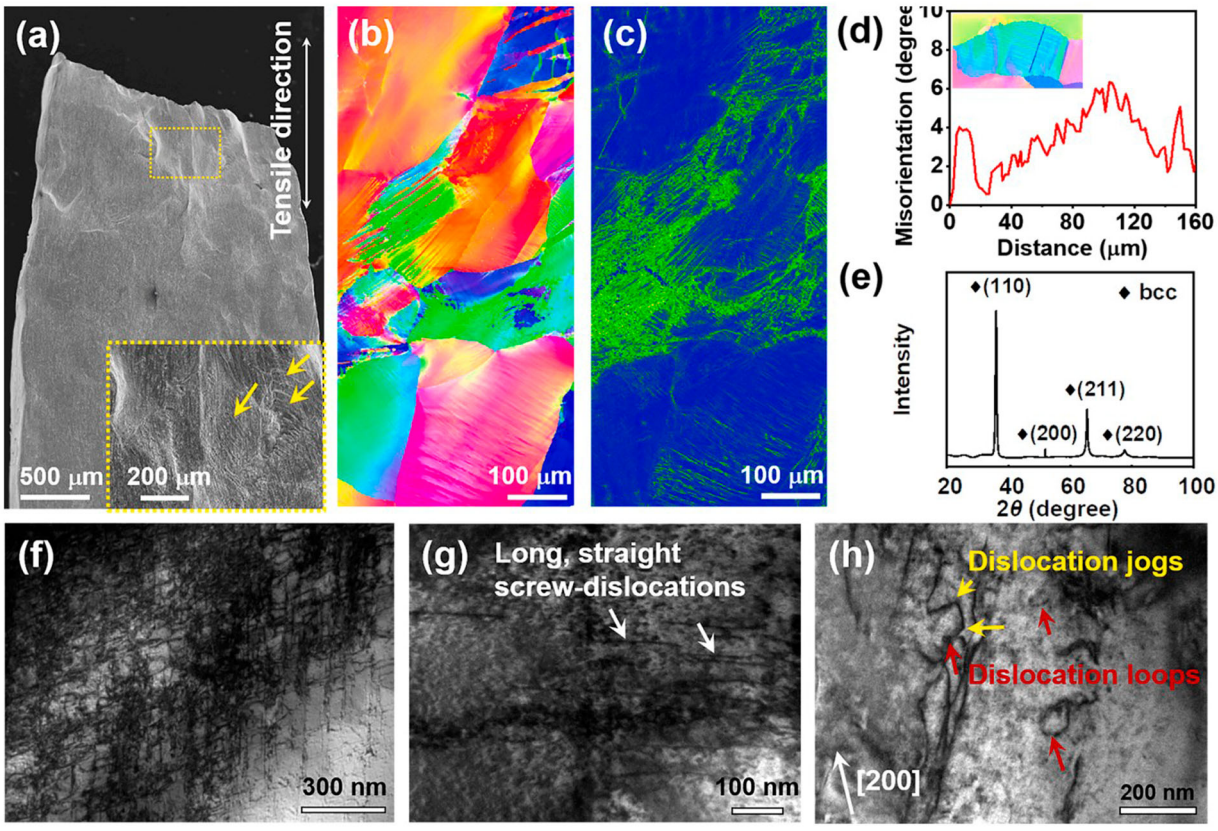

Figure 10. Microstructure of the deformed AM TiZrHfNb RHEA along the horizontal direction. (a) The lateral SEM image, (b) the EBSD inverse pole figure, and (c) the kernel average misorientation map. (d) The local misorientation variation, (e) XRD pattern near the fracture. TEM images near the fracture: (f) high-density dislocations, (g) long and straight dislocations, (h) dislocation jogs [159].

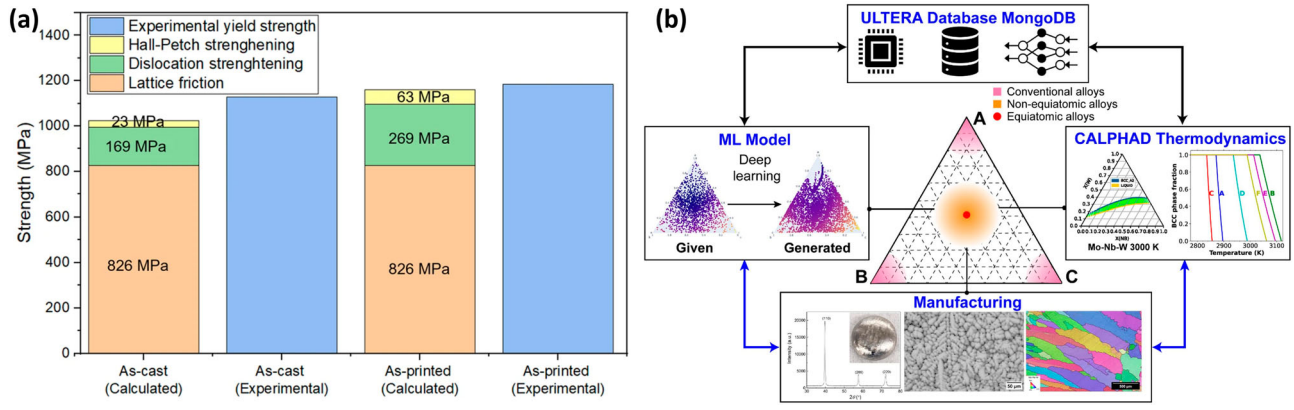

Figure 11. Properties of AM-RAs. (a) Comparison of experimentally measured and theoretically calculated yield strength in TiZrNbTa [255], (b) Iterative design loop incorporating ML, CALPHAD calculation, manufacturing, and a dynamic Database (ULTERA) for the Mo-Nb-W system [258].

experimental validation, particularly acute in AM of refractory alloys. For example, Li et al. [258] implemented an ML + CALPHAD framework for designing Mo–Nb–W alloys and validated hardness experimentally. Sheikh et al. [259] developed an integrated printability mapping framework that combines thermal, microstructural, and defect models, and then compared the predictions with actual AM data. Wen et al. [260] applied CALPHAD-driven strategies to mitigate cracking in Al-Mg-Si-Ti alloys during LPBF, thereby linking design intents to real-world outcomes. Bridging this divide demands well-designed experiments specifically aimed at verifying and correcting computational outputs for refractory alloy systems.

4.2.4. Performance

The performance assessment of AM-RAs is increasingly conducted using various mesoscale plasticity models and ML-based surrogate models, driven by advancements in high-performance computing (HPC) and the availability of robust ML toolkits. For example, the crystal plasticity framework within the finite element method (CPFEM) or the Fast Fourier Transform (CPFFT) approach enables predictions of elastic and plastic anisotropic mechanical behaviour of polycrystals based on the material's crystal structure. These microstructure-aware mesoscale approaches are particularly effective for AM materials due to their non-traditional, highly anisotropic microstructures. These models employ single-crystal constitutive models that account for grain-scale microstructures and defects, including grain morphology (size and shapes), crystallographic texture, and defects such as dislocations, secondary particles, and voids, all of which can significantly influence the mechanical properties of AM-RAs.

In addition, CP-based models incorporate key phenomenological deformation features, such as dislocation slip, deformation twinning, shear band formation, and damage evolution. These deformation mechanisms are critical for accurately simulating the complex behaviour of materials under various loading conditions. The software packages commonly used for CPFEM and CPFFT simulations include DAMASK [261], MOOSE [262], PRISMS [263], and ABAQUS [264]. Each of these tools offers unique capabilities, and the integration of these computationally expensive mesoscale modelling with ML surrogate models is actively pursued to achieve more refined and efficient assessments and optimizations of AM-RAs.

He et al. [265] implemented ML models to predict strength and fracture strain in RHEAs under compression, focusing on the Nb-Ta-Ti-V-W system. This approach has the potential to replace the traditional 'trial and error approach' for property prediction. Steingrimsson et al. [266] developed a physics-based ML

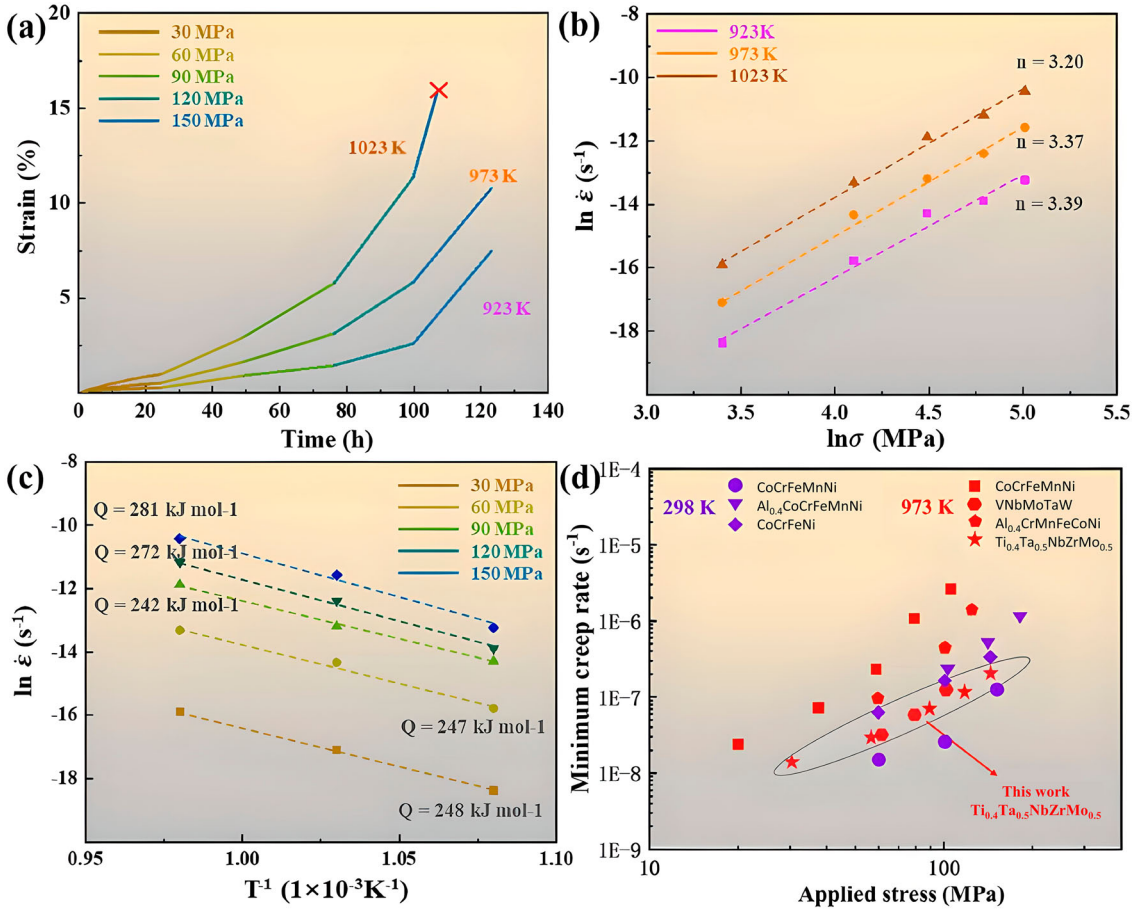

Figure 12. (a) Creep curves of $Ti_{1.5}Ta_{0.5}NbZrMo_{0.5}$ RHEA at different temperatures and stresses as well as creep rate versus strain, (b) Minimum creep rates versus applied stress from 973 K to 1073 K, (c) minimum creep rates versus the reciprocal of the absolute temperatures from 30 to 150 MPa, (d) Creep rate vs. stress for the $Ti_{1.5}Ta_{0.5}NbZrMo_{0.5}$ at 973 K in comparison with previously reported HEAs [267].

approach for modelling the temperature-dependent yield strengths of medium – or high-entropy alloys. In addition, Ren et al. [266] proposed a physics-guided neural network (PGNN) model to predict the fatigue life of multi-principal element alloys (MPEA). In another study, Feng et al. [267] studied the high-temperature creep mechanism of Ti-Ta-Nb-Mo-Zr refractory high-entropy alloys prepared by LPBF, as shown in Figure 12. Table 5 summarises the reviewed PSPP literature for additively manufactured refractory alloys.

Additionally, several recent studies demonstrate how data-driven workflows can be applied to address failure-related challenges in additive manufacturing. For example, Garg et al. [268] reviewed AI-enabled mechanical analysis of auxetic metamaterials, highlighting how machine learning can complement physics-based models to accelerate performance evaluation. Babu et al. [269] surveyed the integration of machine learning at different stages of the AM workflow, providing insights into how predictive analytics can enhance PSP understanding. More specifically, Lei et al. [270] proposed a multi-source data-driven ML framework for predicting fatigue crack paths in polycrystalline superalloys by combining synthetic, simulated, and in-situ experimental datasets, demonstrating how transfer learning can overcome data scarcity. It is worth noting that, since AM-RA parts remain a relatively new approach, systematic evaluations of such components under real service conditions are still scarce. Future research must extend PSPP studies beyond manufacturing and performance to encompass long-term service reliability (Table 6).

4.3. Fabrication

In AM, robust in-situ monitoring and control systems are desired to detect part imperfections and reduce the

Table 6. Reviewed PSPP literature for additively manufactured refractory alloys.

DA Tool	Material	AM	Process	Structure	Property	Performance	Ref
FE	W	L-PBF	Melt pool simulation Input laser influence	Grain morphology Crack	Thermal conductivity Young's module	–	[254]
CPFFT	NbZr1	WAAM	Build direction Deposition direction	Grain size distribution Deformation behaviour	Tensile strength Yield strength	–	[211]
CFD FEM	Mo	EBSM	Melt pool Temperature field	Phase transformation Porosity, voids	Surface roughness	–	[271]
CFD BPNN	Mo	PBF	Melt pool Spreading velocity	Balling Porosity	–	–	[272]
FEM	W	LM	Scan track thermal model	Crack network Morphology	DBTT Residual stress	–	[63]
CP	W	L-PBF	Temp. gradient Microstructure	Crack Dislocation behaviour Crystal orientation	Residual stress	–	[273]
CALPHAD PF	Ti-Nb	L-PBF	Process conditions Melt pool Thermal profile	Grain growth Segregation Solidification kinetics	–	–	[274]
CALPHAD	$Al_{0.5}CrMoNbTa_{0.5}$	EBM	–	Grain size Phase contents	–	–	[158]
CALPHAD	$Cr_{10}Mo_{25}Ta_{25}Ti1_5V_{25}$	VAM DED	Parameters optimisation	Phase formation	Compressive strength	–	[275]
RF GB	TiNbHfTaW CrNbHfTaW VNbHfTaW	SLM	–	–	Hardness Young's modulus Conductivity	–	[276]
GBT	TiZrNbTa	L-PBF	Process window	Anisotropy	Yield strength Tensile strength	–	[255]
GAN DL	RHEAs database [277]	LAM	–	–	Hardness	–	[278]
NSGA-II RF GBDT	Ti-Al-Nb-Zr	L-PBF	Process parameters	Porosity dilution	Microhardness		[248]
–	TiZrHfNb	LMD	Process window	Phase evolution Element distribution	Tensile strength Deformation	–	[159]
–	W	SLM	Process window	Density Surface morphology Pore, Crack	Compressive strength Fracture morphology	–	[103]
–	MoNbTaW	L-DED	–	Microstructure analysis Chemical composition	Hardness	–	[39]
–	TiZrNbTa	LMD	Melt pool size Pulse energy	In-situ alloying Texture Equiatomic composition	Microhardness	–	[156]
–	TiTaNbMoZr	L-PBF	–	Phase constituent Morphology evolution Strengthening Deformation		Creep	[267]
–	C103 Nb alloy	L-PBF	–	–	Tensile strength	Creep	[279]

uncertainty of part performance. Recent advances in AM offer the ability to minimise undesired defects such as balling, porosity, cracking, and other anomalies. However, research efforts on real-time monitoring and control of AM-RA face difficulties due to challenges in the acquisition of technically meaningful data and a lack of knowledge in AM-RA.

4.3.1. Real-time monitoring

To improve part quality, NIST reported the need to develop monitoring methods and a robust feedback control system [280]. In such systems, the first step is to acquire sufficient and reliable real-time data as feedback signals from the AM process. Since the interactions in the metal AM are highly complex, numerous processes and part signatures are required to be monitored. Process monitoring systems can help understand the deposition process, defect formation, and evolution, and ultimately ensure a high-quality final product. This can be achieved by utilising physically accurate signatures to link process parameters with part quality. These signatures can be 1D (e.g. voltage, current, height, and temperature), 2D (e.g. high-dynamic-range images and thermal images), or 3D (e.g. CMM) [281]. A few studies have been conducted on real-time monitoring of AM-RA. For instance, a study conducted by Kim et al. [282] presents a convolutional neural network (CNN)-based real-time monitoring algorithm to detect an abnormal WAAM process for Mo. The effectiveness of the CNN classifiers was validated by applying a class-activation mapping method. It was concluded that the CNN classifiers were adequately trained since they captured the critical regions in voltage images for both normal and abnormal cases. In addition, Cho et al. [283] employed a CNN to detect anomalies during the WAAM process for fabricating Mo alloys. The details of the procedure employed can be observed in Figure 13. Table 7 presents the various real-time monitoring methods and the types of data acquired for AM-RA. As the literature suggests, this area remains highly unexplored, and many approaches employed for different materials have not been applied to study refractory alloys.

4.3.2. In-situ control

After gathering and labelling process monitoring data, the subsequent step involves establishing a link between this data and observed defects or quality levels. Given the complex, nonlinear, and currently incomplete understanding of this relationship, ML provides a suitable and effective approach. Supervised CNNs are the most commonly used method due to their exceptional performance in image processing and speech recognition tasks [287]. Reinforcement learning can be used to optimise metal AM processes by adjusting parameters like power, speed, and layer thickness in real-time to mitigate defects and ensure quality [288]. In a study, Wasmer et al. [289] attempted to employ reinforcement learning methods for identifying melt pool behaviour under different energy inputs. In addition, Knaak et al. [290] suggested employing reinforcement learning to develop feedback control models and successfully showed that this method could optimise parameters during the process.

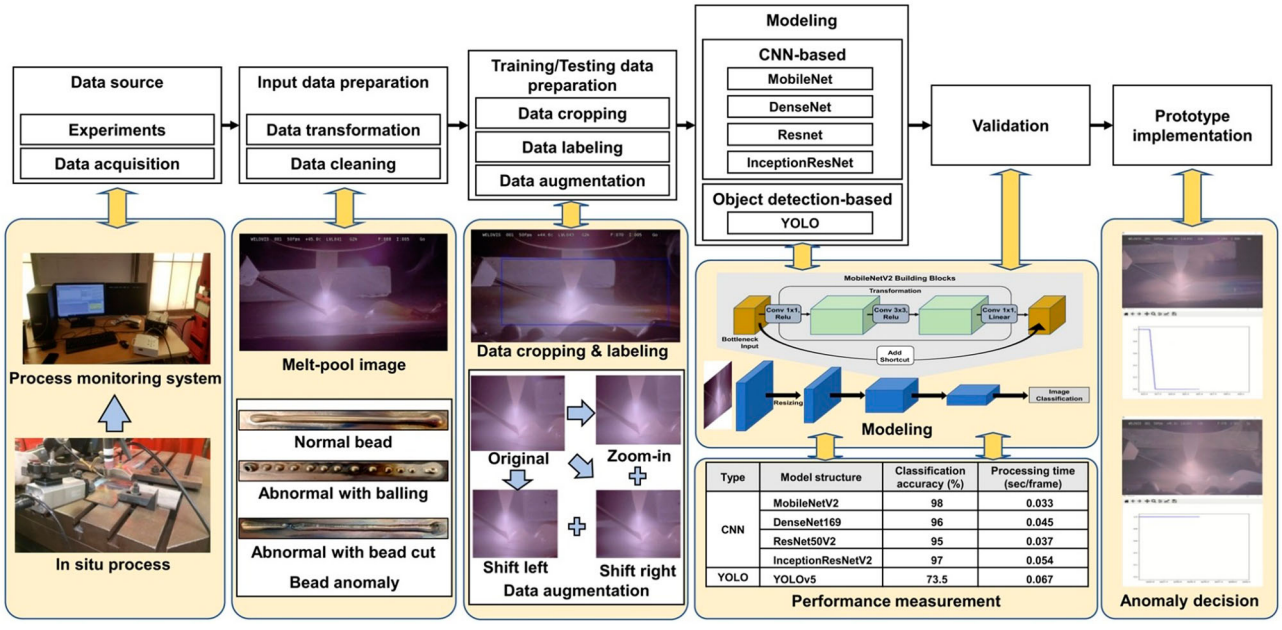

Figure 13. Procedural steps in the proposed method [283].

Table 7. Real-time monitoring methods for AM-RA.

Data Type	Objective	AM process	Material	DA Tool	Ref
Power	Defect Detection	WAAM	Mo	CNN	[282]
High-Speed IR Camera	Temperature maps	L-PBF	Nb-based alloy C103	Stefan-Boltzmann scaling	[284]
HDRI	Balling, Bead cut	WAAM	Mo	CNN	[283]
DXR (with high-speed IR)	Solidification analysis, Melt pool morphology	L-PBF	$Ti_{0.4}Zr_{0.4}Nb_{0.1}Ta_{0.1}$ $Ti_{0.486}V_{0.375}Cr_{0.111}Ta_{0.028}$	CALPHAD (ThermoCalc and TCHEA4 database)	[285]
Synchrotron X-ray	In-situ alloying observation, Melt flow dynamics	L-DED	MoNbTiV	–	[286]
IR Imaging					
CMM	Geometry	–	–	–	–
Pyrometer	Defect Detection	–	–	–	–
Acoustic Emissions	Overheating, Cracking	–	–	–	–
Ultrasonic	Porosity, Balling	–	–	–	–

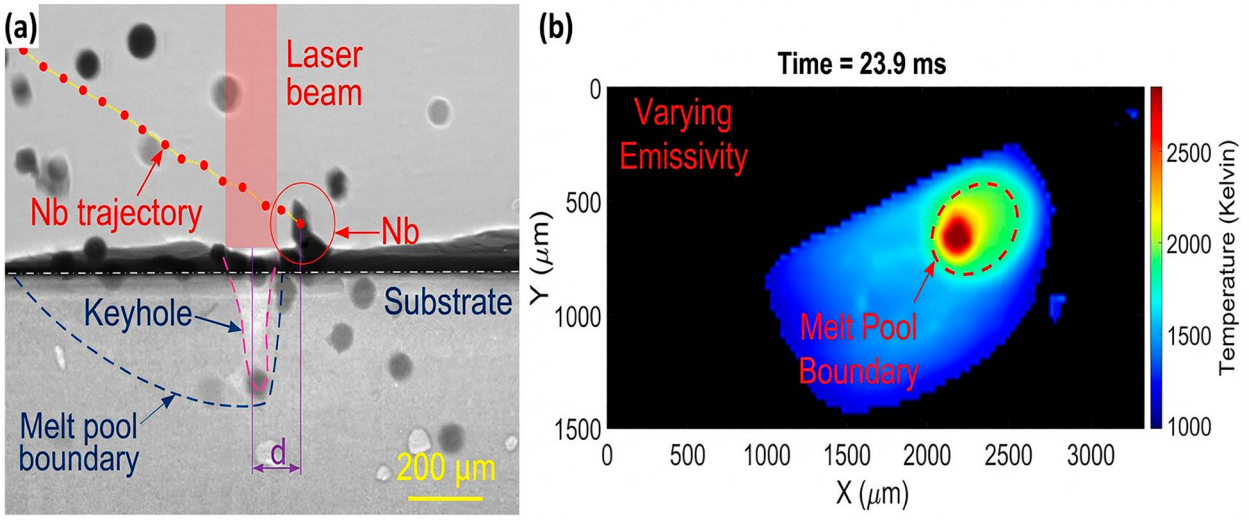

Figure 14. (a) A representative X-ray image of laser-matter interactions, (b) melt pool boundary and temperature distribution at a specific time frame during the deposition process [286].

Another approach to achieve in-situ process control is to employ thermal or mechanical strategies [3,39]. They enable favourable characteristics, such as a refined microstructure, minimised porosity, reduced distortion/warpage, and a preferred stress state. Rolling can be either interpass rolling [291] (i.e. as a cold work after the deposition) or in-situ rolling [292] (i.e. as an immediate hot work above recrystallization temperature)., Wang et al. [286] studied the in-situ X-ray and thermal imaging to observe melt pool dynamics during alloying utilising laser-directed deposition, as shown in Figure 14. Table 8 shows the different thermal and mechanical

Table 8. In-situ control strategies used for non-refractory alloys that can be implemented for AM-RA.

Approach	Objective	AM Process	Material	Ref. (non-RA)
Rolling (in-situ, interpass)	Enhancing ductility and tensile microstructure refinement	WAAM	Inconel 718	[291,293]
Laser shock forging	Enhancing fatigue life, reducing residual stress	LMD	316L SS	[294]
Hot forging	Refining the microstructure, reducing process defect	LPBF	AlSi10Mg	[295]
Induction heating	Reduction in residual stress, microstructure refinement	SLM	Ni-superalloys	[296]
Magnetic field	Microstructure refinement, altering weave structure	LDED	TC 11[a]	[297]
In-situ shot peening	Microstructure refinement, improving mechanical properties	SLM	GH3230[b]	[298]
Ultrasonic impact peening	Grain refinement, recrystallization	WAAM	Ti-6Al-4V	[299]
Friction-stir processing	Enhancing mechanical properties, grain refinement	WAAM	Al-Zn-mg-cu	[300]
Electromagnetic stirring	Enhancing tensile strength, microhardness, and corrosion resistance	WAAM	Inconel625 – HSLA steel FGMs	[301]
Hot hammering	Repairing layers, enhancing mechanical properties	WAAM	Steel	[302]
Cryogenic cooling	Improving surface quality and integrity	LMD	Ti64	[303]

[a]Ti-based alloy.
[b]Ni-based superalloy.

strategies employed for in-situ control in the metal AM process. For AM-RA, our review indicates no in-situ control strategies have been employed so far; hence, there is a substantial research gap and potential for future studies in this area.

4.4. Post-processing

In AM-RAs, post-processing includes the removal of support material and enhancement of surface texture (e.g. shot peening and polishing), accuracy (e.g. machining), aesthetics (e.g. painting, priming, and polishing), and properties. Among these processes, heat treatment (HT), hot isostatic pressing (HIP), and subtractive processes will be further discussed.

4.4.1. Heat treatment and hot isostatic pressing (HIP)

HT and HIP are used to improve the part properties through (1) residual stress reduction, (2) porosity reduction, (3) generation of fine and uniform microstructure, and (4) increases in ductility. Studies have shown HIP with 1800°C, 4 hr., and 180 MPa can remove cracks in AMed tungsten [97]. Therefore, these post-processes should be available to optimise an RA material's properties [304]. Knowledge of HT and HIP for AM-RAs is significantly lacking due to the cost-intensive AM processing and the additional requirement of specialised post-processing equipment (e.g. furnaces). Therefore, to date, few studies have been conducted to explore this research area. For instance, Tanvir et al. [305] evaluated the effectiveness of hot isostatic pressing (HIP) in mitigating porosity in TZM-NbZr1 bimetallic structures fabricated via the WAAM process. Two distinct HIP conditions and a combined HIP and heat treatment (HT) were investigated. The pore area fraction decreased from 4 ± 0.05% in the as-built condition to 3.05 ± 0.02% and 1 ± 0.01% after treatment at (HIP1: 1200°C) and (HIP2: 1500°C), respectively. Porosity was further reduced to 0.01 ± 0.005% with HIP at 1800°C followed by HT, as shown in Figure 15. In another study by Qin et al. [306], the effects of HIP treatment (850°C/1350°C, 150 MPa, 4 h) on the microstructure and mechanical properties of LPBF Ta were investigated. After HIP, all the mechanical properties of LPBF Ta were significantly improved. The hardness, ultimate tensile strength, and elongation of Ta improved to 273 HV, 551 MPa, and 43.4%, with a relative increase of 40.72%, 16.24%, and 18.26%, respectively.

Recent work has shown that composition tuning, and process optimisation can effectively mitigate cracking and elemental segregation in complex concentrated alloys. For example, Song et al. [307] demonstrated that hot isostatic pressing combined with microalloying strategies improved both strength and ductility of LPBF-fabricated Al-Cr-Fe-Ni-V high-entropy alloys by promoting microcrack closure and precipitation strengthening. Similarly, Wang et al. [308] reported that in Haynes 230, nanoprecipitate transformations induced during HIP enabled effective crack inhibition and a transition in deformation mechanisms, thereby enhancing mechanical performance. These cases highlight that targeted alloy design and process adjustments provide a complementary path to addressing the inherent challenges of AM-fabricated refractory and high-entropy alloys.

As AM for RAs is relatively new, databases to support their analysis are currently lacking. Near-optimal HT/HIP conditions are difficult to determine with experiments because infinite combinations in RHEAs are possible, thus necessitating DA approaches to fill this gap. The CALPHAD analysis can be used to determine the near-optimal heat treatment and HIP conditions [309]. For example, to study precipitation kinetics during intrinsic

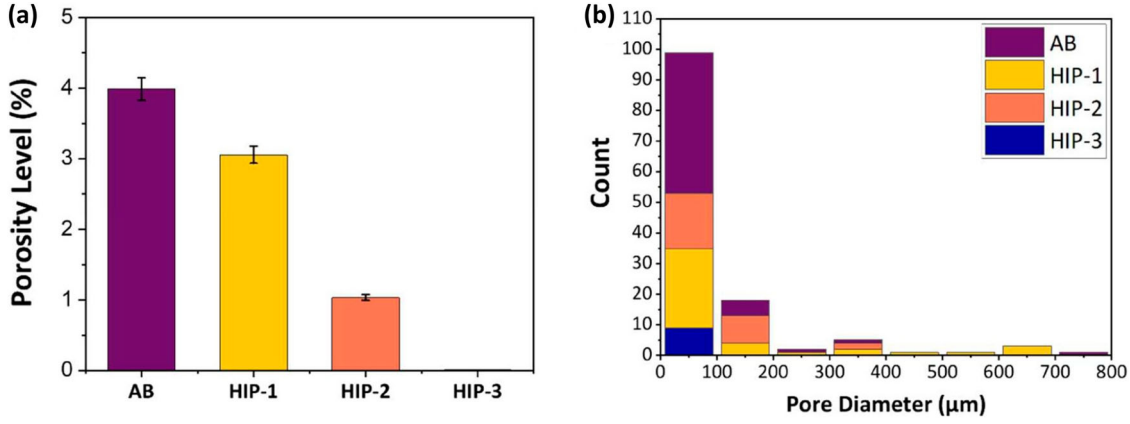

Figure 15. (a) Average pore area fraction (in %) of all conditions, indicating a porosity level in the cross-section of the TZM/NbZr1 bimetal interface (calculated using ImageJ software), and (b) Histogram of pore size (diameter) distribution at the interface before and after HIP treatments [305].

HT, a model alloy can be selected based on initial simulations using the TC Prisma precipitation module in ThermoCalc. Then, in-situ (e.g. Differential Scanning Calorimetry) and ex-situ (e.g. Atom Probe Tomography) measurements can be performed using linear time-temperature profile HT to capture the precipitation kinetics for simple time-temperature profiles [310]. A number of studies have employed Gleeble [311] and JMatPro [312] to extract thermo-mechanical properties. For instance, Huang et al. [313] studied the mechanical properties of $Al_5Mo_xNb_{36}Hf_{13}Ti_{46-x}$ at high temperatures, including 600, 700, and 800°C, using a Gleeble 3800 thermal simulation testing machine.

4.4.2. Subtractive process

Due to the process repeatability and part reproducibility issues [314], AM parts often need to be machined for geometrical accuracy and property enhancement/surface roughness. Typically, RAs are difficult to machine since they have low ductility and preserve high mechanical properties at elevated temperatures, which result in intensive tool wear, increased cutting force, chatter, and vibrations [315]. The DBTT in refractory alloys is usually above the room temperature (e.g. for tungsten, it is ~200-400°C) [3].

AM processes can cause an increase in DBTT in RAs, making their machining significantly more complicated. To address these difficulties, experimental and computational approaches have been employed. Experiment-based approaches include (1) optimising the machining parameters, (2) employing coolant systems, (3) optimising tool selection (e.g. polycrystalline diamond (PCD) tools), (4) utilising assisted machining (e.g. laser [316], ultrasonic [317], and vibration [318] assisted machining) and (5) adopting non-conventional methods (e.g. electro discharge machining (EDM), electrochemical machining (ECM) and abrasive water jet [319]). Computational modelling approaches such as finite element methods (FEM) [320] and crystal plasticity (CP) [321] can be used to simulate the machining by estimating the cutting forces and observing the impact of variations in process parameters (e.g. cutting velocity) and tool geometry (e.g. rake angle).

To the best of our knowledge, so far, there are very few studies focusing on the machining of AM-RAs [322]. Yang et al. [323] studied the cutting performance and chip characteristics of $WNbMoTaZr_{0.5}$ RHEA during machining with different feed rates and cutting speeds. Figure 16(a) shows the serrated chips formed during the deposition process. However, computational methods, including FEM and CPFEM, have been shown to be more accessible (Figure 16(b)) [324–326]. For instance, a FEM-based digital twin for difficult-to-machine materials [327] can be developed for RAs to predict tool wear, microstructural changes, and variables for machining process optimisation, such as cutting forces, temperature gradient, and metal chip formation. Coupling AM with material removal processes (e.g. milling and turning) has become common.

In most cases of adopting subtractive manufacturing for post-processing, computer numerical control (CNC) machining is integrated with DED, and the post-processing is achieved with milling and turning [328]. For precisely manufacturing complex parts or moulds (such as those with cooling channels), a viable approach is to use AM to create a near-net-shape part, followed by layer-by-layer milling. Studies using intermediate milling on each layer of maraging steel samples have shown improvements in surface quality, hardness, microstructure, and anisotropy [329]. Recently, the influence of distinct AM and subtractive manufacturing parameters has been analyzed for property improvement using experiments conducted on a fully integrated hybrid manufacturing process for non-refractory metals [330–332]. As the literature suggests, no studies have been conducted on hybrid manufacturing of AM-RA.

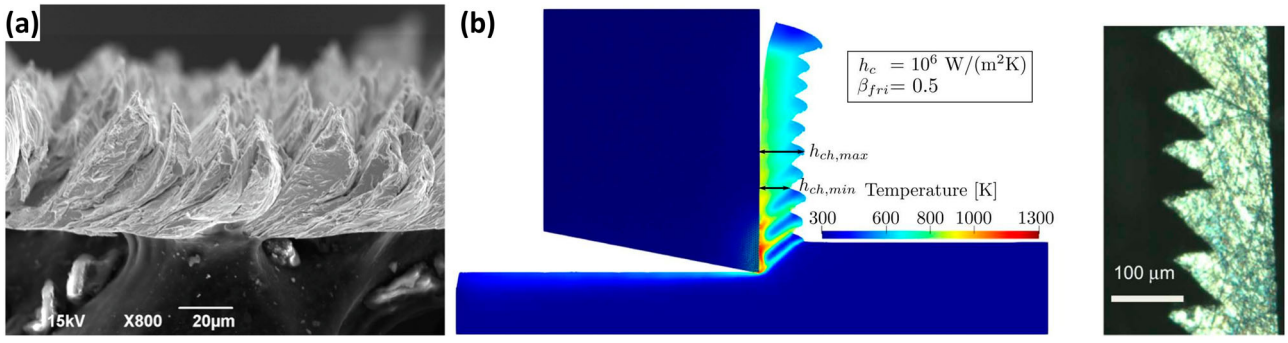

Figure 16. (a) Micrographs of serrated chip formation during machining of $WNbMoTaZr_{0.5}$ [323], (b) Comparison of simulated and experimental results for chip formation in Ti6V4 [326].

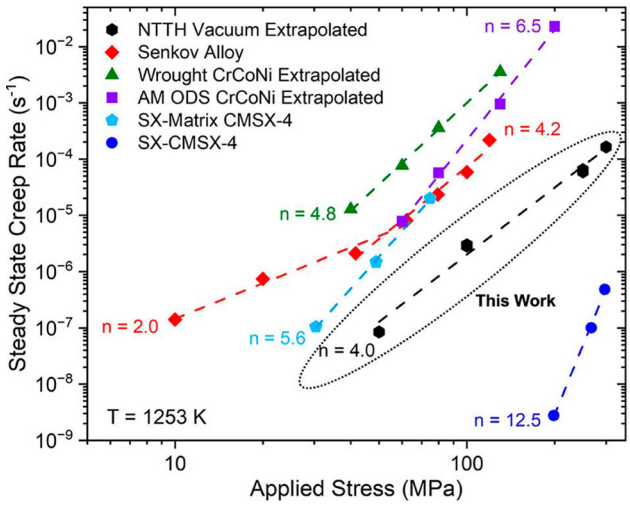

Figure 17. Comparison of steady-state creep rates among several different types of HEAs: BCC Nb45Ta25Ti15Hf15 (or NTTH investigated in [337]), TaNbHfZrTi (or the Senkov alloy [338]), wrought FCC CrCoNi [339], AM oxide dispersion strengthened (ODS) CrCoNi [340], a commercial single crystal FCC/L12 two-phase Ni-based superalloy CMSX-4, as well as the FCC matrix of CMSX-4 (also a concentrated solid solution) [341].

4.5. Test, qualification, and certification

Compared to the additively manufactured high-strength alloys (e.g. Inconel 625 and Ti-6Al-4V), RAs can be widely used in extremely harsh environments. Therefore, to maintain higher quality, detailed material characterisation and rigorous testing at extreme temperatures are required. Accordingly, different methods of test, qualification, and certification have been proposed, including geometric dimensioning and tolerancing [333,334], round-robin tests [335], materials characterisation in extreme environments, and non-destructive evaluation (NDE) techniques. This subsection will discuss the materials characterisation in extreme environments and with NDE.

4.5.1. Material characterisation at extreme environments

The material properties obtained through conventional characterisation approaches may not accurately represent the material's performance in extreme environments. For instance, at high temperatures, the effect of oxidation is likely to become much more prevalent. This highlights the importance of considering high-temperature oxidation behaviours, which directly influence the high-rate/high-pressure mechanical behaviour of materials. The stochastic nature of AM processes and the brittle behaviour of RAs present additional challenges, and large statistical datasets are required to describe the distribution of material failure modes. These challenges are compounded when considering extreme environments (e.g. the combined effect of temperature, corrosion, and pressure). For high-temperature tests, these challenges have limited the range of maximum test temperature to ~1500°C. For the cryogenic temperatures, these tests can be performed in a coolant such as liquid helium (~−260°C) or liquid nitrogen (~−190°C) [336]. In a recent study, the tensile creep behaviour of a vacuum arc-melted $Nb_{45}Ta_{25}Ti_{15}Hf_{15}$ refractory high entropy alloy was investigated over a constant true stress range of 50-300 MPa at a temperature of 900°C [337]. Figure 17 shows the comparison of creep rates for different RHEAs.

Because data in materials science is often scarce due to the expense of experiments and simulations, there should be greater emphasis on ML techniques that guide data acquisition. This includes methods such as active learning, Bayesian optimisation, bandit optimisation, and reinforcement learning, which utilise ML models in a closed loop to determine which experiments to conduct iteratively, simulations to perform, or expert queries to make. Active learning and Bayesian optimisation are becoming increasingly popular for designing experiments in materials science. Prior work in the past few years [342–346] has demonstrated that active learning and Bayesian optimisation hold great potential for efficient experimental design in extreme environments, offering substantial improvements over traditional approaches, such as factorial design. While rapid and accurate materials development and evaluation remain challenging, progress has been made toward AI-driven high-throughput methods that pave the way for accelerated materials development for combined extreme conditions. For materials designed for these extreme environments, the parameter space for composition, synthesis, and even characterisation is extremely complex and not well-suited to traditional reductionist methods [347]. This complex space necessitates rapid decision-making, which AI/ML methods can provide. Specifically, ML techniques that incorporate existing or hypothesised physical and chemical principles are expected to be highly effective in accelerating the development of materials for extreme conditions.

4.5.2. Non-destructive evaluation (NDE)

Non-destructive evaluation (NDE) methods such as X-ray computed tomography (CT) and micro-focus CT (μ-CT) are widely used for inspecting intricate AM parts (as demonstrated by NASA [348] and NIST [349]). These techniques are currently employed to identify porosity, cracks, and dimensional inaccuracies in AM components [350]. However, these methods have not been shown to be suitable for inspecting refractory metal parts because these

metals have high atomic numbers, resulting in high radiopacity. These properties lead to significant scatter, shallow penetration, and a poor signal-to-noise ratio, producing unusable images for defect detection. Furthermore, ultrasonic inspection is generally challenging to apply to AM parts due to their inherent surface roughness, requiring surface preparation for proper application. Therefore, the existing NDE methods still have several limitations. First, it is not a closed-loop control approach, indicating that real-time inspection during the AM process is not feasible. Second, most NDE methods focus on defect detection (e.g. porosity and cracks), but microstructures and mechanical properties are also important aspects and should be investigated for qualification.

Automating NDE can guarantee consistent and precise analysis of test results, including signals, data, images, and patterns. AI/ML methods show great promise for achieving automated and efficient evaluation of NDE data and test results. Recently, AI has been successfully integrated with various NDE applications [351]. For example, statistical ML techniques can predict defect characteristics by leveraging existing defect datasets, utilising their capability to estimate unknown values from training data [352]. Furthermore, the use of neural networks in NDE is a growing trend in material structural design and material performance. Specific examples of neural network implementation in NDE can be found in the study by Saleem et al. [353].

Leveraging NDE technologies for testing and qualification, particularly concerning refractory alloys, remains largely unexplored. NDE 4.0, which integrates advanced technologies and digital transformation into traditional NDE practices, is gradually becoming more prevalent. However, the future, referred to as NDE 5.0, is currently being shaped by the collaboration of humans and intelligent machines working together through real-time evaluation, computation, and communication. Currently, the digital twin concept [354] and digital twin-based qualification offer a potential near-term solution [355], particularly when used to monitor performance, enabling the determination of key remaining useful life (RUL) parameters of the physical twin. Other valuable applications of digital twins in NDE include early warning systems, anomaly detection, prediction, and optimisation, which will be discussed in detail in Section 5.5.

Beyond digital twin-assisted DE, recent developments in NDE for AM have introduced advanced approaches particularly relevant for refractory alloys, which pose unique inspection challenges due to their high atomic number and density. Wu et al. [356] highlighted the integration of machine learning and digital-twin-driven frameworks to improve the detection accuracy, data processing, and reliability of NDE in large and complex metal AM components. Complementarily, Yoon et al. [357] demonstrated the application of high-energy X-ray computed tomography and advanced ultrasonic imaging for tungsten-based alloys, emphasising the potential of hybrid multi-modal inspection systems to overcome signal attenuation and achieve sub-surface defect localisation. These emerging techniques demonstrate the increasing feasibility of intelligent, physics-aided NDE systems that integrate with digital twin environments for real-time quality assurance in AM-RA.

Studies have shown that using AI/ML techniques like CNNs can double the accuracy of defect detection and characterisation (such as sizing) compared to traditional methods [358]. These technological advancements will significantly transform the future of NDE and maintenance, repair, and overhaul operations across nearly all industries.

5. Integration from the data analytics perspective

This section describes the knowledge gaps and research issues from the top-down perspective, while Section 4 describes them from the bottom-up perspective. In the following section, VV&UQ, with a focus on AM-RA, will be discussed first. Then design rule establishment and the related efforts and challenges will be reviewed. Subsequently, ICME tools and their applications in design rule establishment and the PSPP relationship will be discussed. Finally, a multi-criteria decision-making and integration framework for quality assurance will be investigated.

5.1. VV&UQ

As with AM in general, AM-RA faces process repeatability and part reproducibility issues [314]. AM models and simulations (such as physics-based, data-driven, or physics-informed data-driven models) provide an attractive means to study the variabilities in the quantities of interest (QoIs) (such as geometric accuracy, porosity, residual stress, or strength), and to support process optimisation and control. AM is a complicated, multi-scale, multi-physics process; therefore, analytics approaches benefit from multiple models to describe the various aspects of the process [359,360]. Each of these models encompasses its own sources of uncertainty [361]. In addition, uncertainties inherent in the experimental setup, measurements, and data processing algorithms may introduce uncertainty in the prediction results of ML models developed using experimental data.

Therefore, to effectively improve AM processes (e.g. process design, process control, and resource allocation) using ML models, it is crucial to verify and validate these models, account for various sources of uncertainty (i.e. aleatory and epistemic), and continuously update them as real-time data becomes available. This subsection will discuss model verification and validation, review proposed approaches in the existing literature, and provide an in-depth explanation of uncertainty elements, including quantification, propagation, and management.

It is worth noting that, despite growing interest in developing quantitative PSPP linkages for AM-RA, rigorous validation frameworks remain largely underdeveloped. Recent advances in thermophysical modelling and UQ for refractory systems, such as those by Bowling et al. [362]on niobium alloys, have highlighted how uncertainty in thermal conductivity and elastic modulus measurements can reach up to 20%, influencing subsequent model calibration. Similarly, Nonato et al. [363] proposed a probabilistic UQ framework using Latin Hypercube Sampling to quantify the variability in mass and atomic radii in high-entropy alloys, demonstrating the sensitivity of phase prediction to small uncertainties in elemental composition. At a broader scale, Giles et al. [364] incorporated both aleatory and epistemic uncertainties into deep-learning models predicting yield strength and plasticity in refractory HEAs, emphasising that experimental variability often exceeds model uncertainty. Complementary efforts by Shargh et al. [240] and Li et al. [258] have begun bridging prediction and validation by integrating deep learning, CALPHAD, and experimental synthesis to verify microstructure and phase-formation predictions. These studies highlight that establishing multi-physics PSPP validation frameworks with embedded uncertainty quantification and propagation remains an essential, yet still largely unexplored, future direction for AM-RA.

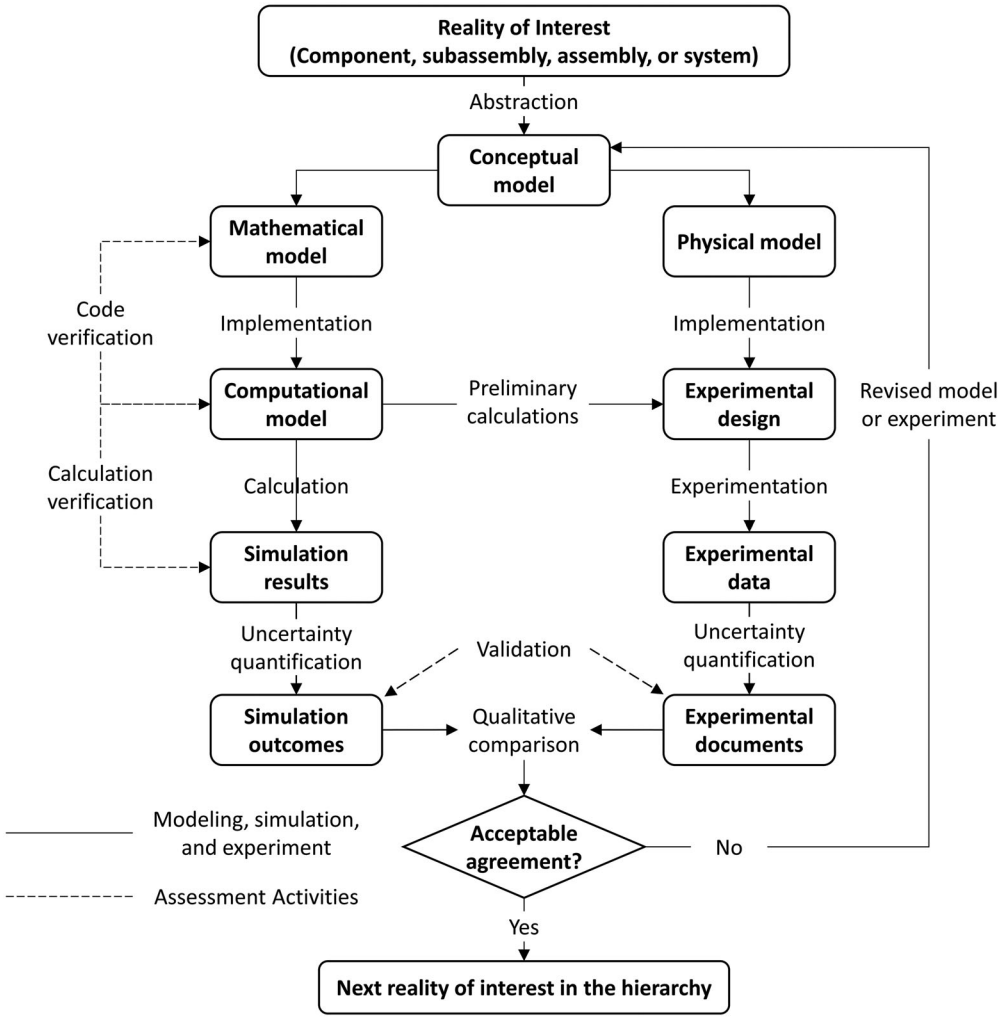

Figure 18. VV activities by ASME [367].

5.1.1. Model verification and validation

Verification is 'the process of determining that a model or simulation implementation and its associated data accurately represent the developer's conceptual and mathematical description and specifications' [365]. Validation is 'the process of determining the degree to which a model or a simulation is an accurate representation of the real world from the perspective of the intended uses of the model or the simulation' [360]. The V&V process is necessary to utilise any developed simulations and DA results for performance prediction of the process [366]. Figure 18 identifies the activities and products in a recommended V&V approach [367]. Two elements of verification are identified in this framework: code verification and calculation verification. More details can be found on [367].

Different researchers have explored the verification of physics-based computational models of AM-RA, such as the melt pool [368], solidification [369], and residual stress [211]; however, validation is significantly lacking in this regard. When the AM process model is used for decision-making, validation can be carried out at two stages: validation of (1) physics-based model prediction and (2) model-based process decisions. The former is performed by quantifying the difference between the model prediction and experimental observation [258], and the latter (e.g. process parameter optimisation) is done by conducting experiments at optimal and nonoptimal process parameter values [3]. In AM, experimental data is used to validate individual physics-based models, such as the melt pool model and solidification model. For instance, Wang et al. [273] developed a thermo-mechanical coupled dislocation density-based CP model and applied this model to investigate the evolution of temperature, stress, and dislocation behaviours in single crystal and polycrystalline W during AM. They also validated the mechanical model by predicting the yield stresses of single-crystal W at different temperatures and comparing them with the experimental data. Modelling and simulation of the AM-RA process is in its initial stage, and its V&V is yet to be thoroughly studied. To the best of our knowledge, no research has been published in this area.

5.1.2. Uncertainty quantification

UQ for AM-RA requires explicit identification and quantification of epistemic uncertainty (due to lack of knowledge) and aleatory uncertainty (due to natural variability). Epistemic uncertainty is subdivided into model uncertainty and data uncertainty [370–372]. The former is caused by uncertainty regarding the calibration of model parameters, model formulation, and solution approximation error. The latter can be due to sparse data (e.g. data generation and performing experiments are expensive for AM-RA), imprecise data (interval data), measurement error (e.g. it is very challenging to measure the peak temperature during AM of W), and qualitative data. Aleatory uncertainty mainly originates from equipment, process parameters, and inherent variability in material properties [360,373]. A detailed classification of uncertainty types, sources, and examples is listed in Table 9.

Current research on UQ in AM processes can be categorised as: (1) experimental UQ of AM, (2) UQ of melt pool models, and (3) UQ of solidification (microstructure) models. For (1) at the process level, AM experiments are repeated with varying process parameters. Statistical analysis (e.g. analysis of variance (ANOVA) and signal-to-noise ratio (SNR) [374]) is then employed to assess the impact of these parameters on product quality, using the resulting data. Because experimental data for AM-RA is limited and costly to obtain, efficient DoE [375] and sampling techniques (e.g. random, stratified,

Table 9. Uncertainty sources [370–372].

Uncertainty type		Sources		Examples
Epistemic	Model uncertainty	Model parameters	Measurement error	Conflicting data, human error
			Experiment data	Systematic error, random error, sensor error
		Model form	Model approximations	Truncation, numerical treatment, mathematical formulations
			Simplification	Dimension reduction, assumptions, model conceptualizations
			Subjectivity	Model preference, knowledge limitation
		Solution approximation	Surrogate model error	Model assumptions
			Numerical approx.	Iterative convergence, discretization errors, roundoff error
			Programming mistakes	Inefficient code
	Data uncertainty		Imprecise data	Sparse data, qualitative data, subjective data
			Sparse data	Inadequate experimentations
			Measurement error	Missing Data
Aleatory	Equipment		Measurement errors	Instrument calibration
	Process parameters		Input parameters	Powder particle radius, fluctuation of laser scan speed
			Boundary conditions	Interpass temperature, system excitation
	Material properties		Thermal properties	Diffusion coefficient, absorption coefficient
			Mechanical properties	Friction coefficient

and Poisson disk sampling) have only been partially explored [376].

Concerning potential AM-RA adaptations, notably, (2) UQ of the melt pool is crucial since its result can be used as input for other models. In this regard, Garg et al. [377] performed uncertainty and sensitivity analysis for the melt pool model to identify the most sensitive parameters. Anderson and Delplanque [378] implemented DAKOTA and ALE3D software to explore the UQ of the melting process. For (3) UQ of solidification, limited studies have been conducted due to the cost and time intensity of AM-RAs. For example, Ma et al. [379] used DoE and FE models to identify the critical variables in LPBF. Loughnane [380] developed a UQ framework for microstructure characterisation in AM, and Cai and Mahadevan [381] studied the effect of cooling rate on the microstructure and considered various sources of uncertainty during the solidification process. In terms of UQ explicitly for AM-RAs, to the best of our knowledge, no research has been carried out due to a lack of experimental data, which is challenging to acquire. Refractory alloys are more prone to specific uncertainties than other materials. To generate a simulation model of AM-RA, researchers must take simplified assumptions, which can induce uncertainties in the results.

5.1.3. Uncertainty propagation and aggregation

Quantifying uncertainty propagation (UP) in AM-RA is challenging due to (1) difficulties in data generation (i.e. epistemic) and (2) process variations (i.e. aleatory). Uncertainties are propagated and aggregated throughout the modelling process. Each step in a modelling approach (either data-driven, physics-based, or physics-informed data-driven) induces some uncertainty in the calculation. For example, in the CPFEM model generation, uncertainty is propagated from the first step (i.e. determination of process parameters) to the last (i.e. mechanical performance diagrams). In addition, Ye et al. [382] demonstrated the P-S-P surrogate linkages, i.e. multi-fidelity Gaussian process (MFGP), multi-output Gaussian process (MOGP), functional Gaussian process (FGP), involve models of GP and its variants that accompany uncertainties, as shown in Figure 19. The common approach for analyzing UP through a model is sampling (e.g. Monte Carlo sampling) [383]. Although sampling methods are conceptually simple, large datasets are needed, which is extremely challenging and time – and cost-intensive in the case of AM-RA. More advanced approaches for UP analysis that may be more suitable for AM-RA include polynomial chaos [384], stochastic collocation [385], response surface approximation methods [371], and Bayesian inference, along with a Taylor expansion [386].

In addition, modelling the complete AM process involves multiple levels. Lower-level model outputs (like those from powder bed or heat source models) feed into higher-level models (such as melting pool or solidification models). Because various parameters and model outputs are interconnected, understanding how uncertainty propagates from process and environmental parameters to the final quantities of interest (QoIs) requires multi-level UQ methods and uncertainty aggregation analysis. Besides this multi-level UQ, some analysis models may also involve coupling between different simulation models (for example, coupling between FE and CA models).

In a study conducted by Tapia et al. [387], UP analysis was performed on two different simulation models for LPBF: a reduced-order thermal model and a higher-fidelity finite element thermal model. A UP framework was generated based on generalised polynomial chaos expansion to quantify the uncertainty in melt pool predictions as a function of uncertainty in process parameters that are input to the models. The UP framework was employed to validate these models using experimental measurements obtained from the LPBF system. In another study, Kotha et al. [386] developed an uncertainty-quantified parametrically homogenised constitutive model (PHCM) for dual-phase titanium alloys (e.g. Ti6242S). They employed Bayesian inference and a Taylor-expansion-based UP method to quantify and propagate different uncertainties in PHCM, such as model reduction error, data sparsity error, and microstructural uncertainty. As the literature suggests, no studies have been conducted on the analysis of uncertainty propagation and aggregation of AM-RA, though the reviewed approaches appear adoptable.

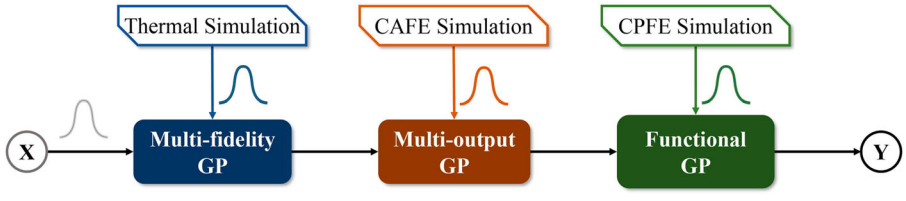

Figure 19. Uncertainty propagation through PSP surrogates [382].

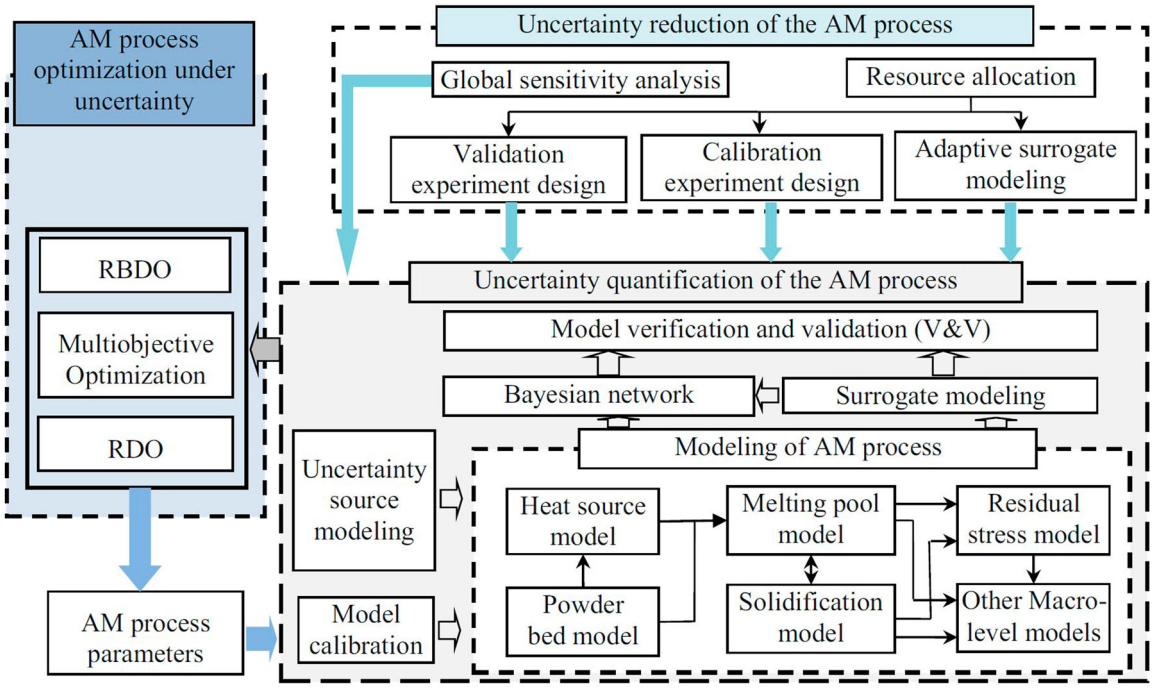

Figure 20. Overall UQ and UM frameworks for the AM process [372].

5.1.4. Uncertainty management

In uncertainty management, three issues need to be addressed: reducing the number of variables, reducing the uncertainty of AM models, and optimising the process parameters to reduce the effect of uncertainty sources, as shown in Figure 20 [372]. Dimensional reduction aims to omit the less important variable in AM by performing global sensitivity analysis (GSA), which ranks the contribution of each variable based on QoIs. For uncertainty reduction, adaptive surrogate models must be generated, and experimental designs must be collaborated to validate and verify the model [388]. For this, a physics-informed, data-driven approach with UQ is the viable solution. The details are discussed in Section 4.3. The final goal, which is AM-RA optimisation, can be pursued through reliability-based design optimisation (RBDO) or robust design optimisation (RDO). More details can be found in [24]. It will be discussed in more detail in Section 5.4, the multi-criteria decision-making (MCDM).

5.2. Design rules establishment

For the design rule establishment, including the establishment of PSPP relationships, DA techniques can be utilised at multi-scale, multi-stage, and multi-physics to understand and elucidate the AM-RAs. However, it remains significantly challenging to characterise relationships and establish the design rules with respect to the different AM processes, materials, and requirements due to the curse of dimensionality. In addition, the number of combinations of RAs is almost infinite, indicating that it is nearly impossible to investigate all possible combinations, especially in RHEA [21,50,257]. To address these issues, the following subsections will discuss transfer learning, ontological mapping, and a physics-informed ML approach.

5.2.1. Transfer learning

Utilising ML techniques, the relationships between process, structure, property, and performance can be elucidated [389]. Transfer learning (TL) is a promising group of approaches where the model of one product (source) may be reused for another product (target) with limited new target data [390], and it has been utilised to tackle the curse of dimensionality in AM [391]. The TL for AM studies is well-discussed in the study of Tang et al. [392]. In the following paragraphs, TL and its applications in AM will be discussed, and then its advantages in AM-RA will be introduced.

Mehta and Shao [393] used federated learning to train a laser powder bed fusion (LPBF) source defect detection model. Then they adapted it to the binder jetting process using rapid fine-tuning with just four images. While the resulting target model was adequate for defect detection, its accuracy was slightly lower than the original LPBF model. Regarding knowledge transfer between materials, Vigneashwara et al. [390]

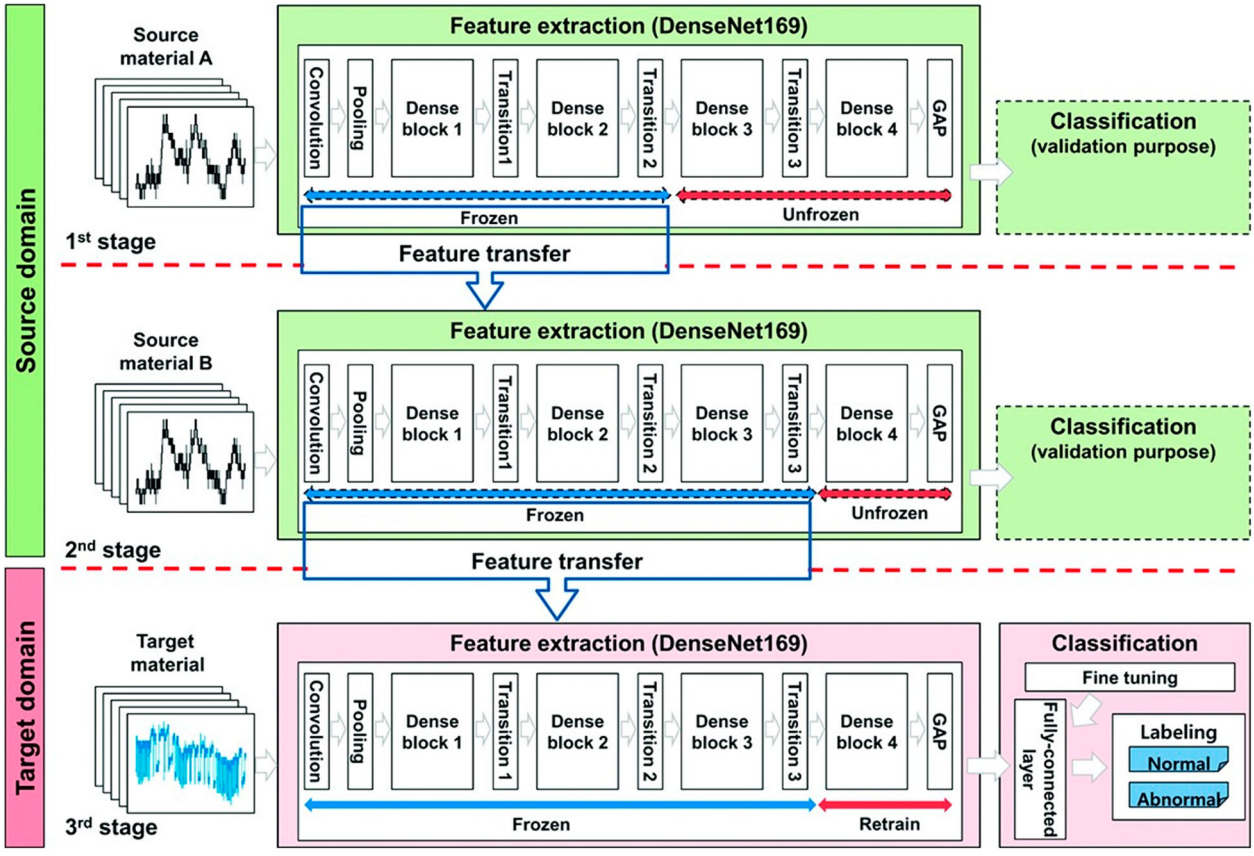

Figure 21. Conceptual representation of transfer learning from low carbon steel to high entropy alloy [394].

developed a TL classification framework to detect LPBF defects, specifically balling, lack-of-fusion pores, conduction mode, and keyhole pores. They initially trained two source CNN models (VGG16 and ResNet18) using spectrogram images of acoustic signals from stainless steel 316L line tracks. Target models were then created by fine-tuning the final layers of these source models with target data consisting of bronze (CuSn8) spectrogram images. Their experiments showed a decrease in prediction accuracy when transferring knowledge between different materials. Shin et al. [394] also proposed using CNN to extract sufficient image features from multi-source materials (low carbon steel and stainless steel), then transferred and fine-tuned the models for anomaly detection in the target material (Inconel), as shown in Figure 21. They applied stepwise learning to extract image features sequentially from individual source materials, and composite learning is employed to assign the optimal frozen ratio for converging transferred and existing features.

5.2.2. Ontological mapping

To overcome the limitations, such as the lack of physical interpretability and a holistic view of AM life cycles, as discussed in Section 5.2.1, ontological mapping (OM) methods can be employed. The main idea is to extract relationships among AM parameters and the resulting parts, i.e. establishing design rules. NIST and other research groups have been investigating ontological mapping to efficiently relate complex, scattered knowledge [395], as shown in Figure 22.

Roh et al. [396,397] developed an ontology for AM to represent information for different process models for laser, thermal, microstructure, and mechanical properties for metal-based AM of Ti-6Al-4 V. Liang [398] developed a novel 'AM-OntoProc' ontology that promotes the modelling and re-utilisation of knowledge towards the AM process planning, where the AM process is supposed to start from the utilisation of CAD software during the design stage until the final AM prototype is developed. Hagedorn et al. [399] utilised the Innovative Capabilities of Additive Manufacturing (ICAM) ontology, a structured knowledge model that links business and technical insights to AM processes. The information in ICAM covers basic product attributes from the NIST Core Product Model (CPM) relating to materials, geometry, and design function, as well as types of manufacturing processes and services taken over from the manufacturing service description language (MSDL). Most recently, Ko et al. [395] proposed a novel framework, the data-

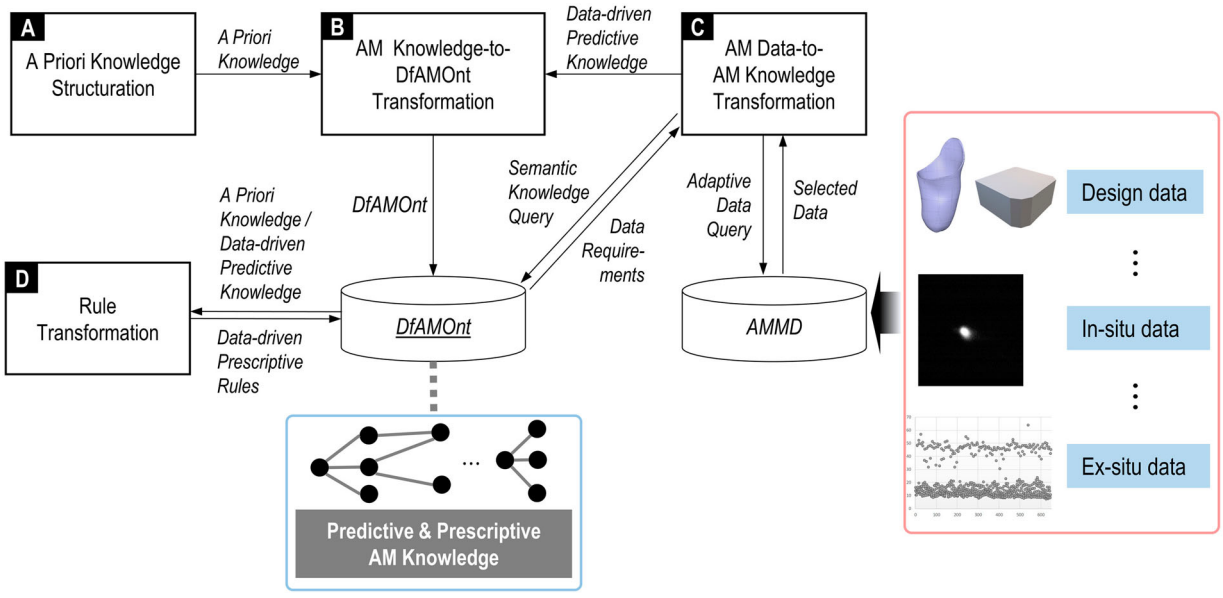

Figure 22. Overall data-knowledge-design rule framework [395].

knowledge-design-rule, in which they aimed to extract knowledge from a public AM database and update prior knowledge. It can automatically and autonomously improve knowledge of AM design. In another study, Park et al. [400] developed a data analytics knowledge base (DAKB) using the Web Ontology Language (OWL), which captures diverse knowledge from the experts to identify DA opportunities.

In the case of AM-RA, integrating transfer learning and ontological mapping can effectively address data scarcity. However, a substantial amount of data is required to achieve improved prediction accuracy, which poses non-trivial challenges. In addition, imbalanced data is another issue faced by the AM processes, especially for RAs. This indicates that while collecting process signatures using sensors and other data acquisition devices is inexpensive and well-established, characterising microstructural features and mechanical performance/properties is significantly time- and cost-intensive and, in many cases, requires destructive tests. This statement will be elaborated on in Section 5.2.3. Integrated TL and ontological mapping, especially in the case of multisource TL, can induce accumulated uncertainties, which reduces the process repeatability and part reproducibility [394]. This issue will be comprehensively discussed in Section 5.2.4.

5.2.3. Physics-informed machine learning (PIML)

The effectiveness of using ML as a reliable modelling tool depends on ensuring consistency with physical principles. In addition, data scarcity and imbalanced data are hindering the modelling of AM-RA processes. To address these issues, physics-informed machine learning (PIML), a hybrid method that integrates physics-based knowledge with big data [401], is gaining significant interest. Its main goal is to achieve interpretable models and establish design rules by transforming raw data into PSPP knowledge. This transformation enables a comprehensive understanding of the underlying physics of AM-RA processes, which in turn can be leveraged to reduce process defects and increase process repeatability and part reproducibility.

Although still in its infancy, the PIML paradigm has already attracted an increasing level of attention due to its potential for future exploration. Du et al. [402] showed that a combination of PIML, mechanistic modelling, and experimental data can reduce the occurrence of common defects in AM. By analyzing experimental data on the defect formation mechanism, they identified several key variables that reveal the underlying physical phenomenon. Guo et al. [401] proposed five predominant ways to integrate physics into ML: (1) model input, (2) model training, (3) model components, (4) model architecture, and (5) model output. An example of model input is described in the study of Guo et al. [403], where PIML-driven NNs, as shown in Figure 23, were proposed. They extracted features from thermal images of melt pools with a CNN and concatenated the features with physical measures from finite-element analysis (FEA) simulations before feeding them to a subsequent ML algorithm for porosity prediction. In another study, Ko et al. [404] proposed a novel framework driven by physics-guided ML, which included both physics knowledge and AM data from measurement and monitoring. The research enabled a systematic approach for combining physics knowledge with real-

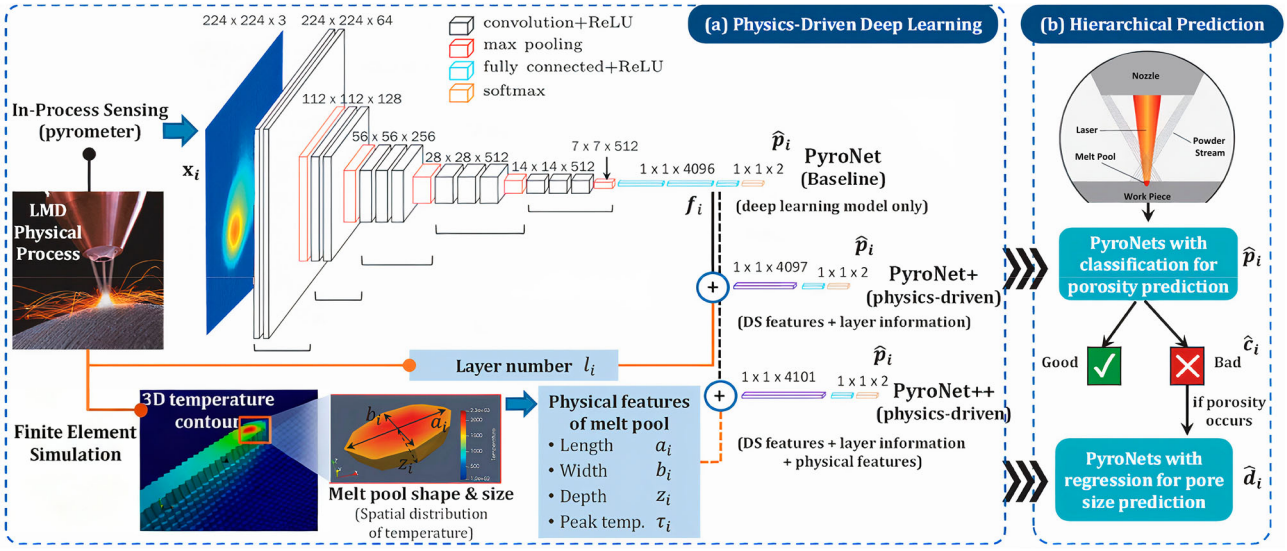

Figure 23. PIML-driven PyroNet + and PyroNet++ [403].

world data, facilitating the development, validation, and verification of PSP linkages.

The prevailing advantage of PIML is that it enhances model interpretability and composability, since these models are underpinned by physical principles. This approach maintains the high performance of ML, making it well-suited for modelling and simulating AM-RA processes. Since physics-based models are frequently used as sources of the PIML training data for the metal AM, it is crucial for these models to be as accurate as possible, especially in the case of RAs, where experiments are expensive. Therefore, it is important to recognise inherent assumptions, simplifications, and approximations in physics-based models that can compromise accuracy [405]. Hence, UQ is one of the most effective approaches to address these issues. The accumulation of process repeatability and part reproducibility issues in AM, along with the stochastic behaviour of RAs, necessitates the use of UQ for PIML. Ma et al. [379] pointed out that the quality and properties of AM deposits can vary significantly even when the same materials, processing parameters, and type of AM machine are used. For example, the fatigue life of AM parts can vary based on the process signatures and induced defects. To tackle these issues, PIML studies must be integrated with uncertainty considerations, as discussed in detail in Section 5.1.

5.2.4. Synthetic data generation

One of the most promising yet underexplored approaches to addressing data scarcity in the AM-RA is the use of synthetic data generation. Due to the high experimental costs and the limited number of available datasets for refractory systems, researchers are increasingly relying on computationally derived datasets and hybrid learning strategies. However, as noted by Singh et al. [406], synthetic data generation must be handled with caution, particularly for refractory or high-entropy systems, since synthetic oversampling may distort the phase-property relationships inherent to experimentally verified data. Their study highlighted that while the use of SMOTE-Tomek augmentation can improve classification accuracy, it cannot reliably guarantee structural fidelity for complex systems such as refractory HEAs. Consequently, rigorous physical validation remains indispensable when extending these methods to AM-RAs.

Recent work by Rahman et al. [407] reviewed the integration of synthetic datasets with machine learning (ML) frameworks across multiple alloy systems, demonstrating how generative adversarial networks (GANs) and conditional GANs can expand sparse data domains while maintaining statistically realistic feature distributions. In particular, they emphasised the utility of combining CALPHAD, DFT, and experimental data to generate synthetic training sets that bridge gaps between scales. Similarly, Swateelagna et al. [238] proposed explainable ML workflows in which synthetic datasets generated from thermodynamic simulations are used to train interpretable models for alloy design, improving predictive accuracy by integrating physical constraints. These frameworks – although mainly applied to non-refractory alloys-offer transferable methodologies for future AM-RA research, where limited datasets constrain the development of robust predictive models.

Complementary efforts by Kannan and Nandwana [408] have demonstrated data-driven synthetic alloy

discovery pipelines combining virtual high-throughput screening with deep generative models. Their approach integrates latent space sampling from trained neural networks with physical descriptors to generate hypothetical alloy compositions exhibiting plausible microstructural and thermodynamic stability. While such methods have yet to be validated for refractory alloy systems, they offer a scalable path forward for generating synthetic microstructure-property datasets. In the context of AM-RAs, combining physics-based models (e.g. phase-field or cellular automata) with generative frameworks can enable the creation of realistic synthetic datasets that accurately reproduce melt-pool behaviour, defect formation, and thermal history effects under extreme processing conditions. Nevertheless, extensive experimental validation is still required before synthetic data generation can be fully trusted for the qualification of refractory alloys.

5.3. Integrated computational materials engineering (ICME)

An integrated computational materials engineering (ICME) framework has been recognised as a powerful tool that can improve the AM process [409]. Its primary goals are to (1) support decisions in materials selection and design processes, as discussed in Section 4.1, and (2) establish the PSPP relationships with uncertainty consideration, as discussed in Section 5.2. It aims to realise the concept of 'manufacture the alloy and structure you need' [410]. Computational models differ in terms of their length and time scales, stages, and physical aspects. Therefore, creating a single computational model to simulate the holistic PSPP response in metal AM is challenging. In this context, the hierarchical integration of multi-scale multi-physics models based on the ICME approach to link PSPP has emerged as a pragmatic solution [411]. ICME tools encompass density functional theory (DFT), molecular dynamics (MD), coarse-graining atomistic modelling methods, kinetic Monte Carlo (KMC), dislocation dynamics (DD), microscopic and mesoscopic phase field (PF), FEA, and CP simulation.

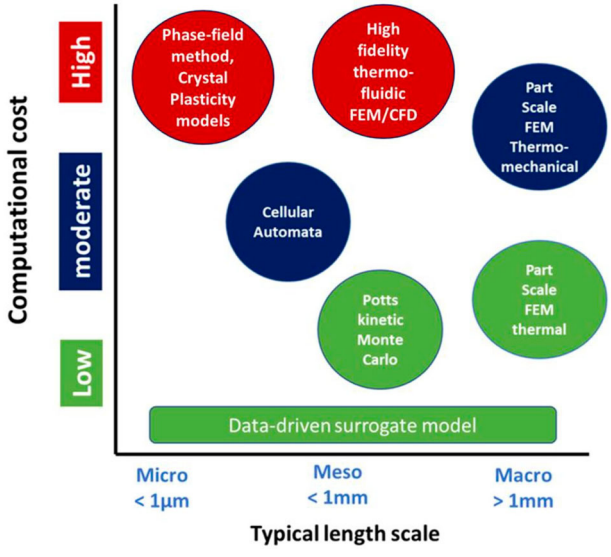

Figure 24. Categorisation of different phenomenological computational models, based on length scales and computational cost [411].

Multi-scale characteristics (different phenomena occur at different scales) induce inherent complexity in the metal AM process. Figure 24 illustrates various models and their corresponding length scales, along with their computational costs. Micro-scale models focus on local phenomena such as the interaction between the heat source and powder, heat absorption, the heat-affected zone, grain evolution, and melt pool phase transformations. Meso-scale models simulate changes in composition, thermo-mechanical behaviour, and temperature-dependent metallurgical properties. Macro-scale models, which encompass a broader scope, address process evolution. They use thermal, thermo-mechanical, and thermo-metallurgical models to predict temperature fields, molten pool geometry/residual stress, and distortion/microstructural phase transformations, respectively [50].

The AM modelling process is inherently complex due to the multitude of physical phenomena involved, ranging from the formation of the powder layer to the melting and solidification of the additive layer. They include molten pool physics such as temperature profile, heat transfer, fluid flow, viscosity, vaporisation, solidification, volume shrinkage, phase transformation, and morphology of molten pool, as well as process-wise physical mechanisms, including energy source-particle interaction, powder layer formation, and heat transfer [50]. As multiscale CA/PF/KMC models enhance our understanding of the link between processing and the resulting structure, there is a growing demand for modelling frameworks that can simulate the entire metal AM fabrication process. This represents a shift in modelling paradigm, integrating process-structure (PS) and structure–property (SP) models into a complete PSPP framework. This integrated approach is promising because it can directly connect process parameters to the mechanical behaviour of AM components through microstructural models. A significant challenge lies in developing a reliable information exchange algorithm to effectively manage data flow between the different multiscale modelling platforms [411]. Table 10 shows the ICME tools employed in different research. Here, 'x' denotes that the research has studied the corresponding

Table 10. ICME tools and multi-scale, multi-stage, multi-physics analysis.

ICME tool		Material	AM Process	Multi-scale					PSPP (Multi-stage)				Ref.
				Macro	Meso	Micro	Nano	Atom	Process	Structure	Property	Performance	
Multi-physics	FE	W	LPBF	×	×	×	–	–		×	×	–	[254]
	CPFFT	NbZr1	WAAM	×	×	×	–	–	×	×	×	–	[211]
	CFD	Mo	PBF	×	–	–	–	–	×	×	–	–	[272]
			EBSM	×	×	–	–	–	×	×	×	–	[271]
	FEM	W	LPBF	×	×	×	–	–	×	×	×	–	[63]
	CP	W	LPBF	×	–	×	–	–	×	×	×	–	[273]
	CALPHAD	$Al_{0.5}CrMoNbTa_{0.5}$	EBM	–	×	×	–	–	–	×	–	–	[158]
		$Cr_{10}Mo_{25}Ta_{25}Ti_5V_{25}$	VAM	×	×	×	–	–	×	×	×	–	[275]
	CALPHAD-PF	Ti-Nb	LPBF	×	×	×	×	×	×	×	–	–	[274]

aspect, and '-' denotes that it has not been investigated. As the literature suggests, inadequate research has been dedicated to using ICME tools to investigate materials that might help reveal the underlying aspects of AM-RA, and a huge gap still exists in this area. For instance, to the best of the authors' knowledge, no comprehensive survey has been conducted to study and model the performance of AM-RA using ICME tools.

Current ICME tools and studies are still unable to establish comprehensive PSPP linkages, particularly in the case of AM-RA, and a holistic approach remains unexplored. Motaman et al. [44] illustrated an example of ICME-based PSPP linkage in metal AM, along with a hybrid physics-based data-driven strategy for its application in the optimal design of a component. They predicted the performance for design parameter combination via the ICME-based PSPP linkage. In another study, Jalalahmadi et al. [412] developed a modelling tool that enables the performance prediction of AM parts, considering microstructural properties and fatigue cracks. This tool, called DigitalClone® for Additive Manufacturing (DCAM), is an ICME tool that includes models of crack initiation and damage progression with the high-fidelity process and microstructure modelling approaches. However, very few studies have considered uncertainties associated with the ICME tools arising from model, structure, parameters, and simplifications, which are intensified in the case of AM-RA due to their stochastic nature. Quantifying these uncertainties is necessary to enable robust decision-making and reliable PSPP linkage. Figure 25 shows an overview of the ICME approach for establishing the process-signature-structure–property-performance (PS^2P^2), which could be applied in this regard.

5.4. Multi-criteria decision making for PA: interoperability and integration issues

The ultimate goal of DA for AM-RAs can be the 'performance assurance (PA)' [413], which can be achieved by an integrated, high-level perspective framework. This framework is necessary for better and robust decision support since AM inherently has manufacturability, repeatability, and reproducibility issues [314], issues compounded in AM-RAs. AM-RAs can be more intensified due to the (1) complexity of AM-RAs; (2) uncertainty induced mainly from the nascent knowledge; and (3) volatility and variability of processes leading to measurement errors. To tackle these issues, all the previously mentioned sections need to be seamlessly integrated to realise the MCDM with uncertainty consideration [414,415]. The MCDM is applied to satisfy conflicting requirements and goals. It needs to manage

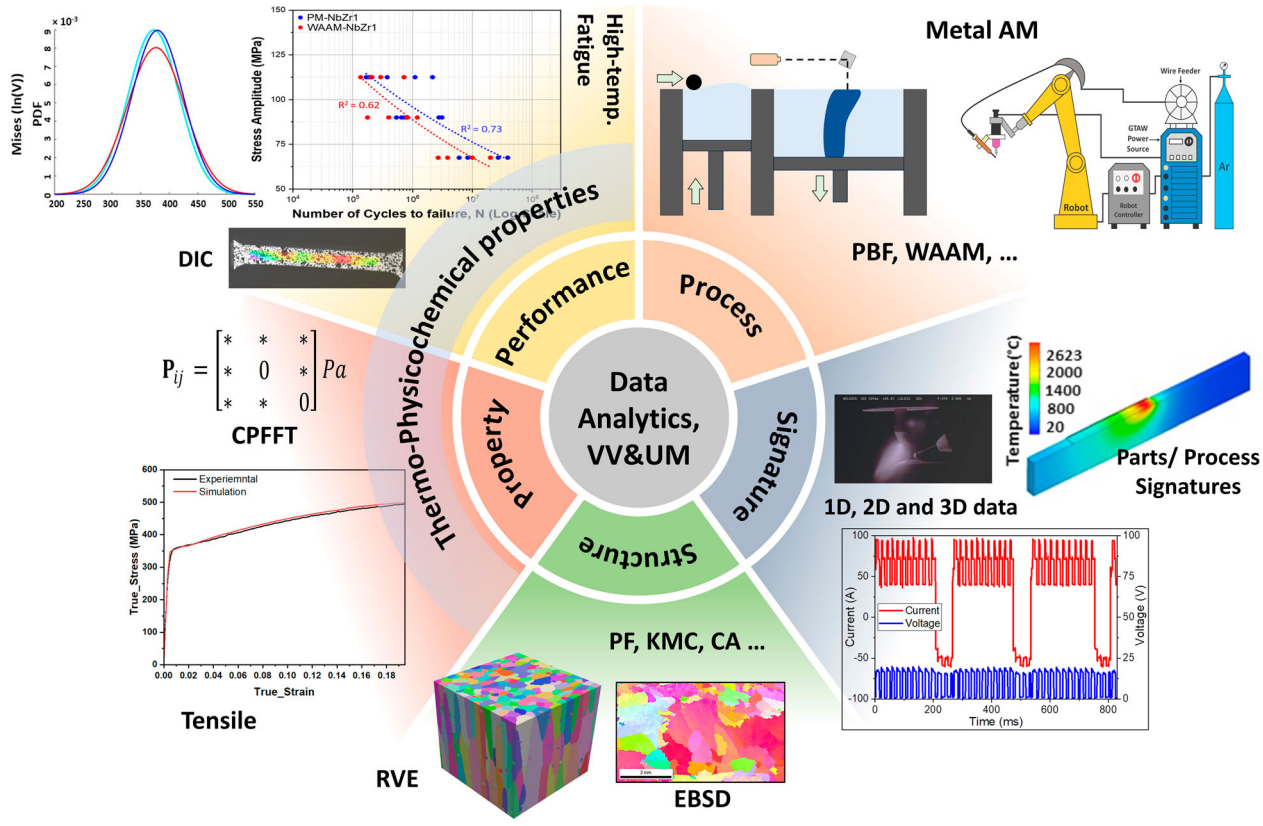

Figure 25. Schematic overview of the ICME-based PS^{2}P^2 linkage for performance prediction of AM-RA.

multiple conflicting objectives with heterogeneous data and models with uncertainty considerations at multi-scale, multi-stage, and multi-physics. This produces two critical questions: (1) model composition and (2) uncertainty aggregation. The following two paragraphs discuss them.

First, there are interoperability and integration issues because the MCDM needs to manage a large amount of information and different types of data and models [416]. In the case of AM-RA, the issues are intensified due to the additional complexities and uncertainties. For example, consider the question 'How to compose disparate analytical problems into a unified analytical problem?'. Addressing this question requires an investigation into which types of models are best suited for various features of input/output data (e.g. input type, availability, fidelity, and size) and manufacturing conditions (e.g. objectives, constraints, and key performance indicators). The characterisation of methods is necessary for scaling, normalisation, weighting, and aggregation (SNWA) [417] with respect to the different data characteristics (e.g. type and integrity), model features (e.g. type and fidelity), and other conditions (e.g. objectives and constraints). Each step and method in MCDM should be carefully determined since the choice of these significantly affects the decision results.

An additional question may be, 'Can the aggregated model be considered reliable even if each model satisfies the required confidence level?' The quantification of uncertainty in the aggregated model is challenging because it involves multiple criteria with subjective normalisation and weighting factors. In other words, the uncertainties associated with each data and model need to be scaled, normalised, and weighted. Additionally, the propagation and aggregation of these uncertainties must be managed to facilitate the final MCDM analysis. For example, consider the generation of surrogate models from high-fidelity computational models and/or DoEs in AM. For successful MCDM, these models need to be aggregated into a global surrogate model (GSM) that considers uncertainty considerations following the SNWA procedures to support final decision-making [418]. In this regard, a reliable and robust method needs to be developed to integrate analytical problems from different manufacturing resources for MCDM, considering uncertainty. However, such a method does not currently exist.

To tackle these issues, a seamlessly integrated MCDM framework for AM-RAs is necessary. In the AM community, several research groups have been investigating and developing the integrated decision-support framework, such as (1) Integrated computational materials

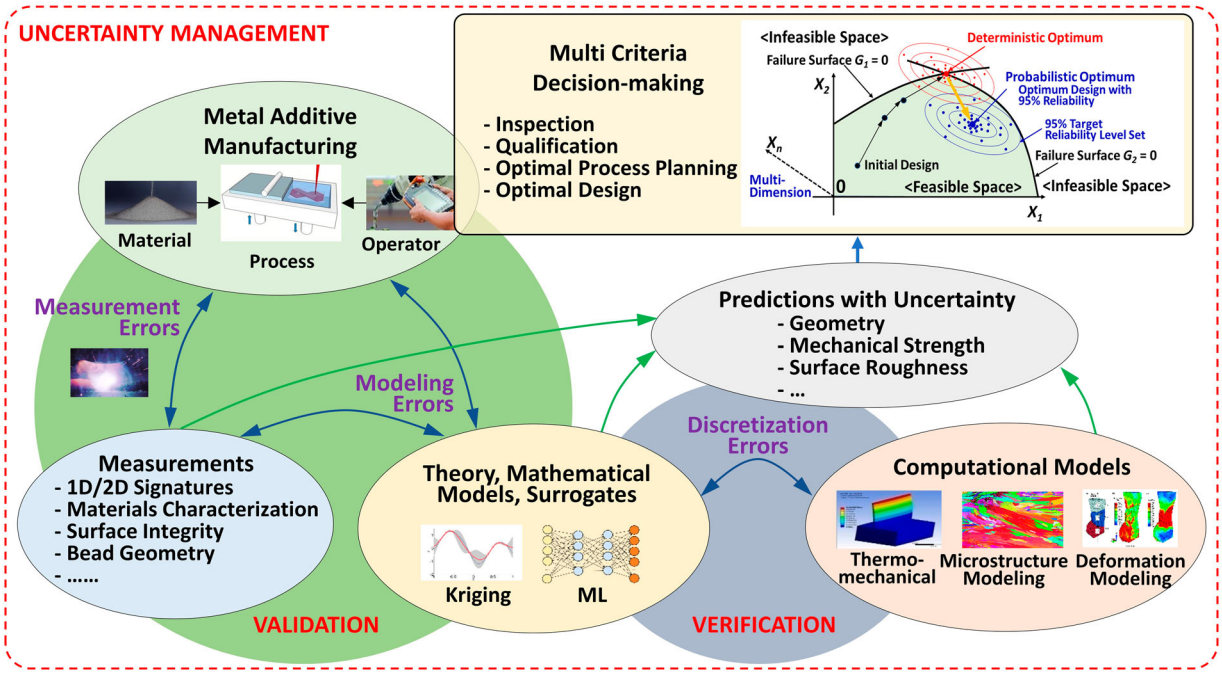

Figure 26. VV and UM for MCDM. Reproduced from [420].

engineering (ICME) discussed in Section 5.3, (2) NIST Data-driven decision support for additive manufacturing [400], and (3) NIST Data Integration and management for additive manufacturing [419]. Efforts such as these should be leveraged to facilitate a seamlessly integrated MCDM framework for AM-RAs with uncertainty consideration. As an example, we regenerated the conceptual schematic diagram of MCDM with uncertainty consideration, based on the previously discussed thoughts and concepts from [420], as shown in Figure 26. It consists of several components discussed in the previous sections such as (1) AM process complexities in Section 2 and 3, (2) measurement techniques in Section 4, (3) surrogate models in Section 4, (4) computation models in Sections 4 and 5, (5) prediction with uncertainty (knowledge) in Section 5, (6) MCDM in Section 5. It also displays measurement, modelling, and discretization errors, as well as VVUQ. The errors are discussed in Section 4, while VVUQ is discussed in Section 5.

5.5. Integrated framework for quality assurance

Complete qualification of a new AM process and materials often requires thousands of individual tests, millions of dollars, and years to complete in the aerospace industry [421]. Even though the process is well-established for general components, each AM part needs to be tested in many cases to ensure process repeatability and product reproducibility [422]. In recent years, AMed parts have made great strides, with guidelines and paths provided through agencies in standards guidance. However, in the case of AM-RAs, AM issues will be further magnified, presenting greater challenges and incurring higher costs, as described in Section 4.5. This will be one of the main hindrances for its wide adoption. In accordance with this, reliable and efficient qualification methods are essential for the AM-RA structures, as they are intended for use in extreme environments (e.g. high temperatures and radioactivity).

To address these issues, research groups are actively investigating DA and digital twins from a holistic perspective [423,424]. This research mainly aims to digitally analyze measured process signatures and validate/qualify a part, rather than conducting physical tests, which are one of the NDE methods. In Huang et al. [425,426], the concept 'certify-as-you-build' is first presented, which is an integrated framework for quality assurance (QA). In addition, a digital twin-driven rapid qualification method has been proposed, as shown in Figure 27 [355]. Seo et al. [413] proposed a QA framework consisting of four stages: QA plan, prospective, concurrent, and retrospective validations. Despite its potential, no studies have comprehensively demonstrated the effectiveness of digital twin-driven qualification frameworks in metal AM.

Although digital twins offer a promising path toward closed-loop control in additive manufacturing, their realisation for refractory alloys presents especially severe demands. In extreme processing environments,

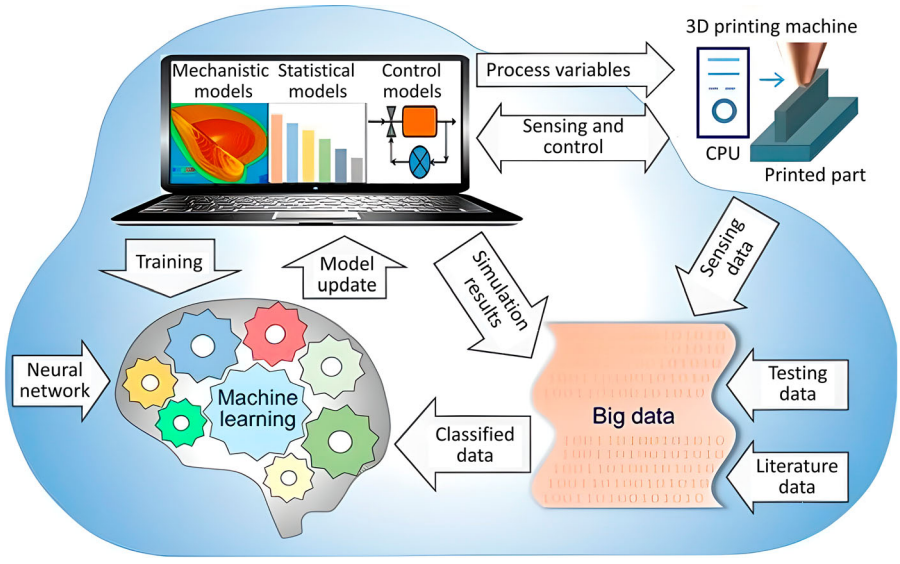

Figure 27. Schematic representation of the Digital Twin [355].

integrating multi-sensor data streams (e.g. thermal imaging, acoustic emission, coaxial melt pool vision, and laser line scanning) into a robust digital twin architecture is nontrivial. For instance, Chen et al. [427] developed a multi-sensor fusion-based digital twin for robotic DED that synchronises acoustic, thermal, vision, and scanning data within the 3D volume to detect defects and drive corrective toolpath adjustments in real time. Liu et al. [428] proposed a deep neural operator-enabled digital twin for LPBF that merges physics-based melt pool simulations with in-situ sensor feedback to predict future states and adapt parameters dynamically. Li et al. [429] introduced a parameterised physics–based twin model that calibrates between simulation and experiment to predict defects and surface quality. These examples highlight how sensor fusion, model assimilation, and real-time analytics can be integrated in a DT framework [430]. However, due to the harsher conditions and sensor challenges in AM of refractory alloys, achieving reliable digital twin architectures remains a key open challenge and a focus for future investigations.

In addition, Since process signatures can represent the complicated interactions of process parameters with multi-physics (e.g. surface tension, viscosity, and thermo-capillary effects), which ultimately define final part quality, it can be hypothesised that they can provide valuable information for qualifying the part through an analytical approach. However, a full data-driven approach is required for qualifying the AM part via the digital twin-driven qualification since only real-time process signatures can contain information related to the process repeatability and part reproducibility issues [314]. Although the computational modelling approach can support the qualification, it cannot be directly used for the qualification since it is unable to handle the dynamically changing real-time process signatures. Therefore, it is important to acquire physically accurate and enough process signatures for a reliable qualification analysis. However, it is challenging to acquire the physically correct and/or enough data from the AM-RA due to the difficulties in measurement as well as aleatory/epidemic sources, as discussed in Sections 4.3 and 5.1, respectively. While DT approaches are promising for AM part qualification, they are not yet mature enough for providing a viable option.

6. Summary, challenges and outlook

Currently, nickel-based superalloys (e.g. Inconel 718) are the most widely used metallic materials in components that operate at temperatures exceeding 500°C (e.g. turbine blades). However, its maximum operating temperature is limited by its relatively low melting temperature. Recently, refractory alloys, including RHEAs, have been considered as a great potential for application at temperatures beyond the working temperature of nickel-based superalloys (above ~1000-1100°C), due to their extraordinary thermo-physicochemical properties. Research has demonstrated [431,432] how advanced experimental and modelling approaches can elucidate temperature-dependent deformation and plasticity loss mechanisms in Ni-based superalloys. Such studies provide valuable guidance for extending similar methodologies to AM of refractory alloys in future research.

In addition, utilising the benefits of AM, geometrically complex and multi-functional refractory structures can

be fabricated successfully, which is nearly impossible in conventional manufacturing processes. Unfortunately, many RAs face significant challenges, including rapid oxidation at high temperatures and intrinsic brittleness at room temperature. Additionally, non-equilibrium repeated thermal cycles and sharp thermal gradients that occur during AM induce residual stresses and microstructural anisotropy within the component. Furthermore, as an evolving technology, AM faces challenges related to process repeatability and part reproducibility. These issues can be intensified for AM-RAs due to the requirement of higher heat input to melt them, leading to significant complexity, uncertainty, and challenges.

6.1. Summary and response to research questions

This study explored the state-of-the-art AM for refractory alloys across various stages of design, process planning, manufacturing, post-processing, and test/qualification/certification. Next, it identified the knowledge gaps and critical research issues in each stage as well as potential solutions. It can be summarised that an integrated experimental and computational approach is essential for elucidating the underlying physics and applying the knowledge to real-life manufacturing. Since the AM for refractory alloy structures is both cost-intensive and time-consuming, the computational modelling approach is preferable.

In Section 2.4, six research questions were identified, and through this study, we have addressed them as follows:

- *RQ1: What are the limitations, critical research issues, and technical challenges for AM-RAs?*

AM-RAs exacerbate core AM issues, including manufacturability, repeatability, and reproducibility, due to higher heat input, non-equilibrium thermal cycles, residual stresses, and microstructural anisotropy. These factors increase complexity and uncertainty, particularly in high-temperature service applications.

- *RQ2: What DA techniques are used to investigate multi-physics/multi-scale phenomena and defect formation, and what are their limitations?*

The current study discusses a range of DA techniques, from convolutional neural networks applied to thermal imaging for porosity detection to PIML frameworks that link PSPP relationships with process signatures. These approaches demonstrate strong potential but remain constrained by sparse and imbalanced datasets, approximations in physical models, and limited uncertainty quantification. The review emphasises that for AM-RAs, data scarcity and experimental inaccessibility make the coupling of DA with uncertainty management particularly critical.

- *RQ3: What are the VV&UQ and performance assurance (PA) criteria in AM-RA?*

The study emphasises that robust verification and validation necessitate both code- and calculation-level checks, as well as rigorous comparison of simulations with experimental benchmarks. Uncertainty quantification is treated as essential, addressing both aleatory variability and epistemic gaps across multi-model workflows. Ultimately, performance assurance in AM-RAs depends on integrated frameworks that combine VV&UQ with multi-criteria decision-making to ensure reliability under operational conditions.

- RQ4: What are the design-rule establishment approaches in AM-RA?

Design rules in AM-RAs are framed within the ICME paradigm, where process–structure–property–performance relations provide the foundation for codified guidelines. The current study highlights the role of data-driven knowledge bases, ontology-supported frameworks, and design-rule extraction methods that can evolve dynamically as more RA data becomes available. This emphasises that design rules must remain adaptive and data-informed, rather than static or prescriptive.

- *RQ5: What are the digital-twin-driven qualification methods?*

Our study focused on digital twin-driven rapid qualification approaches, including 'certify-as-you-build' strategies that link real-time monitoring with simulation-based prediction. While these methods hold promise for accelerating qualification, the manuscript notes their current immaturity for metallic systems, especially RAs, given the demand for high-fidelity process signatures and validated multi-scale models. Nevertheless, digital twin integration is positioned as a transformative path toward reducing qualification time and cost in future AM-RA applications.

- RQ6: What are the future research and development tasks for AM-RAs?

Finally, the outlook emphasises that future progress requires tighter integration of experimental and

computational approaches, with computation increasingly used to reduce cost and time. It highlights the need for DA-ready frameworks that can handle heterogeneous data, conflicting objectives, and uncertainty propagation in qualification. Establishing systematic physicochemical databases, advancing PIML and transfer learning, and embedding these within digital twins are identified as essential steps for the next generation of AM-RA research.

6.2. Challenges

AM-RAs present a unique set of challenges and opportunities across the entire value chain, from initial design to final certification. Unlike conventional superalloys, refractory alloys possess exceptionally high densities and operate in extreme environments, requiring careful attention to both geometric and compositional design. Moreover, the complexity of their PSPP relationships demands integrated experimental and computational approaches at every stage, from process planning to qualification. The following sections synthesise the key considerations and current gaps across five critical domains of design, process planning, fabrication, post-processing, and test/qualification.

- **Design:** Design can be divided into geometric design and chemical composition design. Refractory alloys typically have a higher density compared to superalloys. Since refractory alloys can be widely used in aerospace applications, a more stringent geometric design is necessary to ensure lightweight and safety. This can be achieved by topological optimisation and generative design approaches. For chemical composition design, an integrated experimental and computational approach is necessary to avoid unwanted features and satisfy requirements, since its design space is enormous. However, investigations are significantly lacking, and related ICME is absent for refractory metals and alloys.
- **Process planning:** Due to the curse of dimensionality and the high cost in AM for refractory alloys, the establishment of design rules is significantly challenging. An integrated experimental and computational approach is necessary to investigate the PSPP. In particular, computational modelling approaches, e.g. (1) numerical thermomechanical FEM for residual stress, (2) solidification models (e.g. cellular automata, kinetic Monte Carlo, and phase field) for the prediction and analysis of microstructure, and (3) CPFEM for the analysis of the deformation behaviour, can be effectively used to understand the underlying physics and subsequent correlations. To achieve this objective, further investigations on experiments (e.g. neutron diffraction) and computations (e.g. JMatPro) are necessary. HTEM and transfer learning can be effective ways to develop design rules of AM for refractory alloys.
- **Fabrication:** To ensure part quality, real-time monitoring and process control systems are necessary. This step involves the accurate measurement of physical process signatures and pre-processing them for further analysis. It can be challenging due to the lack of knowledge and difficulties in measurements and calibration. For process control, reinforcement learning and transfer learning can be effective solutions. However, its related knowledge and investigations remain significantly limited in AM RAs. Also, further investigations into (1) in-situ control (e.g. machining and cold rolling) for performance improvement and (2) multi-materials for enhanced multi-functionality are needed.
- **Post-processing:** To improve mechanical properties and optimise component performance, post-processing (e.g. heat treatment and machining) is often necessary. However, significant investigation efforts are lacking due to limited facility accessibility and associated high cost. Thus, computational modelling approaches, such as CALPHAD for the heat treatment and CPFEM for the machining, can be effectively implemented to gain additional insights.
- **Test/qualification/certification:** Additively manufactured refractory alloys require significantly higher quality standards and stricter testing compared to nickel – or titanium-based alloys due to their potential use in extreme environments, such as nuclear reactors. Such testing and qualification methods are not fully developed. Non-destructive evaluation (NDE) can be considered an effective method in this regard, provided it is available. The digital twin-driven NDE method, based on ML models (e.g. LSTM) derived from process signatures, is promising.

6.3. Outlook

To overcome these challenges and to realise the concept of 'apply the alloy you have' to 'manufacture the alloy and structure you need' and 'certify-as-you-build,' data analytics (DA) is necessary from an integrated, high-level perspective. Future research directions can include:

- **Integrated Computational Materials Engineering (ICME) for Performance Assurance:** The integrated decision support framework must manage

heterogeneous, multiple, and conflicting objectives, data, and models across multi-scale, multi-stage, and multi-physics domains, as well as uncertainty and its propagation. In this situation, the seamlessly integrated MCDM method is considered as one of the possible solutions to resolve this highly complex problem. The decision-support techniques have several critical hurdles: (1) their high uncertainty and complexity; (2) their inability to deal with multiple, conflicting objectives; and (3) the dynamicity of the evolving manufacturing systems. Integrated decision-support efforts in AM can include NIST Data-driven decision support for additive manufacturing, (2) NIST Data Integration and management for additive manufacturing, and ICME. Nonetheless, the research efforts need to be extended to support decision-making for AM of refractory alloy structures. Such frameworks are directly applicable to aerospace propulsion and nuclear energy systems, where ICME-driven multi-objective optimisation can accelerate the qualification of molybdenum-based thruster nozzles and rhenium–tungsten heat shields, reducing costly experimental iterations.

- **PSPP establishment:** It is significantly challenging to establish the PSPP design rules in AM-RA, due to the curse of dimensionality as well as the infinite compositional combinations in RHEA. A multi-fidelity computational and experimental modelling approach is necessary to effectively elucidate the underlying physics and to establish the PSPP design rules. For example, HTEM can be a low-fidelity experimental modelling approach. In addition, transfer learning can be a possible solution to tackle the curse of dimensionality via transferring the well-established design rules to cases with incomplete or limited data. A validated PSPP framework would directly support fusion and high-temperature energy applications, such as the design of tungsten divertor plates [433].
- **Interoperability and integration for heterogeneous data and models:** Various types of datasets must be incorporated for predictive models, and different predictive models need to be combined for further in-depth analysis. However, this process is challenging, as it involves multiple criteria with subjective normalisation and weighting factors. Reliable and robust methods are needed to address analytical problems arising from disparate manufacturing resources in multi-criteria decision-making scenarios. For this purpose, it is necessary to characterise methods for scaling, normalisation, weighting, and aggregation (SNWA) with respect to the different data characteristics (e.g. type and integrity), surrogate model features (e.g. type and fidelity), and other conditions (e.g. objectives and constraints).
- **Verification/Validation and Uncertainty Quantification:** Due to the complexity and uncertainty in AM-RA, more issues related to manufacturability, process repeatability, and part reproducibility are expected to arise. To manage these issues, VV&UQ is required, including uncertainty management. However, it is challenging to generate enough data due to the difficulties and high costs of AM-RA. For this, a physics-informed, data-driven approach can be the possible solution. For example, a CPFEM-informed, ML approach with uncertainty quantification can predict the tensile strength with its variations.
- **Integrated framework for quality assurance:** Since AM-RA structures can be widely used in harsh environments, their quality should be strictly assured before their use, compared to high-performance alloys (e.g. Ti-6Al-4 V and Inconel 625). For this, real-time process monitoring and in-situ control are necessary. In addition, the digital twin-based NDE method, which analyzes process signatures, can be a potential solution to realise the paradigm of 'certify-as-you-build.'

In summary, AM's complexity-free fabrication capability, with its exceptional and unique properties, can be utilised across various industries. Due to their outstanding properties, refractory alloy structures will be used in high-temperature, corrosion, and irradiation applications, including but not limited to the aerospace industry, turbine blades, land-based power plants, nuclear reactors, radiation-shielding systems, and biomedical applications. The authors believe that this critical review and perspective will provide the research community with proper guidance and an outline regarding future research directions for refractory metals and alloys.

Acknowledgments

The authors of this paper acknowledge the Center for Manufacturing Research (CMR) and Tennessee Technological University's Department of Manufacturing and Engineering Technology for their support.

Author contributions

CRediT: **Duck Bong Kim:** Conceptualization, Data curation, Funding acquisition, Methodology, Project administration, Supervision, Visualization, Writing – original draft; **Mahdi Sadeqi Bajestani:** Conceptualization, Data curation, Formal analysis, Investigation, Methodology, Visualization, Writing –

review & editing; **Md Abdul Karim:** Conceptualization, Data curation, Visualization, Writing – review & editing; **Saiful Islam:** Conceptualization, Methodology, Writing – review & editing; **Oleg N. Senkov:** Conceptualization, Data curation, Writing – review & editing; **Peter K. Liaw:** Conceptualization, Data curation, Writing – review & editing; **Hojun Lim:** Conceptualization, Data curation, Writing – review & editing; **Paul Witherell:** Conceptualization, Data curation, Writing – review & editing; **Yousub Lee:** Conceptualization, Data curation, Visualization, Writing – review & editing; **Peeyush Nandwana:** Conceptualization, Data curation, Writing – review & editing; **Xuesong Fan:** Conceptualization, Data curation, Writing – review & editing; **Wonjong Jeong:** Data curation, Visualization, Writing – review & editing; **Jiwon Mun:** Conceptualization, Data curation, Writing – review & editing; **Yongho Jeon:** Conceptualization, Data curation, Funding acquisition, Writing – review & editing; **Ho Jin Ryu:** Conceptualization, Data curation, Writing – review & editing.

Disclosure statement

No potential conflict of interest was reported by the author(s).

Funding

This work was supported by the National Science Foundation under grant number 2141905; the National Research Foundation of Korea (NRF) grant funded by the Korea government (MSIT) under grant number RS-2024-00346883; the National Research Foundation of Korea (NRF) grant funded by the Korean government under grant number NRF-2022R1A5A1030054; the US Department of Energy Advanced Materials and Manufacturing Technologies Office (AMMTO) within the Energy Efficiency and Renewable Energy Office under grant number DE-AC05-00OR22725 with UT-Battelle LLC; the Air Force on-site contract by MRL Materials Resources LLC, Xenia, OH, USA under grant number FA8650-21-D-5270; the Army Research Office Project under grant number W911NF-13-1-0438 and W911NF-19-2-0049; the National Science Foundation under grant number DMR-1611180, 1809640, and 2226508; the Department of Energy under grant number DOE DE-EE0011185; and the Air Force Office of Scientific Research under grant number AF AFOSR-FA9550-23-1-0503.

Data availability statement

The data that support the findings of this study are openly available in Harvard Dataverse at doi:10.7910/DVN/PXHUEE.

References

[1] Shabalin IL. Ultra-High temperature materials II: refractory carbides I (Ta, Hf, Nb and Zr carbides), 1st ed. Dordrecht: Springer Netherlands; 2019. doi:10.1007/978-94-024-1302-1

[2] Guler SH, Yakin A, Guler O, et al. A critical review of the refractory high-entropy materials: RHEA alloys: composites, ceramics, additively manufactured RHEA alloys. Curr Appl Phys. 2025;70:87–124.

[3] Talignani A, Seede R, Whitt A, et al. A review on additive manufacturing of refractory tungsten and tungsten alloys. Addit Manufact. 2022;58; doi:10.1016/j.addma.2022.103009

[4] Liu B, Zhang P, Yan H, et al. A review on manufacturing pure refractory metals by selective laser melting. J Mater Eng Perform. 2024;33; doi:10.1007/s11665-024-09693-z

[5] Mukherjee P, Gabourel A, Firdosy SA, et al. Additive manufacturing of refractory metals and carbides for extreme environments: an overview. Sci Technol Weld Joining. 2024;29:99–115. doi:10.1177/13621718241235471

[6] Philips NR, Carl M, Cunningham NJ. New opportunities in refractory alloys. Metall Mater Trans A. 2020;51; doi:10.1007/s11661-020-05803-3

[7] Islam S, Seo G, Ahsan MRU, et al. Investigation of microstructures, defects, and mechanical properties of titanium-zirconium-molybdenum alloy manufactured by wire arc additive manufacturing. Intern J Refract Hard Metals. 2023;110; doi:10.1016/j.ijrmhm.2022.106042

[8] Islam S, Ahsan MRU, Seo G, et al. Investigations of microstructure and mechanical properties in wire + arc additively manufactured niobium–zirconium alloy. Adv Eng Mater. 2023;25; doi:10.1002/adem.202201633

[9] Mireles O, Rodriguez O, Gao Y, et al. Additive manufacture of refractory alloy C103 for propulsion applications, AIAA propulsion and energy 2020. doi:10.2514/6.2020-3500

[10] Marinelli G, Martina F, Lewtas H, et al. Microstructure and thermal properties of unalloyed tungsten deposited by wire + arc additive manufacture. J Nucl Mater. 2019;522; doi:10.1016/j.jnucmat.2019.04.049

[11] Groden C, Traxel KD, Afrouzian A, et al. Inconel 718-W7Ni3Fe bimetallic structures using directed energy deposition-based additive manufacturing. Virt Phys Prototyp. 2022;17; doi:10.1080/17452759.2022.2025673

[12] Gibson I, Rosen D, Stucker B, et al. *Additive manufacturing technologies, third edition*. Cham: Springer; 2021. doi:10.1007/978-3-030-56127-7

[13] Islam Z, Agrawal AK, Rankouhi B, et al. A high-throughput method to define additive manufacturing process parameters: application to haynes. Metall Mater Trans A. 2022;53:282), doi:10.1007/s11661-021-06517-w

[14] Zhao Y, Sargent N, Li K, et al. A new high-throughput method using additive manufacturing for alloy design and heat treatment optimization. Materialia. 2020;13; doi:10.1016/j.mtla.2020.100835

[15] Brennan MC, Keist JS, Palmer TA. Defects in metal additive manufacturing processes. J Mater Eng Perform. 2021;30; doi:10.1007/s11665-021-05919-6

[16] Fu J, Li H, Song X, et al. Multi-scale defects in powder-based additively manufactured metals and alloys. J Mater Sci Technol. 2022;122; doi:10.1016/j.jmst.2022.02.015

[17] Xie D, Lv F, Yang Y, et al. A review on distortion and residual stress in additive manufacturing. Chin J Mech Eng Addit Manufact Front. 2022;1; doi:10.1016/j.cjmeam.2022.100039

[18] Tomar B, Shiva S, Nath T. A review on wire arc additive manufacturing: processing parameters: defects, quality improvement and recent advances. Mater Today Commun. 2022;31; doi:10.1016/j.mtcomm.2022.103739

[19] Fang L, Cheng L, Glerum JA, et al. Data driven analysis of thermal simulations, microstructure and mechanical properties of Inconel 718 thin walls deposited by metal additive manufacturing, arXiv preprint, 2021. doi:10.48550/arXiv.2110.07108
[20] Balamurugan R, Chen J, Meng C, et al. Data-driven approaches for fatigue prediction of Ti–6Al–4 V parts fabricated by laser powder bed fusion. Int J Fatigue. 2024;182; doi:10.1016/j.ijfatigue.2024.108167
[21] Wang Z, Yang W, Liu Q, et al. Data-driven modeling of process, structure and property in additive manufacturing: A review and future directions. J Manufact Processes. 2022;77; doi:10.1016/j.jmapro.2022.02.053
[22] Hu Z, Yan W. Data-driven modeling of process-structure-property relationships in metal additive manufacturing. npj Adv Manuf. 2024;1; doi:10.1038/s44334-024-00003-y
[23] Farrag A, Yang Y, Cao N, et al. Physics-informed machine learning for metal additive manufacturing. Progr Addit Manufact. 2025;10:171–185.
[24] Wang Z, Liu P, Ji Y, et al. Uncertainty quantification in metallic additive manufacturing through physics-informed data-driven modeling. JOM. 2019;71; doi:10.1007/s11837-019-03555-z
[25] Yarlapati A, Aditya YN, Kumar D, et al. Recent advances in additive manufacturing of refractory high entropy alloys (RHEAs): A critical review. J Alloys Metall Syst. 2024;8:100120.
[26] Li W, Xie D, Li D, et al. Mechanical behavior of high-entropy alloys. Progr Mater Sci. 2021;118; doi:10.1016/j.pmatsci.2021.100777
[27] Cantor B, Chang ITH, Knight P, et al. Microstructural development in equiatomic multicomponent alloys. Mater Sci Eng. A Struct Mater Propert Microstruct Process. 2004: 375–377. doi:10.1016/j.msea.2003.10.257
[28] Senkov ON, Wilks GB, Scott JM, et al. Mechanical properties of Nb25Mo25Ta25W25 and V20Nb20Mo20Ta20W20 refractory high entropy alloys. Intermetallics. 2011;19; doi:10.1016/j.intermet.2011.01.004
[29] Senkov ON, Wilks GB, Miracle DB, et al. Refractory high-entropy alloys. Intermetallics. 2010;18; doi:10.1016/j.intermet.2010.05.014
[30] Chen S, Qi C, Liu J, et al. Recent advances in W-containing refractory high-entropy alloys – An overview. Entropy (Basel, Switzerland). 2022;24; doi:10.3390/e24111553
[31] Hua X, Hu P, Xing H, et al. Development and property tuning of refractory high-entropy alloys: A review. Acta Metall Sin (Engl Lett). 2022;35; doi:10.1007/s40195-022-01382-x
[32] Zhou J, Cheng Y, Chen Y, et al. Composition design and preparation process of refractory high-entropy alloys: A review. Intern J Refract Metals Hard Mater. 2022;105; doi:10.1016/j.ijrmhm.2022.105836
[33] Srikanth M, Annamalai AR, Muthuchamy A, et al. A review of the latest developments in the field of refractory high-entropy alloys. Crystals (Basel). 2021;11; doi:10.3390/cryst11060612
[34] Senkov ON, Miracle DB, Chaput KJ, et al. Development and exploration of refractory high entropy alloys – A review. J Mater Res. 2018;33; doi:10.1557/jmr.2018.153
[35] Gorsse S, Miracle DB, Senkov ON. Mapping the world of complex concentrated alloys. Acta Mater. 2017;135; doi:10.1016/j.actamat.2017.06.027
[36] Senkov ON, Gorsse S, Miracle DB. High temperature strength of refractory complex concentrated alloys. Acta Mater. 2019;175; doi:10.1016/j.actamat.2019.06.032
[37] Whitfield TE, Pickering EJ, Owen LR, et al. An assessment of the thermal stability of refractory high entropy superalloys. J Alloys Compds. 2021;857; doi:10.1016/j.jallcom.2020.157583
[38] Liu C, Li Y, Li J, et al. A novel low-density and high-strength Fe-Ni-base high-entropy superalloy with stable γ/γ′ coherent microstructure at 1023 K. Scr Mater. 2024;252; doi:10.1016/j.scriptamat.2024.116236
[39] Melia MA, Whetten SR, Puckett R, et al. High-throughput additive manufacturing and characterization of refractory high entropy alloys. Appl Mater Today. 2020;19; doi:10.1016/j.apmt.2020.100560
[40] Marinelli G, Martina F, Lewtas H, et al. Functionally graded structures of refractory metals by wire arc additive manufacturing. Sci Technol Weld Join. 2019;24; doi:10.1080/13621718.2019.1586162
[41] Kim J, Wakai A, Moridi A. Materials and manufacturing renaissance: additive manufacturing of high-entropy alloys. J Mater Res. 2020;35; doi:10.1557/jmr.2020.140
[42] Anonymous. (2022). BS EN ISO/ASTM 52900:2021: Additive manufacturing. General principles Fundamentals and vocabulary, https://bsol.bsigroup.com/Bibliographic/BibliographicInfoData/000000000030448424.
[43] Järvenpää A, Kim DB, Mäntyjärvi K. Chapter 14 – metal additive manufacturing, welding of metallic materials. Elsevier. 2023: 493–536. doi:10.1016/B978-0-323-90552-7.00007-9
[44] Motaman SAH, Kies F, Köhnen P, et al. Optimal design for metal additive manufacturing: An integrated computational materials engineering (ICME) approach. JOM. 2020;72; doi:10.1007/s11837-020-04028-4
[45] Tandoc C, Hu Y, Qi L, et al. Mining of lattice distortion, strength, and intrinsic ductility of refractory high entropy alloys. npj Comput Mater. 2023;9:53. doi:10.1038/s41524-023-00993-x
[46] Liu X, Zhang J, Yin J, et al. Monte Carlo simulation of order-disorder transition in refractory high entropy alloys: a data-driven approach. Comput Mater Sci. 2021;187:110135.
[47] Bong Kim D, Shao G, Jo G. A digital twin implementation architecture for wire + arc additive manufacturing based on ISO 23247. Manufact Lett. 2022;34; doi:10.1016/j.mfglet.2022.08.008
[48] Vela B, Khatamsaz D, Acemi C, et al. Data-augmented modeling for yield strength of refractory high entropy alloys: a Bayesian approach. Acta Mater. 2023;261:119351.
[49] Tran A, Tranchida J, Wildey T, et al. Multi-fidelity machine-learning with uncertainty quantification and Bayesian optimization for materials design: application to ternary random alloys. J Chem Phys. 2020;153.
[50] Hashemi SM, Parvizi S, Baghbanijavid H, et al. Computational modelling of process–structure–property–performance relationships in metal additive manufacturing: a review. Intern Mater Rev. 2022;67:1–46.
[51] Tian D, Li C, Hu Z, et al. Modeling of the flow field and clad geometry of a molten pool during laser cladding

of CoCrCuFeNi high-entropy alloys. Materials (Basel). 2024;17:564.
[52] Mann A, Kalidindi SR. Development of a robust CNN model for capturing microstructure-property linkages and building property closures supporting material design. Front Mater. 2022;9; doi:10.3389/fmats.2022.851085
[53] Hu X, Zhao J, Chen Y, et al. Structure-property modeling scheme based on optimized microstructural information by two-point statistics and principal component analysis. J Mater Inform. 2022;2:N–A.
[54] Zhou Y, Yang B. Uncertainty quantification of predicting stable structures for high-entropy alloys using Bayesian neural networks. J Energy Chem. 2023;81:118–124.
[55] Yi Wang W, Li J, Liu W, et al. Integrated computational materials engineering for advanced materials: a brief review. Computat Mater Sci. 2019;158; doi:10.1016/j.commatsci.2018.11.001
[56] Ahsan MRU, Tanvir ANM, Ross T, et al. Fabrication of bimetallic additively manufactured structure (BAMS) of low carbon steel and 316L austenitic stainless steel with wire arc additive manufacturing. Rapid Prototyp J. 2020;26:519–530.
[57] Pan S, Yao G, Cui Y, et al. Additive manufacturing of tungsten, tungsten-based alloys, and tungsten matrix composites. Tungsten. 2023;5:1–31.
[58] Yang J, Wang S, Wang K, et al. Molybdenum-rhenium alloy: a focused review of strengthening-toughening mechanism and method. Intern J Refract Met Hard Mater. 2026;134; doi:10.1016/j.ijrmhm.2025.107408
[59] Morcos P, Elwany A, Karaman I, et al. Review: additive manufacturing of pure tungsten and tungsten-based alloys. J Mater Sci. 2022;57; doi:10.1007/s10853-022-07183-y
[60] Chinchanikar S, Shaikh AA. A review on machine learning, Big data analytics, and design for additive manufacturing for aerospace applications. J Materi Eng and Perform. 2022;31; doi:10.1007/s11665-022-07125-4
[61] Qin J, Hu F, Liu Y, et al. Research and application of machine learning for additive manufacturing. Addit Manufact. 2022;52:102691.
[62] Liang Z, Wu J, Liu C, et al. Microcracking in additively manufactured tungsten: experiment and a nano-micro-macro multiscale model. Int J Plast. 2025;186:104264.
[63] Vrancken B, Ganeriwala RK, Matthews MJ. Analysis of laser-induced microcracking in tungsten under additive manufacturing conditions: experiment and simulation. Acta Mater. 2020;194; doi:10.1016/j.actamat.2020.04.060
[64] Vrancken B, King WE, Matthews MJ. In-situ characterization of tungsten microcracking in Selective Laser Melting. Procedia CIRP. 2018;74; doi:10.1016/j.procir.2018.08.050
[65] Wang D, Li K, Yu C, et al. Cracking behavior in additively manufactured pure tungsten. Acta Metall Sin (Engl Lett). 2019;32:127–135.
[66] Guo M, Gu D, Xi L, et al. Selective laser melting additive manufacturing of pure tungsten: role of volumetric energy density on densification, microstructure and mechanical properties. Intern J Refract Met Hard Mater. 2019;84; doi:10.1016/j.ijrmhm.2019.105025
[67] Hu Z, Zhao Y, Guan K, et al. Pure tungsten and oxide dispersion strengthened tungsten manufactured by selective laser melting: microstructure and cracking mechanism. Addit Manufact. 2020;36; doi:10.1016/j.addma.2020.101579
[68] Ledford C, Fernandez-Zelaia P, Graening T, et al. Microstructure and high temperature properties of tungsten processed via electron beam melting additive manufacturing. Intern J Refract Met Hard Mater. 2023;113:106148.
[69] Ren X, Peng H, Li J, et al. Selective electron beam melting (SEBM) of pure tungsten: metallurgical defects, microstructure, texture and mechanical properties. Materials (Basel). 2022;15; doi:10.3390/ma15031172
[70] Dorow-Gerspach D, Kirchner A, Loewenhoff T, et al. Additive manufacturing of high density pure tungsten by electron beam melting. Nucl Mater Energy. 2021;28; doi:10.1016/j.nme.2021.101046
[71] Chen H, Zi X, Han Y, et al. Microstructure and mechanical properties of additive manufactured W-Ni-Fe-Co composite produced by selective laser melting. Intern J Refract Met Hard Mater. 2020;86; doi:10.1016/j.ijrmhm.2019.105111
[72] Wang YP, Ma SY, Yang XS, et al. Microstructure and strengthening mechanisms of 90W–7Ni–3Fe alloys prepared using laser melting deposition. J Alloys Compds. 2020;838; doi:10.1016/j.jallcom.2020.155545
[73] Li K, Wang D, Xing L, et al. Crack suppression in additively manufactured tungsten by introducing secondary-phase nanoparticles into the matrix. Intern J Refract Met Hard Mater. 2019;79; doi:10.1016/j.ijrmhm.2018.11.013
[74] Su S, Lu Y. Densified WCu composite fabricated via laser additive manufacturing. Intern J Refract Met Hard Mater. 2020;87; doi:10.1016/j.ijrmhm.2019.105122
[75] Xue J, Feng Z, Tang J, et al. Selective laser melting additive manufacturing of tungsten with niobium alloying: microstructure and suppression mechanism of microcracks. J Alloys Compds. 2021;874; doi:10.1016/j.jallcom.2021.159879
[76] Rebesan P, Ballan M, Bonesso M, et al. Pure molybdenum manufactured by Laser Powder Bed Fusion: thermal and mechanical characterization at room and high temperature. Addit Manufact. 2021;47; doi:10.1016/j.addma.2021.102277
[77] Leitz K, Grohs C, Singer P, et al. Fundamental analysis of the influence of powder characteristics in Selective Laser Melting of molybdenum based on a multi-physical simulation model. Intern J Refract Met Hard Mater. 2018;72; doi:10.1016/j.ijrmhm.2017.11.034
[78] Oehlerking F, Stawovy MT, Ohm S, et al. Microstructural characterization and mechanical properties of additively manufactured molybdenum and molybdenum alloys. Intern J Refract Met Hard Mater. 2022;109; doi:10.1016/j.ijrmhm.2022.105971
[79] Rock C, Lara-Curzio E, Ellis B, et al. Additive manufacturing of pure Mo and Mo+TiC MMC alloy by electron beam powder Bed fusion. JOM. 2020;72; doi:10.1007/s11837-020-04442-8
[80] Johnson JL, Palmer T. Directed energy deposition of molybdenum. Intern J Refract Met Hard Mater. 2019;84; doi:10.1016/j.ijrmhm.2019.105029

[81] Vanhoose JH. Investigating using titanium zirconium molybdenum for additively manufacturing aerospace components, ProQuest Dissertations & Theses, 2019, https://www.proquest.com/docview/2311651864.
[82] Cho J, Lee D, Seo G, et al. Optimizing the mean and variance of bead geometry in the wire arc additive manufacturing using a desirability function method. Intern J Adv Manufact Technol. 2022;120:7771–7783.
[83] Becker J, Fichtner D, Schmigalla S, et al. Oxidation response of additively manufactured eutectic Mo-Si-B alloys. IOP Confer Ser Mater Sci Eng. 2020;882; doi:10.1088/1757-899X/882/1/012002
[84] Krüger M, Schmelzer J, Fichtner D, et al. Recent advances in additive manufacturing of Mo-Si-B alloys – A status report on the cooperative project LextrA. IOP Confer Ser Mater Sci Eng. 2020;882; doi:10.1088/1757-899X/882/1/012011
[85] Liu M, Zhang J, Chen C, et al. Additive manufacturing of pure niobium by laser powder bed fusion: microstructure, mechanical behavior and oxygen assisted embrittlement. Mater Sci Eng A Struct Mater Propert Microstruct Process. 2023;866; doi:10.1016/j.msea.2023.144691
[86] Terrazas CA, Mireles J, Gaytan SM, et al. Fabrication and characterization of high-purity niobium using electron beam melting additive manufacturing technology. Int J Adv Manuf Technol. 2016;84; doi:10.1007/s00170-015-7767-x
[87] Chen J, Ding W, Tao Q, et al. Laser powder bed fusion of a Nb-based refractory alloy: microstructure and tensile properties. Mater Sci Eng A Struct Mater Propert Microstruct Process. 2022;843; doi:10.1016/j.msea.2022.143153
[88] Awasthi PD, Agrawal P, Haridas RS, et al. Mechanical properties and microstructural characteristics of additively manufactured C103 niobium alloy. Mater Sci Eng A Struct Mater Propert Microstruct Process. 2022;831; doi:10.1016/j.msea.2021.142183
[89] Lian F, Chen L, Wu C, et al. Selective laser melting additive manufactured tantalum: effect of microstructure and impurities on the strengthening-toughing mechanism. Materials (Basel). 2023;16; doi:10.3390/ma16083161
[90] Wang D, Yu C, Zhou X, et al. Dense pure tungsten fabricated by selective laser melting. Appl Sci. 2017;7:430.
[91] Wang J, Yao D, Li M, et al. Hierarchical effects of multi-layer powder spreading in the electron beam bed fusion additive of material. Addit Manufact. 2022: 55:102835.
[92] Zhou K, Chen W, Yang Y, et al. Microstructure and mechanical behavior of porous tungsten skeletons synthesized by selected laser melting. Intern J Refract Met Hard Mater. 2022;103:105769.
[93] Zhou X, Liu X, Zhang D, et al. Balling phenomena in selective laser melted tungsten. J Mater Process Technol. 2015;222:33–42.
[94] Karra VSSA, Webler BA. Processing of W and W-Ta alloys via laser powder feed directed energy deposition. Intern J Refract Met Hard Mater. 2023;116:106360.
[95] Field AC, Carter LN, Adkins N, et al. The effect of powder characteristics on build quality of high-purity tungsten produced via laser powder bed fusion (LPBF). Metall Mater Trans A. 2020;51:1367–1378.
[96] Guo M, Gu D, Xi L, et al. Formation of scanning tracks during selective laser melting (SLM) of pure tungsten powder: morphology, geometric features and forming mechanisms. Intern J Refract Met Hard Mater. 2019;79:37–46.
[97] Chen J, Li K, Wang Y, et al. The effect of hot isostatic pressing on thermal conductivity of additively manufactured pure tungsten. Intern J Refract Met Hard Mater. 2020;87:105135.
[98] Sidambe AT, Tian Y, Prangnell PB, et al. Effect of processing parameters on the densification, microstructure and crystallographic texture during the laser powder bed fusion of pure tungsten. Intern J Refract Met Hard Mater. 2019;78:254–263.
[99] Wen S, Wang C, Zhou Y, et al. High-density tungsten fabricated by selective laser melting: densification, microstructure, mechanical and thermal performance. Opt Laser Technol. 2019;116:128–138.
[100] Xiong Z, Zhang P, Tan C, et al. Selective laser melting and remelting of pure tungsten. Adv Eng Mater. 2020;22:1901352.
[101] Rebesan P, Bonesso M, Gennari C, et al. Tungsten fabricated by laser powder bed fusion. BHM Berg-und Hüttenmännische Monatshefte. 2021;166:263–269.
[102] Iveković A, Montero-Sistiaga ML, Vanmeensel K, et al. Effect of processing parameters on microstructure and properties of tungsten heavy alloys fabricated by SLM. Intern J Refract Met Hard Mater. 2019;82; doi:10.1016/j.ijrmhm.2019.03.020
[103] Ren X, Liu H, Lu F, et al. Effects of processing parameters on the densification, microstructure and mechanical properties of pure tungsten fabricated by optimized selective laser melting: from single and multiple scan tracks to bulk parts. Intern J Refract Met Hard Mater. 2021;96; doi:10.1016/j.ijrmhm.2021.105490
[104] Xie J, Lu H, Lu J, et al. Additive manufacturing of tungsten using directed energy deposition for potential nuclear fusion application. Surf Coat Technol. 2021;409:126884.
[105] Jeong W, Kwon Y, Kim D. Three-dimensional printing of tungsten structures by directed energy deposition. Mater Manuf Process. 2019;34:986–992.
[106] Pixner F, Buzolin R, Warchomicka F, et al. Wire-based electron beam additive manufacturing of tungsten. Intern J Refract Met Hard Mater. 2022;108:105917.
[107] Marinelli G, Martina F, Ganguly S, et al. Development of wire arc additive manufacture for the production of large-scale unalloyed tungsten components. Intern J Refract Met Hard Mater. 2019;82:329–335.
[108] Li J, Wu Y, Xue L, et al. Laser powder bed fusion in-situ alloying of refractory WTa alloy and its microstructure and mechanical properties. Addit Manufact. 2023;67; doi:10.1016/j.addma.2023.103493
[109] Iveković A, Omidvari N, Vrancken B, et al. Selective laser melting of tungsten and tungsten alloys. Intern J Refract Met Hard Mater. 2018;72:27–32.
[110] Li K, Ma G, Xing L, et al. Crack suppression via in-situ oxidation in additively manufactured W-Ta alloy. Mater Lett. 2020;263:127212.
[111] Li K, Li Y, Chen W, et al. Effect of Ta addition on the fuzz formation of additively manufactured W-based materials. Nucl Fus. 2020;60:064004.

[112] Guo Z, Wang L, Wang X. Additive manufacturing of W-12Ta (wt%) alloy: processing and resulting mechanical properties. J Alloys Compds. 2021;868:159193.
[113] Li J, Wei Z, Zhou B, et al. Preparation, microstructure, and microhardness of selective laser-melted W–3Ta sample. J Mater Res. 2020;35:2016–2024.
[114] Chen H, Ye L, Han Y, et al. Additive manufacturing of W–Fe composites using laser metal deposition: microstructure, phase transformation, and mechanical properties. Mater Sci Eng A. 2021;811; doi:10.1016/j.msea.2021.141036
[115] Tan Z, Zhou Z, Wu X, et al. In situ synthesis of spherical WMo alloy powder for additive manufacturing by spray granulation combined with thermal plasma spheroidization. Intern J Refract Met Hard Mater. 2021;95; doi:10.1016/j.ijrmhm.2020.105460
[116] Yang G, Jia W, Wang J, et al. Refined W-3.5Nb alloy fabricated by electron beam melting via doped carbon. Intern J Refract Met Hard Mater. 2023;111; doi:10.1016/j.ijrmhm.2022.106094
[117] F. Miranda, M.O. dos Santos, D. Rodrigues, R.S. Coelho, G.F. Batalha, Ni based tungsten heavy alloy processed by PBF-L additive manufacturing and conventional LPS routes, Mater Today Proc, 2023. doi:10.1016/j.matpr.2023.05.567
[118] Wang G, Sun X, Huang M, et al. Influence of processing parameters on the microstructure and tensile property of 85 W-15Ni produced by laser direct deposition. Intern J Refract Met Hard Mater. 2019;82; doi:10.1016/j.ijrmhm.2019.04.016
[119] Li J, Wei Z, Zhou B, et al. Densification, microstructure and properties of 90W-7Ni-3Fe fabricated by selective laser melting. Metals (Basel). 2019;9; doi:10.3390/met9080884
[120] Schwanekamp T, Müller A, Reuber M, et al. Investigations on laser powder bed fusion of tungsten heavy alloys. Intern J Refract Met Hard Mater. 2022;109; doi:10.1016/j.ijrmhm.2022.105959
[121] Verdonik TW, Pires M, Guo T, et al. Investigation of powder bed laser fusion additive manufacturing of 93W, 5.6Ni, 1.4Fe tungsten heavy alloys. Intern J Refract Met Hard Mater. 2023;111; doi:10.1016/j.ijrmhm.2022.106055
[122] Wei C, Ye H, Zhao Z, et al. Microstructure and fracture behavior of 90W-7Ni-3Fe alloy fabricated by laser directed energy deposition. J Alloys Compds. 2021;865; doi:10.1016/j.jallcom.2021.158975
[123] Wang M, Li R, Yuan T, et al. Selective laser melting of W-Ni-Cu composite powder: densification, microstructure evolution and nano-crystalline formation. Intern J Refract Met Hard Mater. 2018;70; doi:10.1016/j.ijrmhm.2017.09.004
[124] Vrancken B, Ganeriwala RK, Martin AA, et al. Microcrack mitigation during laser scanning of tungsten via preheating and alloying strategies. Addit Manufact. 2021;46:102158. doi:10.1016/j.addma.2021.102158
[125] Gu D, Dai D, Chen W, et al. Selective laser melting additive manufacturing of hard-to-process tungsten-based alloy parts With novel crystalline growth morphology and enhanced performance. J Manufact Sci Eng. 2016;138; doi:10.1115/1.4032192
[126] Chen J, Zhao C, Li K, et al. Effect of TaC addition on microstructure and microhardness of additively manufactured tungsten. J Alloys Compounds. 2022;897; doi:10.1016/j.jallcom.2021.162978
[127] Oehlerking F, Stawovy MT, Ohm S, et al. Microstructural characterization and mechanical properties of additively manufactured molybdenum and molybdenum alloys. Intern J Refract Met Hard Mater. 2022;109; doi:10.1016/j.ijrmhm.2022.105971
[128] Nguyen TDC, Choe J, Ebiwonjumi B, et al. Core design of long-cycle small modular lead-cooled fast reactor. Intern J Energy Res. 2019;43; doi:10.1002/er.4258
[129] Kaserer L, Braun J, Stajkovic J, et al. Fully dense and crack free molybdenum manufactured by selective laser melting through alloying with carbon. Intern J Refract Met Hard Mater. 2019;84; doi:10.1016/j.ijrmhm.2019.105000
[130] Braun J, Kaserer L, Stajkovic J, et al. Molybdenum and tungsten manufactured by selective laser melting: analysis of defect structure and solidification mechanisms. Intern J Refract Met Hard Mater. 2019;84; doi:10.1016/j.ijrmhm.2019.104999
[131] Faidel D, Jonas D, Natour G, et al. Investigation of the selective laser melting process with molybdenum powder. Addit Manufact. 2015;8:88–94.
[132] Zhou Z, He D, Tan Z, et al. Microstructure characters of W-based composites with different immiscible second phases prepared by laser powder bed fusion. J Alloys Compds. 2022;926; doi:10.1016/j.jallcom.2022.166982
[133] Wang G, Qin Y, Yang S. Influence of Ni additions on the microstructure and tensile property of W-Cu composites produced by direct energy deposition. J Alloys Compds. 2022;899; doi:10.1016/j.jallcom.2021.163272
[134] Wang G, Qin Y, Yang S. Characterization of laser-powder interaction and particle transport phenomena during laser direct deposition of W–Cu composite. Addit Manufact. 2021;37; doi:10.1016/j.addma.2020.101722
[135] Makineni SK, Kini AR, Jägle EA, et al. Synthesis and stabilization of a new phase regime in a Mo-Si-B based alloy by laser-based additive manufacturing. Acta Mater. 2018;151; doi:10.1016/j.actamat.2018.03.037
[136] Fichtner D, Schmelzer J, Yang W, et al. Additive manufacturing of a near-eutectic Mo–Si–B alloy: processing and resulting properties. Intermetallics. 2021;128:107025.
[137] Zhou W, Tsunoda K, Nomura N, et al. Effect of hot isostatic pressing on the microstructure and fracture toughness of laser additive-manufactured MoSiBTiC multiphase alloy. Mater Design. 2020;196; doi:10.1016/j.matdes.2020.109132
[138] Zhou W, Sun X, Tsunoda K, et al. Powder fabrication and laser additive manufacturing of MoSiBTiC alloy. Intermetallics. 2019;104; doi:10.1016/j.intermet.2018.10.012
[139] Takeda T, Zhou W, Nomura N, et al. Mechanical responses of additively manufactured MoSiBTiC alloy under tensile and compressive loadings. Mater Sci Eng A. 2022;839; doi:10.1016/j.msea.2022.142848
[140] Candela S, Ottelin J, Hongisto J, et al. W-Ta alloys processed by laser-based powder bed fusion: How microstructure and properties change with ta concentration. Intern J Refract Met Hard Mater. 2025:107324.

[141] Yang J, Huang Y, Liu B, et al. Precipitation behavior in a Nb-5W-2Mo-1Zr niobium alloy fabricated by electron beam selective melting. Mater Characteriz. 2021;174; doi:10.1016/j.matchar.2021.111019
[142] Guo Y, Chen C, Wang Q, et al. Effect of porosity on mechanical properties of porous tantalum scaffolds produced by electron beam powder bed fusion. Trans Nonferr Met Soc China. 2022;32; doi:10.1016/S1003-6326(22)65993-4
[143] Song C, Deng Z, Chen J, et al. Study on the influence of oxygen content evolution on the mechanical properties of tantalum powder fabricated by laser powder bed fusion. Mater Characteriz. 2023;205; doi:10.1016/j.matchar.2023.113235
[144] Guo Y, Chen C, He W, et al. Compressive fatigue behavior of graded tantalum scaffolds produced by electron beam powder bed fusion. J Mater Res Technol. 2023;24:6451–6462. doi:10.1016/j.jmrt.2023.04.235
[145] Liang D, Zhong C, Jiang F, et al. Fabrication of porous tantalum with Low elastic modulus and tunable pore size for bone repair. ACS Biomater Sci Eng. 2023;9; doi:10.1021/acsbiomaterials.2c01239
[146] Thijs L, Montero Sistiaga ML, Wauthle R, et al. Strong morphological and crystallographic texture and resulting yield strength anisotropy in selective laser melted tantalum. Acta Mater. 2013;61; doi:10.1016/j.actamat.2013.04.036
[147] Aliyu AAA, Poungsiri K, Shinjo J, et al. Additive manufacturing of tantalum scaffolds: processing, microstructure and process-induced defects. Intern J Refract Met Hard Mater. 2023;112; doi:10.1016/j.ijrmhm.2023.106132
[148] Jiao J, Hong Q, Zhang D, et al. Influence of porosity on osteogenesis, bone growth and osteointegration in trabecular tantalum scaffolds fabricated by additive manufacturing. Front Bioeng Biotechnol. 2023;11:1117954. doi:10.3389/fbioe.2023.1117954
[149] Wauthle R, van der Stok J, Amin Yavari S, et al. Additively manufactured porous tantalum implants. Acta Biomater. 2015;14; doi:10.1016/j.actbio.2014.12.003
[150] Zhang Y, Aiyiti W, Du S, et al. Design and mechanical behaviours of a novel tantalum lattice structure fabricated by SLM. Virt Phys Prototyp. 2023;18:e2192702. doi:10.1080/17452759.2023.2192702
[151] Balla VK, Bodhak S, Bose S, et al. Porous tantalum structures for bone implants: fabrication, mechanical and in vitro biological properties. Acta Biomater. 2010;6; doi:10.1016/j.actbio.2010.01.046
[152] Bandyopadhyay A, Mitra I, Shivaram A, et al. Direct comparison of additively manufactured porous titanium and tantalum implants towards in vivo osseointegration. Addit Manufact. 2019;28; doi:10.1016/j.addma.2019.04.025
[153] Marinelli G, Martina F, Ganguly S, et al. Microstructure, hardness and mechanical properties of two different unalloyed tantalum wires deposited via wire + arc additive manufacture. Intern J Refract Met Hard Mater. 2019;83; doi:10.1016/j.ijrmhm.2019.104974
[154] Sing SL, Wiria FE, Yeong WY. Selective laser melting of titanium alloy with 50 wt% tantalum: effect of laser process parameters on part quality. Intern J Refract Met Hard Mater. 2018;77; doi:10.1016/j.ijrmhm.2018.08.006
[155] Dobbelstein H, Gurevich EL, George EP, et al. Laser metal deposition of a refractory TiZrNbHfTa high-entropy alloy. Addit Manufact. 2018;24; doi:10.1016/j.addma.2018.10.008
[156] Dobbelstein H, Gurevich EL, George EP, et al. Laser metal deposition of compositionally graded TiZrNbTa refractory high-entropy alloys using elemental powder blends. Addit Manufact. 2019;25:252–262.
[157] Zadorozhnyy V, Tomilin I, Berdonosova E, et al. Composition design, synthesis and hydrogen storage ability of multi-principal-component alloy TiVZrNbTa. J Alloys Compds. 2022;901; doi:10.1016/j.jallcom.2022.163638
[158] Katz-Demyanetz A, Gorbachev II, Eshed E, et al. High entropy Al0.5CrMoNbTa0.5 alloy: additive manufacturing vs. casting vs. CALPHAD approval calculations. Mater Charact. 2020;167; doi:10.1016/j.matchar.2020.110505
[159] Gou S, Gao M, Shi Y, et al. Additive manufacturing of ductile refractory high-entropy alloys via phase engineering. Acta Mater. 2023;248; doi:10.1016/j.actamat.2023.118781
[160] Xiao B, Liu H, Jia W, et al. Cracking suppression in selective electron beam melted WMoTaNbC refractory high-entropy alloy. J Alloys Compds. 2023;948; doi:10.1016/j.jallcom.2023.169787
[161] Zhang H, Zhao Y, Huang S, et al. Manufacturing and analysis of high-performance refractory high-entropy alloy via selective laser melting (SLM). Materials (Basel). 2019;12; doi:10.3390/ma12050720
[162] Zhang H, Zhao Y, Cai J, et al. High-strength NbMoTaX refractory high-entropy alloy with low stacking fault energy eutectic phase via laser additive manufacturing. Mater Des. 2021;201; doi:10.1016/j.matdes.2021.109462
[163] Chen Y, Li B. Double-phase refractory medium entropy alloy NbMoTi via selective laser melting (SLM) additive manufacturing. J Phys Conf Ser. 2023;2419; doi:10.1088/1742-6596/2419/1/012074
[164] Wang F, Kang L, Lin S, et al. High compressive plasticity refractory medium entropy alloy fabricated by laser powder bed fusion using elemental blended powders. Mater Sci Eng A. 2023;880; doi:10.1016/j.msea.2023.145363
[165] Dobbelstein H, Thiele M, Gurevich EL, et al. Direct metal deposition of refractory high entropy alloy MoNbTaW. Phys Procedia. 2016;83; doi:10.1016/j.phpro.2016.08.065
[166] Huber F, Bartels D, Schmidt M. In-Situ alloy formation of a WMoTaNbV refractory metal high entropy alloy by laser powder Bed fusion (PBF-LB/M). Materials (Basel). 2021;14; doi:10.3390/ma14113095
[167] Li Q, Zhang H, Li D, et al. Wxnbmota refractory high-entropy alloys fabricated by laser cladding deposition. Materials (Basel). 2019;12; doi:10.3390/ma12030533
[168] Liu C, Zhu K, Ding W, et al. Additive manufacturing of WMoTaTi refractory high-entropy alloy by employing fluidised powders. Powder Metall. 2022;65; doi:10.1080/00325899.2022.2031718
[169] Xiao B, Jia W, Wang J, et al. Selective electron beam melting of WMoTaNbVFeCoCrNi refractory high-entropy alloy. Mater Charact. 2022;193; doi:10.1016/j.matchar.2022.112278
[170] Zhao S, Taheri M, Shirvani K, et al. Microstructure of NbMoTaTiNi refractory high-entropy alloy coating fabricated by ultrasonic field-assisted laser cladding process. Coatings. 2023;13; doi:10.3390/coatings13060995

[171] Wang BW, Luo P, Zhang LJ, et al. Selective laser melting of multi-principal NiCrWFeTi alloy: processing, microstructure and performance. Mater Sci Forum. 2019;944; doi:10.4028/www.scientific.net/MSF.944.182
[172] Yang X, Zhou Y, Xi S, et al. Additively manufactured fine grained Ni6Cr4WFe9Ti high entropy alloys with high strength and ductility. Mater Sci Eng A. 2019;767; doi:10.1016/j.msea.2019.138394
[173] Jia Y, Chen H, Liang X. Microstructure and wear resistance of CoCrNbNiW high-entropy alloy coating prepared by laser melting deposition. Rare Met. 2019;38; doi:10.1007/s12598-019-01342-y
[174] Wang B, An X, Huang Z, et al. Nitrogen doped Co-Cr-Mo-W based alloys fabricated by selective laser melting with enhanced strength and good ductility. J Alloys Compds. 2019;785; doi:10.1016/j.jallcom.2019.01.178
[175] Sarswat PK, Sarkar S, Murali A, et al. Additive manufactured new hybrid high entropy alloys derived from the AlCoFeNiSmTiVZr system. Appl Surf Sci. 2019;476; doi:10.1016/j.apsusc.2018.12.300
[176] Jeong H, Lee C, Kim D. Manufacturing of Ti-Nb-Cr-V-Ni-Al refractory high-entropy alloys using direct energy deposition. Materials (Basel). 2022;15; doi:10.3390/ma15196570
[177] Abed H, Malek Ghaini F, Shahverdi HR. Characterization of Fe49Cr18Mo7B16C4Nb6 high-entropy hardfacing layers produced by gas tungsten arc welding (GTAW) process. Surf Coat Technol. 2018;352; doi:10.1016/j.surfcoat.2018.08.019
[178] Su B, Li J, Yang C, et al. Microstructure and mechanical properties of a refractory AlMo0.5NbTa0.5TiZr high-entropy alloy manufactured by laser-directed energy deposition. Mater Lett. 2023;335:133980. doi:10.1016/j.matlet.2022.133748
[179] Ye X, Zhang M, Wang D, et al. Carbon nanotubes (CNTs) reinforced CoCrMoNbTi0.4 refractory high entropy alloy fabricated via laser additive manufacturing: processing optimization, microstructure transformation and mechanical properties. Crystals (Basel). 2022;12; doi:10.3390/cryst12111678
[180] Preisler D, Krajňák T, Janeček M, et al. Directed energy deposition of bulk Nb-Ta-Ti-Zr refractory complex concentrated alloy. Mater Lett. 2023;337:133980. doi:10.1016/j.matlet.2023.133980
[181] Agbedor S, Wu H, Yang D, et al. Inhibiting grain boundary cracking in laser additively-manufactured MoNbTaVTiCu refractory complex concentrated alloys by tuning the Cu/Ti content. Manufact Lett. 2025;43; doi:10.1016/j.mfglet.2024.10.008
[182] Mohd Jani J, Leary M, Subic A, et al. A review of shape memory alloy research, applications and opportunities. Mater Design (1980-2015). 2014: 56), doi:10.1016/j.matdes.2013.11.084
[183] Yi X, Wang Y, Liu W, et al. Unraveling role of Co addition in microstructure and mechanical properties of biomedical Ti-Nb based shape memory alloy. Mater Characteriz. 2023;200; doi:10.1016/j.matchar.2023.112848
[184] Alagha AN, Hussain S, Zaki W. Additive manufacturing of shape memory alloys: A review with emphasis on powder bed systems. Mater Design. 2021;204; doi:10.1016/j.matdes.2021.109654
[185] Khimich MA, Prosolov KA, Mishurova T, et al. Advances in laser additive manufacturing of Ti-Nb alloys: from nanostructured powders to bulk objects. Nanomaterials. 2021;11; doi:10.3390/nano11051159
[186] Mehrpouya M, Alberto Biffi C, Lemke JN, et al. Additive manufacturing of architected shape memory alloys: a review. Virt Phys Prototyp. 2024;19:e2414395.
[187] Kim YS, Yun D, Han JH, et al. Bimetallic additively manufactured structure (BAMS) of inconel 625 and austenitic stainless steel: effect of heat-treatment on microstructure and mechanical properties. Intern J Adv Manufact Technol. 2022;121:7539–7549.
[188] Ostolaza M, Arrizubieta JI, Lamikiz A, et al. Latest developments to manufacture metal matrix composites and functionally graded materials through AM: A state-of-the-Art review. Materials (Basel). 2023;16:1746.
[189] Zhang C, Chen F, Huang Z, et al. Additive manufacturing of functionally graded materials: A review. Mater Sci Eng A. 2019;764:138209.
[190] Blakey-Milner B, Gradl P, Snedden G, et al. Metal additive manufacturing in aerospace: A review. Mater Des. 2021;209:110008.
[191] Wei C, Liu L, Gu Y, et al. Multi-material additive-manufacturing of tungsten – copper alloy bimetallic structure with a stainless-steel interlayer and associated bonding mechanisms. Addit Manufact. 2022;50; doi:10.1016/j.addma.2021.102574
[192] Tan C, Zhou K, Kuang T. Selective laser melting of tungsten-copper functionally graded material. Mater Lett. 2019;237; doi:10.1016/j.matlet.2018.11.127
[193] Jadhav S, Tanvir G, Karim MA, et al. Microstructures and mechanical behaviour of bimetallic structures of tungsten alloy (90WNiFe) and nickel alloy (In625) fabricated by wire-arc directed energy deposition. Virt Phys Prototyp. 2024;19; doi:10.1080/17452759.2024.2370957
[194] Jadhav S, Bajestani MS, Islam S, et al. Materials characterization of Ti6Al4 V to NbZr1 bimetallic structure fabricated by wire arc additive manufacturing. Mater Today Communic. 2023;36; doi:10.1016/j.mtcomm.2023.106934
[195] Abdul Karim M, Jeon Y, Bong Kim D. Trailblazing multi-material structure: niobium alloy to tungsten–copper composite using wire-arc additive manufacturing. Mater Lett. 2024;375; doi:10.1016/j.matlet.2024.137246
[196] Reichardt A, Shapiro AA, Otis R, et al. Advances in additive manufacturing of metal-based functionally graded materials. Intern Mater Rev. 2021;66; doi:10.1080/09506608.2019.1709354
[197] He B, Wu D, Pan J, et al. Effect of heat treatment on microstructure and mechanical properties of laser deposited TA15/Ti2AlNb gradient composite structures. Vacuum. 2021;190:110309.
[198] Liu Y, Zhang Y. Microstructure and mechanical properties of TA15-Ti2AlNb bimetallic structures by laser additive manufacturing. Mater Sci Eng A. 2020;795:140019.
[199] Chen H, Liu Z, Cheng X, et al. Laser deposition of graded γ-TiAl/Ti2AlNb alloys: microstructure and nanomechanical characterization of the transition zone. J Alloys Compds. 2021;875; doi:10.1016/j.jallcom.2021.159946
[200] Kang N, Lin X, Mansori ME, et al. On the effect of the thermal cycle during the directed energy deposition application to the in-situ production of a Ti-Mo alloy

functionally graded structure. Addit Manufact. 2020;31; doi:10.1016/j.addma.2019.100911
[201] Dobbelstein H, George EP, Gurevich EL, et al. Laser metal deposition of refractory high-entropy alloys for high-throughput synthesis and structure-property characterization. IJEM. 2020;3:015201. doi:10.1088/2631-7990/abcca8
[202] Moorehead M, Bertsch K, Niezgoda M, et al. High-throughput synthesis of Mo-Nb-Ta-W high-entropy alloys via additive manufacturing. Mater Design. 2020;187; doi:10.1016/j.matdes.2019.108358
[203] Liu S, Grohol CM, Shin YC. High throughput synthesis of CoCrFeNiTi high entropy alloys via directed energy deposition. J Alloys Compds. 2022;916; doi:10.1016/j.jallcom.2022.165469
[204] Wang B, Lu B, Zhang L, et al. Rapid in situ alloying of CoCrFeMnNi high-entropy alloy from elemental feedstock toward high-throughput synthesis via laser powder bed fusion. Front Mech Eng. 2023;18; doi:10.1007/s11465-022-0727-x
[205] Vela B, Acemi C, Singh P, et al. High-throughput exploration of the WMoVTaNbAl refractory multi-principal-element alloys under multiple-property constraints. Acta Mater. 2023;248; doi:10.1016/j.actamat.2023.118784
[206] Qiao L, Liu Y, Zhu J. A focused review on machine learning aided high-throughput methods in high entropy alloy. J Alloys Compds. 2021;877; doi:10.1016/j.jallcom.2021.160295
[207] Zhu C, Li C, Wu D, et al. A titanium alloys design method based on high-throughput experiments and machine learning. J Mater Res Technol. 2021;11:2336–2353. doi:10.1016/j.jmrt.2021.02.055
[208] Feng R, Zhang C, Gao MC, et al. High-throughput design of high-performance lightweight high-entropy alloys. Nat Commun. 2021;12; doi:10.1038/s41467-021-24523-9
[209] Chen B, Zhuo L. Latest progress on refractory high entropy alloys: composition, fabrication, post processing, performance, simulation and prospect. Intern J Refract Met Hard Mater. 2022;110:105993.
[210] Ouyang G, Singh P, Su R, et al. Design of refractory multi-principal-element alloys for high-temperature applications. npj Computat Mater. 2023: 9:141.
[211] Islam S, Jadhav S, Park T, et al. Crystal plasticity approach for predicting mechanical responses in wire-arc directed energy deposition of NbZr1 refractory alloy. Addit Manufact. 2024;84; doi:10.1016/j.addma.2024.104107
[212] Kim DB, Witherell P, Lipman R, et al. Streamlining the additive manufacturing digital spectrum: A systems approach. Addit Manufact. 2015;5; doi:10.1016/j.addma.2014.10.004
[213] Thompson MK, Moroni G, Vaneker T, et al. Design for additive manufacturing: trends, opportunities, considerations, and constraints. CIRP Ann. 2016;65; doi:10.1016/j.cirp.2016.05.004
[214] Jiang J, Xiong Y, Zhang Z, et al. Machine learning integrated design for additive manufacturing. J Intell Manuf. 2022;33; doi:10.1007/s10845-020-01715-6
[215] Vaneker T, Bernard A, Moroni G, et al. Design for additive manufacturing: framework and methodology. CIRP Ann. 2020;69; doi:10.1016/j.cirp.2020.05.006
[216] Gandhi Y, Minak G. A review on topology optimization strategies for additively manufactured continuous fiber-reinforced composite structures. Appl Sci. 2022;12; doi:10.3390/app122111211
[217] Vasan R, Dany D, Rao CK, et al. Design optimization and additive manufacturing of an aircraft seat. AIP Confer Proc. 2023: 2788), doi:10.1063/5.0148590
[218] Liu J, Gaynor AT, Chen S, et al. Current and future trends in topology optimization for additive manufacturing. Struct Multidisc Optim. 2018;57; doi:10.1007/s00158-018-1994-3
[219] Sachin S, Amancio-Filho ST, Paulo DJ. Design and topology optimization for additive manufacturing of multilayer (SS316L and AlSi10Mg) piston. Adv Met Addit Manufact. 2023: 1.), doi:10.1016/B978-0-323-91230-3.00002-0
[220] Ibhadode O, Zhang Z, Sixt J, et al. Topology optimization for metal additive manufacturing: current trends, challenges, and future outlook. Virt Phys Prototyp. 2023;18; doi:10.1080/17452759.2023.2181192
[221] Jankovics D, Barari A. Customization of automotive structural components using additive manufacturing and topology optimization. IFAC-PapersOnLine. 2019;52; doi:10.1016/j.ifacol.2019.10.066
[222] Mishra V, Ayas C, Langelaar M. Design for material properties of additively manufactured metals using topology optimization. Mater Des. 2023;235; doi:10.1016/j.matdes.2023.112388
[223] Briard T, Segonds F, Zamariola N. G-DfAM: a methodological proposal of generative design for additive manufacturing in the automotive industry. Int J Interact Des Manuf. 2020;14; doi:10.1007/s12008-020-00669-6
[224] Oh S, Jung Y, Kim S, et al. Deep generative design: integration of topology optimization and generative models. J Mech Des. 2019;141; doi:10.1115/1.4044229
[225] Li J, Ye H, Wei N, et al. ResUNet involved generative adversarial network-based topology optimization for design of 2D microstructure with extreme material properties. Math Mech Solids. 2024;29; doi:10.1177/10812865241233013
[226] Venugopal V, Anand S. Structural and thermal generative design using reinforcement learning-based search strategy for additive manufacturing. Manufact Lett. 2023;35; doi:10.1016/j.mfglet.2023.08.030
[227] Chandrasekera T, Hosseini Z, Perera U. Can artificial intelligence support creativity in early design processes? Intern J Architect Comput. 2024. doi:10.1177/14780771241254637
[228] Fang C, Zhu Y, Fang L, et al. Generative AI-enhanced human-AI collaborative conceptual design: A systematic literature review. Des Stud. 2025;97; doi:10.1016/j.destud.2025.101300
[229] Kim DB, Bajestani MS, Lee JY, et al. Introduction of human-in-the-loop in smart manufacturing (H-SM). Intern J Precis Eng Manufact Smart Technol. 2024;2; doi:10.57062/ijpem-st.2024.00115
[230] Kim DB, Bajestani MS, Shao G, et al. n.d. Conceptual architecture of digital twin With human-in-the-loop-based smart manufacturing. Adv Manufact; 3; doi:10.1115/IMECE2023-112791
[231] Ng WL, Goh GL, Goh GD, et al. Progress and opportunities for machine learning in materials and processes

of additive manufacturing. Advanced Materials (Weinheim. 2024;36; doi:10.1002/adma.202310006
[232] Ali S, Prajapati MJ, Bhat C, et al. Additive manufactured enabled digital metallurgy processes, challenges and future prospects. Appl Mater Today. 2025;42:102580.
[233] Mu H, He F, Yuan L, et al. Online distortion simulation using generative machine learning models: A step toward digital twin of metallic additive manufacturing. J Industr Inform Integr. 2024;38; doi:10.1016/j.jii.2024.100563
[234] Bandyopadhyay A, Traxel KD, Lang M, et al. Alloy design via additive manufacturing: advantages, challenges, applications and perspectives. Mater Today. 2022;52; doi:10.1016/j.mattod.2021.11.026
[235] Catal AA, Bedir E, Yilmaz R, et al. Machine learning assisted design of novel refractory high entropy alloys with enhanced mechanical properties. Computat Mater Sci. 2024;231:112612.
[236] Gao T, Gao J, Yang S, et al. Data-driven design of novel lightweight refractory high-entropy alloys with superb hardness and corrosion resistance., npj Computat Mater. 2024;10:256.
[237] Gupta KK, Barman S, Dey S, et al. Explainable machine learning assisted molecular-level insights for enhanced specific stiffness exploiting the large compositional space of AlCoCrFeNi high entropy alloys. Mach Learn Sci Technol. 2024;5:025082.
[238] Swateelagna S, Singh M, Rahul MR. Explainable machine learning based approach for the design of new refractory high entropy alloys. Intermetallics. 2024;167:108198.
[239] Liu S, Bocklund B, Diffenderfer J, et al. A comparative study of predicting high entropy alloy phase fractions with traditional machine learning and deep neural networks., npj Comput Mater. 2024;10; doi:10.1038/s41524-024-01335-1
[240] Shargh AK, Stiles CD, El-Awady JA. Deep learning accelerated phase prediction of refractory multi-principal element alloys. Acta Mater. 2025;283:120558.
[241] Yi W, Gao J, Zhang L. A CALPHAD thermodynamic model for multicomponent alloys under pressure and its application in pressurized solidified Al–Si–Mg alloys. Adv Powder Mater. 2024;3; doi:10.1016/j.apmate.2024.100182
[242] Singh P, Acemi C, Kuchibhotla A, et al. Alloying effects on the transport properties of refractory high-entropy alloys. Acta Mater. 2024;276; doi:10.1016/j.actamat.2024.120032
[243] Michael FN, Sowards JW. CALPHAD Models to Guide Refractory Alloys Additive Manufacturing: In-Situ Compounds Formation, Nanoparticles, and Impurities Considerations, 2023. https://ntrs.nasa.gov/citations/20230006677.
[244] Shahzad K, Mardare AI, Hassel AW. Accelerating materials discovery: combinatorial synthesis, high-throughput characterization, and computational advances, science and technology of advanced materials. Methods. 2024;4; doi:10.1080/27660400.2023.2292486
[245] Jadhav S, Jeong GH, Bajestani MS, et al. Investigation of surface roughness, microstructure, and mechanical properties of overhead structures fabricated by wire + arc additive manufacturing. Int J Adv Manuf Technol. 2024;131; doi:10.1007/s00170-024-13330-3
[246] Fang Q, Xiong G, Zhao M, et al. Probabilistic data-driven modeling of a melt pool in laser powder bed fusion additive manufacturing. IEEE Trans Autom Sci Eng. 2024;22:4908–4925.
[247] Cao Y, Chen C, Xu S, et al. Machine learning assisted prediction and optimization of mechanical properties for laser powder bed fusion of Ti6Al4 V alloy. Additive Manufacturing. 2024;91:104341.
[248] Dai R, Guo H, Liu J, et al. Predictive modeling and optimization of layer-cladded Ti-Al-Nb-Zr high-entropy alloys using machine learning. Coatings. 2024;14:1319.
[249] Dong F, Yuan Y, Li W, et al. Hot deformation behavior and processing maps of an equiatomic MoNbHfZrTi refractory high entropy alloy. Intermetallics. 2020;126; doi:10.1016/j.intermet.2020.106921
[250] NASA/NIST/FAA. Technical Interchange Meeting on Computational Materials Approaches for Qualification by Analysis for Aerospace Applications, 2021. https://search.proquest.com/docview/2656866383.
[251] Panicker N, Prabhune B, Delchini M, et al. Integrated Process and Materials Modeling for Development of Additive Manufacturing of Refractory Materials for Critical Applications, 2024. https://www.osti.gov/servlets/purl/2397457.
[252] Doan D. Microstructure-dependent nanoindentation deformation behavior of TaTiZrV refractory high-entropy alloy. Intern J Refract Met Hard Mater. 2024;123; doi:10.1016/j.ijrmhm.2024.106769
[253] Vanani BB, Islam S, Bajestani MS, et al. Microstructure evolution and mechanical behaviors of Ti6Al4 V/NbZr1 bimetallic additively manufactured structure: A molecular dynamics simulation. J Mater Res Technol. 2025;37:3466–3477.
[254] Sharma S, Krishna KVM, Joshi SS, et al. Laser based additive manufacturing of tungsten: multi-scale thermo-kinetic and thermo-mechanical computational model and experiments. Acta Mater. 2023;259; doi:10.1016/j.actamat.2023.119244
[255] Mooraj S, Kim G, Fan X, et al. Additive manufacturing of defect-free TiZrNbTa refractory high-entropy alloy with enhanced elastic isotropy via in-situ alloying of elemental powders. Commun Mater. 2024;5; doi:10.1038/s43246-024-00452-0
[256] Heller L, Karafitov I, Petrich L, et al. Numerical microstructure model of NiTi wire reconstructed from 3D-XRD data. MSMSE. 2020;28; doi:10.1088/1361-651X/ab89c1
[257] Kouraytem N, Li X, Tan W, et al. Modeling process–structure–property relationships in metal additive manufacturing: a review on physics-driven versus data-driven approaches. J Phys Materials. 2021;4; doi:10.1088/2515-7639/abca7b
[258] Li W, Raman L, Debnath A, et al. Design and validation of refractory alloys using machine learning, CALPHAD, and experiments. Intern J Refract Met Hard Mater. 2024;121; doi:10.1016/j.ijrmhm.2024.106673
[259] Sheikh S, Vela B, Honarmandi P, et al. High-throughput alloy and process design for metal additive manufacturing. npj Comput Mater. 2025;11; doi:10.1038/s41524-025-01670-x

[260] Wen T, Li Z, Wang J, et al. CALPHAD aided design of a crack-free Al-Mg-Si-Ti alloy with high strength: heterogeneous nucleation and eutectic filling during additive manufacturing. Virt Phys Prototyp. 2024;19; doi:10.1080/17452759.2024.2378930
[261] Zhang Y, Yang C, Ke H, et al. A study on the microstructure and mechanical behavior of CoCrFeNi high entropy alloy fabricated via laser powder bed fusion: experiment and crystal plasticity finite element modelling. Mater Sci Eng A. 2024;893:146111.
[262] Giudicelli G, Lindsay A, Harbour L, et al. 3.0 – MOOSE: enabling massively parallel multiphysics simulations. SoftwareX. 2024;26; doi:10.1016/j.softx.2024.101690
[263] Yaghoobi M, Ganesan S, Sundar S, et al. PRISMS-Plasticity: An open-source crystal plasticity finite element software. Computat Mater Sci. 2019;169; doi:10.1016/j.commatsci.2019.109078
[264] Rezaei MJ, Sedighi M, Pourbashiri M. Developing a new method to represent the low and high angle grain boundaries by using multi-scale modeling of crystal plasticity. J Alloys Compds. 2023;939:168844.
[265] He J, Li Z, Lin J, et al. Machine learning-assisted design of refractory high-entropy alloys with targeted yield strength and fracture strain. Mater Des. 2024;246; doi:10.1016/j.matdes.2024.113326
[266] Steingrimsson B, Fan X, Feng R, et al. A physics-based machine-learning approach for modeling the temperature-dependent yield strengths of medium – or high-entropy alloys. Appl Mater Today. 2023;31; doi:10.1016/j.apmt.2023.101747
[267] Feng J, Wang B, Zhang Y, et al. High-temperature creep mechanism of Ti-Ta-Nb-Mo-Zr refractory high-entropy alloys prepared by laser powder bed fusion technology. Int J Plast. 2024;181:104080.
[268] Garg A, Sharma A, Zheng W, et al. A review on artificial intelligence-enabled mechanical analysis of 3D printed and FEM-modelled auxetic metamaterials. Virt Phys Prototyp. 2025;20; doi:10.1080/17452759.2024.2445712
[269] Babu SS, Mourad AI, Harib KH, et al. Recent developments in the application of machine-learning towards accelerated predictive multiscale design and additive manufacturing. Virt Phys Prototyp. 2023;18; doi:10.1080/17452759.2022.2141653
[270] Lei Z, Zhou J, Wang Y, et al. A multi-source data-driven machine learning framework for predicting fatigue crack paths in polycrystalline superalloys. Int J Fatigue. 2025;200; doi:10.1016/j.ijfatigue.2025.109072
[271] Zafar MQ, Wu C, Zhao H, et al. Numerical simulation for electron beam selective melting PBF additive manufacturing of molybdenum. Intern J Adv Manufact Technol. 2021;117:1575–1588.
[272] Wu Y, Li M, Wang J, et al. Powder-bed-fusion additive manufacturing of molybdenum: process simulation, optimization, and property prediction. Addit Manufact. 2022;58:103069.
[273] Wang C, Li ZJ, Ji CQ, et al. Crystal plasticity analysis of the evolutions of temperature, stress and dislocation in additively manufactured tungsten. Intern J Refract Met Hard Mater. 2023;110; doi:10.1016/j.ijrmhm.2022.106041
[274] Berry J, Perron A, Fattebert J, et al. Toward multiscale simulations of tailored microstructure formation in metal additive manufacturing. Mater Today. 2021;51:65–86.
[275] Tukaç ÖU. *Development and additive manufacturing of refractory high entropy alloys for extreme environment applications*. Middle East Technical University; 2023.
[276] Buranich V, Rogoz V, Postolnyi B, et al. Predicting the Properties of the Refractory High-Entropy Alloys for Additive Manufacturing-Based Fabrication and Mechatronic Applications, 2020 IEEE 10th International Conference Nanomaterials: Applications & Properties (NAP) 1–5.
[277] Borg CK, Frey C, Moh J, et al. Expanded dataset of mechanical properties and observed phases of multi-principal element alloys. Sci Data. 2020;7:430.
[278] Zhu W, Huo W, Wang S, et al. Machine learning-based hardness prediction of high-entropy alloys for laser additive manufacturing. JOM. 2023;75:5537–5548.
[279] Bell SB, Pint BA, Ridley MJ, et al. High temperature mechanical behavior of refractory alloys with digital image correlation. Adv Mater Technol Power Plants. 2024; 84871:62–73.
[280] Mani M, Feng S, Lane B, et al. Measurement science needs for real-time control of additive manufacturing powder bed fusion processes, 2015.
[281] Ye J, Bab-hadiashar A, Alam N, et al. A review of the parameter-signature-quality correlations through in situ sensing in laser metal additive manufacturing. Int J Adv Manuf Technol. 2023;124; doi:10.1007/s00170-022-10618-0
[282] Kim E, Lee D, Seo G, et al. Development of a CNN-based real-time monitoring algorithm for additively manufactured molybdenum. Sens Actuat A Phys. 2023;352; doi:10.1016/j.sna.2023.114205
[283] Cho H, Shin S, Seo G, et al. Real-time anomaly detection using convolutional neural network in wire arc additive manufacturing: molybdenum material. J Mater Process Technol. 2022;302:117495.
[284] Park H, Mullin KM, Kumar V, et al. Resolving thermal gradients and solidification velocities during laser melting of a refractory alloy, arXiv preprint arXiv:2410.22496, 2024.
[285] Jobes DK, Liu Y, Lopez L, et al. Probing rapid solidification pathways in refractory complex concentrated alloys via multimodal synchrotron X-ray imaging and melt pool-scale simulation. J Mater Res. 2024;40:81–97.
[286] Wang H, Gould B, Moorehead M, et al. In situ X-ray and thermal imaging of refractory high entropy alloying during laser directed deposition. J Mater Process Technol. 2022;299; doi:10.1016/j.jmatprotec.2021.117363
[287] Zhang Y, Yan W. Applications of machine learning in metal powder-bed fusion in-process monitoring and control: status and challenges. J Intell Manuf. 2022;34:2557–2580.
[288] Chung J, Shen B, Law ACC, et al. Reinforcement learning-based defect mitigation for quality assurance of additive manufacturing. J Manuf Syst. 2022;65:822–835.
[289] Wasmer K, Le-Quang T, Meylan B, et al. In situ quality monitoring in AM using acoustic emission: A reinforcement learning approach. J Mater Eng Perform. 2019;28:666–672.

[290] Knaak C, Masseling L, Duong E, et al. Improving build quality in laser powder bed fusion using high dynamic range imaging and model-based reinforcement learning. IEEE Access. 2021;9:55214–55231.
[291] McAndrew AR, Alvarez Rosales M, Colegrove PA, et al. Interpass rolling of Ti-6Al-4 V wire + arc additively manufactured features for microstructural refinement. Addit Manufact. 2018;21; doi:10.1016/j.addma.2018.03.006
[292] Hu Y, Ao N, Wu S, et al. Influence of in situ micro-rolling on the improved strength and ductility of hybrid additively manufactured metals. Eng Fract Mech. 2021;253; doi:10.1016/j.engfracmech.2021.107868
[293] Hönnige J, Seow CE, Ganguly S, et al. Study of residual stress and microstructural evolution in as-deposited and inter-pass rolled wire plus arc additively manufactured inconel 718 alloy after ageing treatment. Mater Sci Eng A. 2021;801; doi:10.1016/j.msea.2020.140368
[294] Zhang Y, Cai S, Yang Z, et al. Laser shock forging – a novel in situ method designed towards controlling residual stresses in laser metal deposition. Int J Adv Manuf Technol. 2023;125:2289–2304. doi:10.1007/s00170-023-10874-8
[295] Ngo A, Kohlhorst N, Fialkova S, et al. Mechanical property improvements of LPBF-AlSi10Mg via forging to modify microstructure and defect characteristics. Manufact Lett. 2024;41; doi:10.1016/j.mfglet.2024.09.072
[296] Warzanskyj W, Özcan B, Luo J, et al. Mechanical and high-temperature characterization of additively manufactured Ni-superalloys at SALSA neutron strain diffractometer. Nucl Instrum Meth Phys Res Sect A Accel Spectrom Detect Assoc Equip. 2024;1067; doi:10.1016/j.nima.2024.169709
[297] Chen C, Sun H, Zhang Z, et al. Grain structure control of TC11 alloy in laser direct energy deposition by a static magnetic field. Materialia. 2024;38; doi:10.1016/j.mtla.2024.102267
[298] Chen L, Li Y, Yu T, et al. Effects of ultrasonic shot peening process on the microstructure and mechanical properties of nickel-based superalloys formed by selective laser melting. J Mater Process Technol. 2025;335; doi:10.1016/j.jmatprotec.2024.118667
[299] Sahu VK, Biswal R, Davis AE, et al. β-Grain refinement in WAAM Ti-6Al-4 V processed with inter-pass ultrasonic impact peening. Materialia. 2024;38; doi:10.1016/j.mtla.2024.102236
[300] Liu J, Miao Y, Wu R, et al. Improved material properties of wire arc additively manufactured Al-Zn-mg-cu alloy through severe deformation interlayer friction stir processing and post-deposition heat treatment. Mater Charact. 2024;218; doi:10.1016/j.matchar.2024.114487
[301] Zhang J, Di X, Li C, et al. Effect of electromagnetic stirring frequency on Inconel625-high strength Low alloy steel functionally graded material fabricated by wire Arc additive manufacturing. J Materi Eng Perform. 2022;31; doi:10.1007/s11665-022-07008-8
[302] Xiong X, Hu Z, Qin X, et al. In-situ fabrication of repairing layers for large structures using follow-up hot-hammering-assisted wire arc additive manufacturing. J Manufact Process. 2023;94; doi:10.1016/j.jmapro.2023.03.023
[303] Ross NS, Mashinini PM, Ananth MBJ, et al. Tribology-driven strategies for tool wear reduction and surface integrity enhancement in cryogenic CO2-cooled milling of laser metal deposited Ti64 alloy. Tribol Int. 2024;198; doi:10.1016/j.triboint.2024.109906
[304] Sure J, Sri Maha Vishnu D, Schwandt C. Preparation of refractory high-entropy alloys by electro-deoxidation and the effect of heat treatment on microstructure and hardness. JOM. 2020;72.
[305] Tanvir G, Karim MA, Jadhav S, et al. Effect of hot isostatic pressing on porosity of wire-arc directed energy deposited TZM/NbZr1 bimetallic structure. Virt Phys Prototyp. 2024;19; doi:10.1080/17452759.2024.2404989
[306] Qin F, Shi Q, Zhou G, et al. Simultaneously enhanced strength and plasticity of laser powder bed fused tantalum by hot isostatic pressing. Mater Lett. 2024;371; doi:10.1016/j.matlet.2024.136957
[307] Song W, Yang J, Liang J, et al. A new approach to design advanced superalloys for additive manufacturing. Addit Manufact. 2024;84; doi:10.1016/j.addma.2024.104098
[308] Wang Y, Guo W, Li H, et al. Nano-scale microstructural evolution and mechanical property enhancement mechanism during crack inhibition in nickel-based superalloys fabricated by laser powder bed fusion. Addit Manufact. 2025;100; doi:10.1016/j.addma.2025.104685
[309] Ocaño PS, Fries SG, Lopez-Galilea I, et al. The AlMo0.5NbTa0.5TiZr refractory high entropy superalloy: experimental findings and comparison with calculations using the CALPHAD method. Mater Des. 2022;217:110593.
[310] Precipitation kinetics during non-linear heat treatment in Laser Additive Manufacturing. https://www.mpie.de/3641061/prec_kin.
[311] Kumawat MK, Alam MZ, Kumar A, et al. Tensile behavior of a slurry Fe-Cr-Si coated Nb-alloy evaluated by gleeble testing. Surf Coat Technol. 2018;349:695–706.
[312] Yi J, Yang L, Wang L, et al. Lightweight, refractory high-entropy alloy, CrNbTa 0.25 TiZr, with high yield strength. Met Mater Intern. 2021;28:448–455.
[313] Huang R, Wang W, Li T, et al. A novel AlMoNbHfTi refractory high-entropy alloy with superior ductility. J Alloys Compds. 2023;940; doi:10.1016/j.jallcom.2023.168821
[314] Kim DB, Witherell P, Lu Y, et al. Toward a digital thread and data package for metals-additive manufacturing. Smart Sustain Manufact Syst. 2017;1:75–99.
[315] Olsson M, Bushlya V, Lenrick F, et al. Evaluation of tool wear mechanisms and tool performance in machining single-phase tungsten. Intern J Refract Met Hard Mater. 2021;94:105379.
[316] You K, Yan G, Luo X, et al. Advances in laser assisted machining of hard and brittle materials. J Manufact Process. 2020;58:677–692.
[317] Yang Z, Zhu L, Zhang G, et al. Review of ultrasonic vibration-assisted machining in advanced materials. Int J Mach Tools Manuf. 2020;156:103594.
[318] Mohammadian A, Sadeqi Bajestani M. Investigation on the cutting force and surface quality in harmonically vibrated broaching (HVB). Adv Tribol. 2023; doi:10.1155/2023/9917497
[319] Wang Y, Wang L, Zhang X, et al. Cutting of tungsten plate for fusion device via pre-mixed abrasive water jet. Fusion Eng Des. 2020;159:111790.

[320] Omole S, Lunt AJ, Kirk S, et al. Investigating the machining of tungsten (W) using finite element analysis, Procedia CIRP, 2023.
[321] Zahedi SA. *Crystal-plasticity modelling of machining* [Doctoral dissertation]. Loughborough University; 2014, http://ethos.bl.uk/OrderDetails.do?uin=uk.bl.ethos.702986.
[322] Omole S, Lunt A, Kirk S, et al. Advanced processing and machining of tungsten and its alloys. J Manufact Mater Process. 2022;6:15.
[323] Yang H, Wang X, Zhang J, et al. On the cutting performance and chip characteristics of WNbMoTaZr0.5 refractory high entropy alloy. Int J Adv Manuf Technol. 2023;128; doi:10.1007/s00170-023-12252-w
[324] Demir E, Mercan C. A physics-based single crystal plasticity model for crystal orientation and length scale dependence of machining response. Int J Mach Tools Manuf. 2018;134; doi:10.1016/j.ijmachtools.2018.06.004
[325] Jawahir IS, Stephenson DA, Wang B. A review of advances in modeling of conventional machining processes: from merchant to the present. J Manuf Sci Eng. 2022;144:110801–110801.
[326] Zhang N, Klippel H, Afrasiabi M, et al. Hybrid SPH-FEM solver for metal cutting simulations on the GPU including thermal contact modeling. CIRP J Manufact Sci Technol. 2023;41; doi:10.1016/j.cirpj.2022.12.012
[327] Sílvia R, Lauro CH, Ana H, et al. Development of FEM-based digital twins for machining difficult-to-cut materials: A roadmap for sustainability. J Manufact Process. 2022;75:739–766.
[328] Dilberoglu UM, Gharehpapagh B, Yaman U, et al. Current trends and research opportunities in hybrid additive manufacturing. Intern J Adv Manufact Technol. 2021;113:623–648.
[329] Du W, Bai Q, Zhang B. A novel method for additive/subtractive hybrid manufacturing of metallic parts. Proc Manufact. 2016;5; doi:10.1016/j.promfg.2016.08.067
[330] Wüst P, Edelmann A, Hellmann R. Areal surface roughness optimization of maraging steel parts produced by hybrid additive manufacturing. Materials (Basel). 2020;13; doi:10.3390/ma13020418
[331] Madireddy G, Feldhausen T, Kannan R, et al. Effect of additive and subtractive sequence on the distortion of cone-shaped part during hybrid direct energy deposition. J Manufact Process. 2024;119; doi:10.1016/j.jmapro.2024.03.080
[332] Lee Y, Feldhausen T, Fancher CM, et al. Prediction of residual strain/stress validated with neutron diffraction method for wire-feed hybrid additive/subtractive manufacturing. Addit Manufact. 2024;79; doi:10.1016/j.addma.2023.103920
[333] Ameta G, Lipman R, Moylan S, et al. Investigating the role of geometric dimensioning and tolerancing in additive manufacturing. J Mech Design. 2015;137:111401.
[334] Lipman RR, Filliben JJ. Testing implementations of geometric dimensioning and tolerancing in CAD software. Computer-aided Design Applic. 2020;17. doi:10.14733/cadaps.2020.1241-1265
[335] Moylan S, Slotwinski J. Assessment of guidelines for conducting round robin studies in additive manufacturing, Proceedings of the 2014 ASPE Spring Topical Meeting–Dimensional Accuracy and Surface Finish in Additive Manufacturing 57 82–85.
[336] Feng R, Feng B, Gao MC, et al. Superior high-temperature strength in a supersaturated refractory high-entropy alloy. Adv Mater. 2021;33:2102401.
[337] Sahragard-Monfared G, Belcher CH, Bajpai S, et al. Tensile creep behavior of the Nb45Ta25Ti15Hf15 refractory high entropy alloy. Acta Mater. 2024;272; doi:10.1016/j.actamat.2024.119940
[338] Liu C, Gadelmeier C, Lu S, et al. Tensile creep behavior of HfNbTaTiZr refractory high entropy alloy at elevated temperatures. Acta Mater. 2022;237; doi:10.1016/j.actamat.2022.118188
[339] Sahragard-Monfared G, Zhang M, Smith TM, et al. The influence of processing methods on creep of wrought and additively manufactured CrCoNi multi-principal element alloys. Acta Mater. 2023;261; doi:10.1016/j.actamat.2023.119403
[340] Sahragard-Monfared G, Zhang M, Smith TM, et al. Superior tensile creep behavior of a novel oxide dispersion strengthened CrCoNi multi-principal element alloy. Acta Mater. 2023;255; doi:10.1016/j.actamat.2023.119032
[341] Glatzel U, Schleifer F, Gadelmeier C, et al. Quantification of solid solution strengthening and internal stresses through creep testing of Ni-containing single crystals at 980°C. Metals (Basel). 2021;11; doi:10.3390/met11071130
[342] Deneault JR, Chang J, Myung J, et al. Toward autonomous additive manufacturing: Bayesian optimization on a 3D printer. MRS Bull. 2021;46; doi:10.1557/s43577-021-00051-1
[343] Kusne AG, Yu H, Wu C, et al. On-the-fly closed-loop materials discovery via Bayesian active learning. Nat Commun. 2020;11; doi:10.1038/s41467-020-19597-w
[344] McDannald A, Frontzek M, Savici AT, et al. On-the-fly autonomous control of neutron diffraction via physics-informed Bayesian active learning. Appl Phys Rev. 2022;9:021408.
[345] Lookman T, Balachandran PV, Xue D, et al. Active learning in materials science with emphasis on adaptive sampling using uncertainties for targeted design. npj Computat Mater. 2019;5:21.
[346] Bateni F, Epps RW, Antami K, et al. Autonomous nanocrystal doping by self-driving fluidic micro-processors. Adv Intellig Syst. 2022;4:2200017.
[347] Reyes KG, Maruyama B. The machine learning revolution in materials? MRS Bullet. 2019;44; doi:10.1557/mrs.2019.153
[348] Waller JM, Saulsberry RL, Parker BH, et al. Summary of NDE of additive manufacturing efforts in NASA, AIP Confer Proc 1650 51–62.
[349] Kim FH, Kim FH, Moylan SP. Literature review of metal additive manufacturing defects. US Department of Commerce, National Institute of Standards and Technology; 2018 doi:10.6028/NIST.AMS.100-16.
[350] Segovia Ramírez I, García Márquez FP, Papaelias M. Review on additive manufacturing and non-destructive testing. J Manuf Syst. 2023;66; doi:10.1016/j.jmsy.2022.12.005
[351] Taheri H, Gonzalez Bocanegra M, Taheri M. Artificial intelligence, machine learning and smart technologies

for nondestructive evaluation. Sensors (Basel, Switzerland). 2022;22; doi:10.3390/s22114055
[352] Harley JB, Sparkman D. Machine learning and NDE: past, present, and future. AIP Confer Proc. 2019;2102:090001.
[353] Saleem M, Gutierrez H. Using artificial neural network and non-destructive test for crack detection in concrete surrounding the embedded steel reinforcement. Struct Concrete J FIB. 2021;22; doi:10.1002/suco.202000767
[354] Mahdi MM, Bajestani MS, Noh SD, et al. Digital twin-based architecture for wire arc additive manufacturing using OPC UA. Robot Comput Integr Manufact. 2025;94; doi:10.1016/j.rcim.2024.102944
[355] Mukherjee T, DebRoy T. A digital twin for rapid qualification of 3D printed metallic components. Appl Mater Today. 2019;14; doi:10.1016/j.apmt.2018.11.003
[356] Wu D, Qu W, Wen Y, et al. The application, challenge, and developing trends of Non-destructive testing technique for large-scale and complex engineering components fabricated by metal additive manufacturing technology in aerospace. J Nondestruct Eval. 2024;43; doi:10.1007/s10921-024-01107-3
[357] Yoon KN, Kim IH, Kim JK, et al. Prediction of yield strength in WTaVTiCr refractory high entropy alloy system via measurement of temperature coefficient of resistivity (TCR). J Alloys Compds. 2025;1036; doi:10.1016/j.jallcom.2025.182004
[358] Pyle RJ, Bevan RL, Hughes RR, et al. Deep learning for ultrasonic crack characterization in NDE. IEEE Trans Ultrason Ferroelectr Freq Contr. 2020;68:1854–1865.
[359] Witherell P, Feng S, Simpson TW, et al. Toward metamodels for composable and reusable additive manufacturing process models. J Manuf Sci Eng. 2014;136; doi:10.1115/1.4028533
[360] Mahadevan S, Nath P, Hu Z. Uncertainty quantification for additive manufacturing process improvement: recent advances. ASCE-ASME J Risk Uncert in Engrg Sys Part B Mech Eng. 2022;8; doi:10.1115/1.4053184
[361] Lopez F, Witherell P, Lane B. Identifying uncertainty in laser powder Bed fusion additive manufacturing models. J Mech Des. 2016;138; doi:10.1115/1.4034103
[362] Bowling LS, Wang AT, Philips NR, et al. Thermophysical modeling of niobium alloys informs materials selection and design for high-temperature applications. Mater Design. 2024;248; doi:10.1016/j.matdes.2024.113456
[363] Nonato RBP, Restivo TAG, Machado Junior JC. Uncertainty quantification in masses of alloy components and atomic radii modification in high-entropy alloys design: thermophysical parameters calculation approach. Mater Res (São Carlos, São Paulo, Brazil). 2025;28; doi:10.1590/1980-5373-mr-2024-0350
[364] Giles SA, Shortt H, Liaw PK, et al. Yield Strength-Plasticity Trade-Off and Uncertainty Quantification for Machine-learning-based Design of Refractory High-Entropy Alloys, 2023. doi:10.48550/arxiv.2304.13932
[365] Office of the Under Secretary of Defense for Research and Engineering. DoD Modeling & Simulation Verification, Validation & Accreditation (VV&A): The Acquisition Perspective, Department of Defense, 2009, https://ndia.dtic.mil/wp-content/uploads/2009/systemengr/8939ThursdayTrack3Truelove.pdf.
[366] Roh B, Simpson TW, Yang H, et al. Ensuring quality in metal additive manufacturing through a V-model framework. Access. 2023;11; doi:10.1109/ACCESS.2023.3327054
[367] ASME, Standard for Verification and Validation in Computational Solid Mechanics V&V 10 - 2019. (2020). https://doclinkonline.com/87a673cb-291a-4027-bf24-5193a92e254a.
[368] Zhu P, Yu Y, Zhang C, et al. V0.5Nb0.5ZrTi refractory high-entropy alloy fabricated by laser addictive manufacturing using elemental powders. Intern J Refract Met Hard Mater. 2023;113; doi:10.1016/j.ijrmhm.2023.106220
[369] Sowards JW, Michael FN, Mireles O. Open-source Numerical Modeling of Solidification Cracking Susceptibility: Application to Refractory Alloy Systems. https://ntrs.nasa.gov/citations/20230012726.
[370] Wang Y, McDowell DL. Uncertainty quantification in multiscale materials modeling, 1st ed. Duxford: Woodhead Publishing, Elsevier; 2020. doi:10.1016/C2018-0-00364-3
[371] Roy CJ, Oberkampf WL. A comprehensive framework for verification, validation, and uncertainty quantification in scientific computing. Comput Meth Appl Mech Eng. 2011;200; doi:10.1016/j.cma.2011.03.016
[372] Hu Z, Mahadevan S. Uncertainty quantification and management in additive manufacturing: current status, needs, and opportunities. Int J Adv Manuf Technol. 2017;93; doi:10.1007/s00170-017-0703-5
[373] Nath P, Hu Z, Mahadevan S. Uncertainty quantification of grain morphology in laser direct metal deposition. MSMS. 2019;27; doi:10.1088/1361-651X/ab1676
[374] Raghunath N, Pandey PM. Improving accuracy through shrinkage modelling by using taguchi method in selective laser sintering. Intern J Mach Tools Manufact. 2007;47; doi:10.1016/j.ijmachtools.2006.07.001
[375] Tapia G, Elwany A. A review on process monitoring and control in metal-based additive manufacturing. J Manuf Sci Eng. 2014;136; doi:10.1115/1.4028540
[376] Kamath C. Data mining and statistical inference in selective laser melting. Int J Adv Manuf Technol. 2016;86; doi:10.1007/s00170-015-8289-2
[377] Garg A, Tai K, Savalani MM. State-of-the-art in empirical modelling of rapid prototyping processes. Rapid Prototyp J. 2014;20; doi:10.1108/RPJ-08-2012-0072
[378] Anderson A, J Delplanque. Development of Physics-Based Numerical Models for Uncertainty Quantification of Selective Laser Melting Processes – 2015 Annual Progress Report, 2015,https://www.osti.gov/servlets/purl/1226942.
[379] Ma L, Fong J, Lane B, et al. Using design of experiments in finite element modeling to identify critical variables for laser powder bed fusion, 2015.
[380] Loughnane GT. A framework for uncertainty quantification in microstructural characterization with application to additive manufacturing of Ti-6Al-4V, Wright State University/Ohio, 2015, http://rave.ohiolink.edu/etdc/view?acc_num=wright1441064431.
[381] Cai G, Mahadevan S. Uncertainty quantification of manufacturing process effects on macroscale material properties. Intern J Multisc Computat Eng. 2016;14; doi:10.1615/IntJMultCompEng.2016015552
[382] Ye J, Saunders RN, Elwany A. Surrogate-based model chains for establishing process-structure-property

linkages with quantified uncertainties in metal additive manufacturing. Manufact Lett. 2023;35; doi:10.1016/j.mfglet.2023.08.099
[383] Zhang J. Modern Monte Carlo methods for efficient uncertainty quantification and propagation: A survey. Wiley Interdiscipl Rev Computat Stat. 2021;13; doi:10.1002/wics.1539
[384] Eldred M. Recent advances in non-intrusive polynomial chaos and stochastic collocation methods for uncertainty analysis and design, 50th AIAA, American Institute of Aeronautics and Astronautics, 2009. doi:10.2514/6.2009-2274
[385] Swiler LP, Eldred MS. Efficient algorithms for mixed aleatory-epistemic uncertainty quantification with application to radiation-hardened electronics. Part I, algorithms and benchmark results, 2009. https://www.osti.gov/servlets/purl/972887.
[386] Kotha S, Ozturk D, Ghosh S. Uncertainty-quantified parametrically homogenized constitutive models (UQ-PHCMs) for dual-phase α/β titanium alloys. npj Comput Mater. 2020;6; doi:10.1038/s41524-020-00379-3
[387] Tapia G, King W, Johnson L, et al. Uncertainty propagation analysis of computational models in laser powder bed fusion additive manufacturing using polynomial chaos expansions. J Manufact Sci Eng. 2018;140:121006.
[388] Senthilnathan A, Nath P, Mahadevan S, et al. Surrogate modeling of microstructure prediction in additive manufacturing. Computat Mater Sci. 2025;247; doi:10.1016/j.commatsci.2024.113536
[389] Razvi SS, Feng S, Narayanan A, et al. A Review of Machine Learning Applications in Additive Manufacturing, ASME 2019 International Design Engineering Technical Conferences and Computers and Information in Engineering Conference2019, Volume 1: 39th Computers and Information in Engineering Conference. doi:10.1115/DETC2019-98415
[390] Pandiyan V, Drissi-Daoudi R, Shevchik S, et al. Deep transfer learning of additive manufacturing mechanisms across materials in metal-based laser powder bed fusion process. J Mater Process Technol. 2022;303; doi:10.1016/j.jmatprotec.2022.117531
[391] Marmarelis MG, Ghanem RG. Data-driven stochastic optimization on manifolds for additive manufacturing. Computat Mater Sci. 2020;181; doi:10.1016/j.commatsci.2020.109750
[392] Tang Y, Dehaghani MR, Wang GG. Review of transfer learning in modeling additive manufacturing processes. Addit Manufact. 2023;61; doi:10.1016/j.addma.2022.103357
[393] Mehta M, Shao C. Federated learning-based semantic segmentation for pixel-wise defect detection in additive manufacturing. J Manufact Syst. 2022;64; doi:10.1016/j.jmsy.2022.06.010
[394] Shin S, Lee J, Jadhav S, et al. Material-adaptive anomaly detection using property-concatenated transfer learning in wire arc additive manufacturing. Intern J Precis Eng Manufact. 2024;25:383–408.
[395] Ko H, Witherell P, Lu Y, et al. Machine learning and knowledge graph based design rule construction for additive manufacturing. Addit Manufact. 2021;37:101620.
[396] Roh B, Kumara SR, Witherell P, et al. Ontology-based process map for metal additive manufacturing. J Mater Eng Perform. 2021;30:8784–8797.
[397] Roh B, Kumara SR, Yang H, et al. Ontology network-based in-situ sensor selection for quality management in metal additive manufacturing. J Comput Inform Sci Eng. 2022;22:060905.
[398] Liang JS. An ontology-oriented knowledge methodology for process planning in additive layer manufacturing. Robot Comput Integr Manufact. 2018;53; doi:10.1016/j.rcim.2018.03.003
[399] Hagedorn TJ, Krishnamurty S, Grosse IR. A knowledge-based method for innovative design for additive manufacturing supported by modular ontologies. J Comput Inf Sci Eng. 2018;18; doi:10.1115/1.4039455
[400] Park H, Ko H, Lee YT, et al. Collaborative knowledge management to identify data analytics opportunities in additive manufacturing. J Intell Manuf. 2023;34; doi:10.1007/s10845-021-01811-1
[401] Guo S, Agarwal M, Cooper C, et al. Machine learning for metal additive manufacturing: towards a physics-informed data-driven paradigm. J Manufact Syst. 2022;62; doi:10.1016/j.jmsy.2021.11.003
[402] Du Y, Mukherjee T, DebRoy T. Physics-informed machine learning and mechanistic modeling of additive manufacturing to reduce defects. Appl Mater Today. 2021;24; doi:10.1016/j.apmt.2021.101123
[403] Guo W, Tian Q, Guo S, et al. A physics-driven deep learning model for process-porosity causal relationship and porosity prediction with interpretability in laser metal deposition. CIRP Ann. 2020;69; doi:10.1016/j.cirp.2020.04.049
[404] Ko H, Lu Y, Yang Z, et al. A framework driven by physics-guided machine learning for process-structure-property causal analytics in additive manufacturing. J Manufact Syst. 2023;67; doi:10.1016/j.jmsy.2022.09.010
[405] Teng C, Gong H, Szabo A, et al. Simulating melt pool shape and lack of fusion porosity for selective laser melting of cobalt chromium components. J Manuf Sci Eng. 2017;139; doi:10.1115/1.4034137
[406] Singh S, Katiyar NK, Goel S, et al. Phase prediction and experimental realisation of a new high entropy alloy using machine learning. Sci Rep. 2023;13; doi:10.1038/s41598-023-31461-7
[407] Rahman A, Hossain MS, Siddique A. Review: machine learning approaches for diverse alloy systems. J Mater Sci. 2025;60; doi:10.1007/s10853-025-11154-4
[408] Kannan R, Nandwana P. Accelerated alloy discovery using synthetic data generation and data mining. Scripta Mater. 2023;228; doi:10.1016/j.scriptamat.2023.115335
[409] Wang X, Xiong W. Uncertainty quantification and composition optimization for alloy additive manufacturing through a CALPHAD-based ICME framework. npj Comput Mater. 2020;6; doi:10.1038/s41524-020-00454-9
[410] Horstemeyer MF. Integrated computational materials engineering (ICME) for metals, 1st ed. Somerset: Wiley; 2012.
[411] Sharma S, Joshi SS, Pantawane MV, et al. Multiphysics multi-scale computational framework for linking process–structure–property relationships in metal

additive manufacturing: a critical review. Intern Mater Rev. 2023;68:943), doi:10.1080/09506608.2023.2169501
[412] Jalalahmadi B, Liu J, Liu Z, et al. An integrated computational materials engineering predictive platform for fatigue prediction and qualification of metallic parts built With additive manufacturing. J Tribol. 2021;143; doi:10.1115/1.4050941
[413] Seo G, Ahsan MR, Lee Y, et al. A functional modeling approach for quality assurance in metal additive manufacturing. Rapid Prototyp J. 2021;27; doi:10.1108/RPJ-12-2018-0312
[414] Qin Y, Qi Q, Shi P, et al. Multi-Attribute decision-making methods in additive manufacturing: The state of the Art. Processes. 2023;11; doi:10.3390/pr11020497
[415] Liu W, Zhu Z, Ye S. A decision-making methodology integrated in product design for additive manufacturing process selection. Rapid Prototyp J. 2020;26; doi:10.1108/RPJ-06-2019-0174
[416] Chandra M, Shahab F, Kek V, et al. Selection for additive manufacturing using hybrid MCDM technique considering sustainable concepts. Rapid Prototyp J. 2022;28; doi:10.1108/RPJ-06-2021-0155
[417] Aytekin A. Comparative analysis of the normalization techniques in the context of MCDM problems. Decision Mak Applic Manage Eng. 2021;4; doi:10.31181/dmame210402001a
[418] Sudret B, Marelli S, Wiart J. Surrogate models for uncertainty quantification: An overview. EuCAP: 793–797. doi:10.23919/EuCAP.2017.7928679
[419] Lu Y, Witherell P, Donmez A. A collaborative data management system for additive manufacturing, Volume 1: 37th computers and information in engineering conference. doi:10.1115/DETC2017-68457
[420] Oden T, Moser R, Ghattas O. Computer predictions with quantified uncertainty, part I, SIAM News 43, 2010, 1–3. https://jtoden.oden.utexas.edu/wp-content/uploads/2013/06/2011-1842-SIAM-NEWS-2010_computerpredictionsPt1.pdf.
[421] Chen Z, Han C, Gao M, et al. A review on qualification and certification for metal additive manufacturing. Virt Phys Prototyp. 2022;17:382–405.
[422] Feng SC, Witherell P, Ameta G, et al. Activity model for homogenization of data sets in laser-based powder bed fusion. Rapid Prototyp J. 2017;23:137–148.
[423] Karkaria V, Goeckner A, Zha R, et al. Towards a digital twin framework in additive manufacturing: machine learning and Bayesian optimization for time series process optimization. J Manuf Syst. 2024;75:322–332.
[424] Chen Y, Karkaria V, Tsai Y, et al. Real-time decision-making for digital twin in additive manufacturing with model predictive control using time-series deep neural networks. J Manuf Syst. 2025;80:412–424.
[425] Huang Y, Leu MC, Mazumder J, et al. Additive manufacturing: current state, future potential, gaps and needs, and recommendations. J Manuf Sci Eng. 2015;137; doi:10.1115/1.4028725
[426] Mazumder J. Design for metallic additive manufacturing machine with capability for "certify as You build". Procedia Cirp. 2015;36:187–192.
[427] Chen L, Bi G, Yao X, et al. Multisensor fusion-based digital twin for localized quality prediction in robotic laser-directed energy deposition. Robot Comput Integr Manufact. 2023;84; doi:10.1016/j.rcim.2023.102581
[428] Liu N, Li X, Rajanna MR, et al. Deep neural operator enabled digital twin modeling for additive manufacturing. ACSE. 2024;2; doi:10.3934/acse.2024010
[429] Li Y, Mojumder S, Lu Y, et al. Statistical parameterized physics-based machine learning digital twin models for laser powder bed fusion process, 2023. doi:10.48550/arxiv.2311.07821
[430] Tudorache L, Babur Ö, Lucas SS, et al. Current approaches to digital twins in additive manufacturing: a systematic literature review. Progr Addit Manufact. 2025. doi:10.1007/s40964-025-01262-7
[431] Liu X, Hu R, Lu W, et al. Temperature-dependent tensile deformation and plasticity loss mechanism of a novel Ni-Cr-W-based superalloy prepared by laser powder bed fusion. Addit Manufact. 2023;78; doi:10.1016/j.addma.2023.103883
[432] Wang Y, Guo W, Li H, et al. High-temperature plasticity improvement by La addition during crack inhibition in laser powder bed fusion fabricated haynes 230. Virt Phys Prototyp. 2025;20; doi:10.1080/17452759.2025.2504079
[433] Fellinger J, Richou M, Ehrke G, et al. Tungsten based divertor development for wendelstein 7-X. Nucl Mater Energy. 2023;37; doi:10.1016/j.nme.2023.101506

Appendix

List of Abbreviations

Abbreviation	Full term
3D	Three-Dimensional
AI	Artificial Intelligence
AM	Additive Manufacturing
BPNN	Back Propagation Neural Network
BTF	Buy-to-Fly (Ratio)
CALPHAD	CALculation of PHAse Diagrams
CFD	Computational Fluid Dynamics
CPFFT	Crystal Plasticity Fast Fourier Transform
DA	Data Analytics
DBTT	Ductile to Brittle Transition Temperature
DED	Directed Energy Deposition
DFAM	Design for Additive Manufacturing
DIC	Digital Image Correlation
DL	Deep Learning
DoE	Design of Experiments
DNN	Deep Neural Network
DT	Digital Twin
DXR	Dynamic Synchrotron X-ray Radiographic
EBM	Electron Beam Melting
FE	Finite Element
FGM	Functionally Graded Material
GAN	Generative Adversarial Network
GBT	Gradient Boosted Tree
GD	Generative Design
HTEM	High-Throughput Experimental Methods
HDRI	High Dynamic Range Image
ICME	Integrated Computational Materials Engineering
IGA	Isogeometric Analysis
ILF	Input Laser Flux
IR	Infrared
LAM	Laser Additive Manufacturing
LPBF	Laser Powder Bed Fusion
L-DED	Laser Directed Energy Deposition

(*Continued*)

Continued.

Abbreviation	Full term
LMD	Laser Metal Deposition
MD	Molecular Dynamics
ML	Machine Learning
MPa	Mega Pascal
MPEAs	Multi-Principal Element Alloys
NSGA-II	Non-dominated Sorting Genetic Algorithm II
OM	Optical Image
PA	Performance Assurance
PCA	Principal Component Analysis
PBF	Powder Bed Fusion
PSPP	Process–Structure–Property–Performance
QA	Quality Assurance
RA	Refractory Alloy
RF	Random Forest
RCCA	Refractory Complex Concentrated Alloy
RHEA	Refractory High-Entropy Alloys
RMPEAs	Refractory Multi-Principal Element Alloy
SLM	Selective Laser Melting
TO	Topology Optimisation
UQ	Uncertainty Quantification
VAM	Vacuum Arc Melting
VV&UQ	Verification, Validation, and Uncertainty Quantification
WAAM	Wire Arc Additive Manufacturing
XAI	Explainable Artificial Intelligence